Convection in pulsating white dwarfs

Auteur : Verhulst, Grégoire
Promoteur(s) : Dupret, Marc-Antoine
Faculté : Faculté des Sciences
Diplôme : Master en sciences spatiales, à finalité approfondie
Année académique : 2018-2019
URI/URL : http://hdl.handle.net/2268.2/6999

University of Liège
Faculty of Sciences
Department of Astrophysics, Geophysics and Oceanography

Master thesis presented for the Master's degree in Space Sciences

Convection in pulsating white dwarfs

Author
Grégoire Verhulst

Supervisor
Prof. Marc-Antoine Dupret

Academic year 2018-2019

Contents

Remerciements

Je tiens en premier lieu à remercier mon promoteur, monsieur Marc-Antoine Dupret, pour avoir présenté ce sujet de mémoire si intéressant et m'avoir soutenu tout au long du développement de celui-ci. Sa disponibilité, ses explications et ses relectures auront grandement contribué à ce travail. Je remercie également madame Valérie Van Grootel pour ses précisions apportées durant l'année.

De plus, je remercie Elisa ainsi que ma famille pour leur soutien continu durant ces cinq années d'étude. Finalement, merci à tous mes amis de bachelier et de master pour tous ces moments passés ensemble et leur aide ponctuelle.

Chapter 1

Introduction

One way to learn more about solar interiors is to use asteroseismology. This technique can provide information on a huge amount of physical quantities which are observationally inaccessible and helps to constraint stellar evolution models. Through the study of the modes observed for a pulsating star, and by comparing them to the predicted pulsation periods obtained from stellar models, the most realistic physical model can hopefully be found.

In this work, the emphasis will be placed on the understating of the theory needed to try to describe correctly the interaction between convection and pulsation. We will shed light on important terms appearing due to turbulent flows and see how we can describe them. Hence, we will present more evolved models that should reproduce the reality with a better fidelity. Finally, to illustrate and compare the different possible models introduced previously, we will study a well-known type of variable stars: the ZZ Ceti white dwarfs. These dying stars are known for their extremely thin but efficient convection envelope (as most white dwarfs) and for their instability strip for which better predictions are still needed in order to match the observations.

1.1 Convection and pulsation

Convection is a phenomenon that can happen in a huge number of places and at a wide variety of spatial scales, from boiling water in a pan to convective flows within stars. In stars, it can have significant consequences on their structure and evolution but also on their oscillation periods when considering pulsating stars. For these, a precise description of convection would be necessary. However, such a full description remains complex as convection is a quite complex phenomenon to model. In this context, several theories have been developed to model the convection in stars and its effect on pulsation.

The approach we will follow is the following: we will present and use the time-dependent convection treatment developed by [Gabriel et al., 1974] and further unified under [Grigahcène et al., 2005] (with the latest improvements) which is based on the mixing-length theory ([Prandtl, 1925]) and for which the solution stability is studied by a linear perturbative method. The mixing-length theory was first developed by [Prandtl, 1925] but further used in two different ways. On one hand, [Gough, 1977] created a theory analogous to the kinetic theory of gases : in this scenario, the mixing-length represents the typical length over which a convective element is accelerated due to the buoyancy force. After having travelled along this distance the element exchanges its thermal energy with the surrounding medium. On the other hand, [Unno, 1967] developed another theory taking the original ideas of [Prandtl, 1925] into account. This time, a fictitious viscosity is introduced, called the turbulent viscosity, and acts in the opposite direction to the buoyancy force. In the stationary case, both approaches should give the same results. The theory of [Gabriel et al., 1974] follows the approach of [Unno, 1967] but with the advantage to be applicable to non-radial modes.

However, as convection is a three-dimensional phenomenon, it would be more appropriate to treat it as such. This can be done for example by using three-dimensional hydrodynamical simulations. These simulations give a much more accurate view of the convection and can help to improve the existing models based on the one-dimensional mixing-length theory.

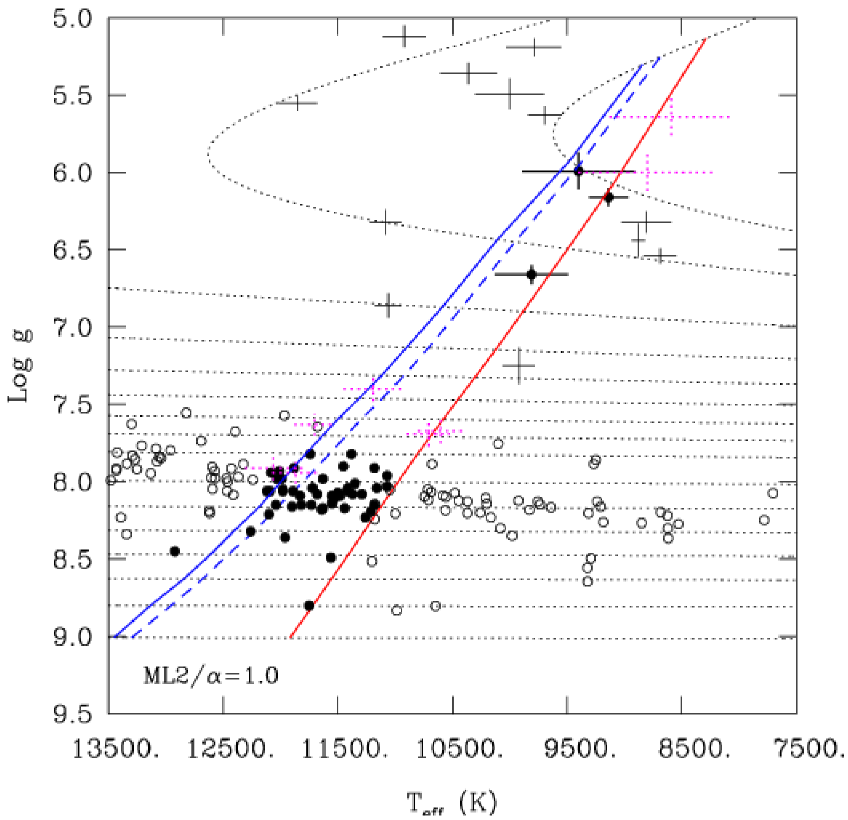

Figure 1.1: Empirical instability domain in the $\log g - T_{\mathrm{eff}}$ domain for the ZZ Ceti white dwarfs. Filled circles represent the positions of the pulsators while open circles show the positions of the non variable stars. (Source: V. Van Grootel)

1.2 ZZ Ceti white dwarfs

As an application to test the different models based on the theory presented beforehand, we will make use of variable white dwarfs. A low or medium mass star ($M < 8M_\odot$) will become at the end of its life a white dwarf after having expelled its envelope. These stars are no more experiencing nuclear reactions in their core and so they slowly cool down. With a rather small radius (of the order of the radius of the Earth) but with masses comparable to that of the Sun, they are compact objects with a high surface gravity g (given by the Newton's law of universal gravitation $g = GM/R^2$). In astrophysics, the surface gravity is often expressed in terms of logarithms ($\log g$) with for example $\log g = 8$ giving $g = 10^8\,cm/s^2$ (to be compared with the surface gravity of the Sun of $g = 27400\,cm/s^2$). As around 97% of all stars are to become someday a white dwarf, they are considered as an interesting field of study. Three main classes of pulsating white dwarf stars are known : the hot GW Vir stars with T_{eff}[1] $\simeq$120 000 K, the cooler V777 Her stars with $T_{\mathrm{eff}} \simeq$ 25 000 K and finally the coolest class of ZZ Ceti stars with $T_{\mathrm{eff}} \simeq$ 11 800 K [Fontaine and Brassard, 2008]. Those of interest in this work will be the ZZ Ceti stars. They belong to the most populated class of white dwarfs (around 86% of all white dwarfs [Aerts et al., 2010]), the DA white dwarfs which are composed of an almost pure hydrogen envelope where all other elements have fallen towards the inner regions due to gravitational settling. At this effective temperature, H located in the outer envelope starts to recombine causing an important increase in the opacity. As a result, it strangles the flow of radiation leading to pulsational instabilities against g-modes (see [Winget et al., 1982]).

Fig. 1.1 shows the piece of the $\log g - T_{\mathrm{eff}}$ diagram where ZZ Ceti stars are located. In this figure, filled circles represent pulsating white dwarfs while the open circles are non varying stars. We clearly see that the empirical boundaries of the instability strip are rather well determined. From these observations, the original idea coming from [Fontaine et al., 1982] stating that the ZZ Ceti strip must be pure seems verified. A pure strip means in that case that all DA white dwarfs are going at some point as they cool across their sequence to become ZZ Ceti pulsators. With a pure strip, studying the whole class of DA white dwarfs can be made through the analysis of ZZ Ceti pulsators. This would not be possible with a mixed strip as an additional parameter would be necessary to make the distinction between constant stars and pulsators. In addition to this, Fig. 1.1 also shows another property of ZZ Ceti stars concerning a $\log g - T_{\mathrm{eff}}$ correlation for the boundaries. Indeed, we see that the edge of the strip occurs at lower effective temperatures for lower surface gravity stars and this effect seems more pronounced at the red edge than at the blue edge as the slope is greater in that case. Although the empirical boundaries are relatively well defined, the predicted edges are still challenging to determine. And more especially the red edge, for which no good theoretical values were found. For these reasons, we will present our results obtained using improved models with the hope of finding the location of the edges. Nevertheless, we do not expect to find the right value for the red edge as the treatment of convection that we will present and use is still far too simplistic.

[1] T_{eff} is the effective temperature, defined as the temperature that the star would have if it were radiating as a black body. In the case of a spherical body of radius R and luminosity L we have : $L = 4\pi R^2 \sigma T_{\mathrm{eff}}$ where σ is the Stefan-Boltzmann constant. Even if the stellar spectrum is in general not the same as a black body spectrum, the effective temperature represents quite well the temperature in the surface layers.

Chapter 2

Theoretical developments

2.1 Mean equations

In what follows, the velocity vector $\mathbf{v}$ will be decomposed in two parts: $\mathbf{u}$ and $\mathbf{V}$ following the idea of [Ledoux and Walraven, 1958]. The first part $\mathbf{u}$, represents the mean velocity of the fluid (noticing that the average of the mean velocity vector is the mean velocity vector itself : $\overline{\mathbf{u}} = \mathbf{u}$) and $\mathbf{V}$ represents the convection contribution. We can write :

$$\mathbf{v} = \mathbf{u} + \mathbf{V}. \tag{2.1.1}$$

This type of decomposition into a mean component and a convective one can be applied to any variable. Let us denote y this variable (which can be the density ρ, the pressure p, the temperature T or any other scalar quantity). The component describing the average model will be written $\overline{y}$ and the component describing the fluctuation due to turbulence will be noted $\mathit{\Delta} y$ such that :

$$y = \overline{y} + \mathit{\Delta} y.$$

It appears clear that $\overline{\mathit{\Delta} y} = 0$. For the rest of the developments we will assume that, on average, the convection is not able to transport matter and so $\overline{\rho \mathbf{V}} = 0$ (note that it is not simply $\overline{\mathbf{V}} = 0$ because the density is also varying with depth). This has as consequence that

$$\begin{aligned} \overline{\rho \mathbf{v}} &= \overline{\rho \mathbf{u}} + \overline{\rho \mathbf{V}} \\ &= \overline{\rho} \mathbf{u} \end{aligned} \tag{2.1.2}$$

where we used the property saying that for any quantity $a = \overline{a} + \mathit{\Delta} a$ and $b = \overline{b} + \mathit{\Delta} b$, the average of their product is :

$$\begin{aligned} \overline{ab} &= \overline{a}\overline{b} + \overline{\mathit{\Delta} a \mathit{\Delta} b} \\ &= \overline{a}\overline{b} + \overline{a \, \mathit{\Delta} b} \\ &= \overline{a}\overline{b} + \overline{b \, \mathit{\Delta} a}. \end{aligned} \tag{2.1.3}$$

However, when one of the quantities is the density, we will often neglect $\overline{\mathit{\Delta}\rho \mathit{\Delta} y}$ so that :

$$\begin{aligned} \overline{\rho y} &= \overline{\rho}\overline{y} + \overline{\mathit{\Delta}\rho \mathit{\Delta} y} \\ &= \overline{\rho}\, \overline{y}. \end{aligned}$$

By definition, we will write the material time derivative $\frac{d}{dt}$ as

$$\frac{d}{dt} = \frac{\partial}{\partial t} + \mathbf{u} \cdot \nabla \tag{2.1.4}$$

which represents the variation of an element following its motion in space.

2.1.1 Equation of mass conservation

The hydrodynamic equation of mass is

$$\frac{\partial \rho}{\partial t} + \nabla \cdot (\rho \mathbf{v}) = 0. \tag{2.1.5}$$

We take the average of Eq. (2.1.5) keeping in mind that $\overline{\rho \mathbf{V}} = 0$. This gives the mean equation of mass :

$$\begin{aligned} &\frac{\partial \overline{\rho}}{\partial t} + \nabla \cdot (\overline{\rho \mathbf{v}}) = 0 \\ \Leftrightarrow\ &\frac{\partial \overline{\rho}}{\partial t} + \nabla \cdot (\overline{\rho} \mathbf{u}) = 0. \end{aligned} \tag{2.1.6}$$

It can also be written using the material derivative :

$$\frac{d\overline{\rho}}{dt} + \overline{\rho} \nabla \cdot \mathbf{u} = 0. \tag{2.1.7}$$

2.1.2 Equation of momentum conservation

The equation of momentum can be written as :

$$\frac{\partial (\rho \mathbf{v})}{\partial t} + \nabla \cdot (\rho \mathbf{v}\mathbf{v}) = -\rho \nabla \Phi - \nabla \cdot (P_g + P_R) \tag{2.1.8}$$

where Φ is the gravitational potential, $P_g = p_g \mathbf{I} - \beta_g$ and $P_R = p_R \mathbf{I} - \beta_R$ are respectively the gaseous and radiative stress tensors ($\mathbf{I}$ is the identity tensor), p_g and p_R being the gaseous and radiative pressures while β_g and β_R are the gaseous and radiative deviatoric (viscous) stress tensors.

One takes the average of Eq. (2.1.8) which gives :

$$\frac{\partial (\overline{\rho \mathbf{v}})}{\partial t} + \nabla \cdot (\overline{\rho \mathbf{v}\mathbf{v}}) = -\overline{\rho} \nabla \overline{\Phi} - \nabla \cdot (\overline{P_g} + \overline{P_R}).$$

The second term of the left-hand side of this equation can be rewritten using Eqs. (2.1.2) and (2.1.3) as :

$$\begin{aligned} \nabla \cdot (\overline{\rho \mathbf{v}\mathbf{v}}) &= \nabla \cdot (\overline{\rho \mathbf{v}}\, \overline{\mathbf{v}} + \overline{\rho \mathbf{V}\mathbf{V}}) \\ &= \nabla \cdot (\overline{\rho} \mathbf{u}\mathbf{u} + \overline{\rho \mathbf{V}\mathbf{V}}). \end{aligned}$$

In addition, we note that in good approximation the convective fluctuation of the gravitational potential can be neglected : $\overline{\Phi} = \Phi$. The mean equation thus becomes :

$$\frac{\partial (\overline{\rho} \mathbf{u})}{\partial t} + \nabla \cdot (\overline{\rho} \mathbf{u}\mathbf{u}) + \nabla \cdot (\overline{\rho \mathbf{V}\mathbf{V}}) = -\overline{\rho} \nabla \Phi - \nabla \cdot (\overline{P_g} + \overline{P_R}). \tag{2.1.9}$$

One can see the apparition of a new tensor $\overline{\rho \mathbf{V}\mathbf{V}}$ in the expression of the mean equation of momentum. This tensor is called the Reynolds stress tensor and represents the viscosity caused by the turbulence (this is the reason why it is often called turbulent viscous tensor). It can be written in a similar way as the viscous stress tensors :

$$\overline{\rho \mathbf{V}\mathbf{V}} = \overline{p_t} \mathbf{I} - \overline{\beta_t}$$

where the isotropic component $\overline{p_t}$ is defined as the turbulent pressure and is given by $\overline{p_t} = \overline{\rho V_r^2}$. The term *pressure* is used in this case because we can see the convection as a phenomenon moving portions of matter up and down, impacting the layers situated at the top, creating a kind of pressure just as the atoms at the microscopic level are creating the gaseous pressure p_g. This tensor has as components :

$$\begin{pmatrix} \overline{\rho V_r V_r} & \overline{\rho V_r V_\theta} & \overline{\rho V_r V_\varphi} \\ \overline{\rho V_\theta V_r} & \overline{\rho V_\theta V_\theta} & \overline{\rho V_\theta V_\varphi} \\ \overline{\rho V_\varphi V_r} & \overline{\rho V_\varphi V_\theta} & \overline{\rho V_\varphi V_\varphi} \end{pmatrix}.$$

At equilibrium , only the diagonal components remain and we can define :

$$A = \frac{1}{2}\frac{\overline{\rho \mathbf{V}_r^2}}{\overline{\rho \mathbf{V}_\theta^2}} = \frac{1}{2}\frac{\overline{\rho \mathbf{V}_r^2}}{\overline{\rho \mathbf{V}_\varphi^2}}.$$

If we are in the isotropic case then $A = \frac{1}{2}$ which comes from the fact that all the diagonal components are equal. For more details, see Section 2.4.

We can write Eq. (2.1.9) in another way taking into account the definitions of the different stress tensors. In order to do that it is first interesting to show how the two first terms of Eq. (2.1.9) can be decomposed :

$$\begin{aligned} \frac{\partial(\overline{\rho}\mathbf{u})}{\partial t} + \nabla\cdot(\overline{\rho}\mathbf{u}\mathbf{u}) &= \frac{\partial\overline{\rho}}{\partial t}\mathbf{u} + \frac{\partial\mathbf{u}}{\partial t}\overline{\rho} + \overline{\rho}\mathbf{u}\cdot\nabla\mathbf{u} + \mathbf{u}\nabla\cdot(\overline{\rho}\mathbf{u}) \\ &= \frac{\partial\mathbf{u}}{\partial t}\overline{\rho} + \overline{\rho}\mathbf{u}\cdot\nabla\mathbf{u} \\ &= \overline{\rho}\frac{d\mathbf{u}}{dt} \end{aligned} \tag{2.1.10}$$

where we use the equation of continuity (2.1.6).

Using the previous equation we then easily get :

$$\overline{\rho}\frac{d\mathbf{u}}{dt} = -\overline{\rho}\nabla\Phi - \nabla(\overline{p_g} + \overline{p_R} + \overline{p_t}) + \nabla\cdot(\overline{\beta_g} + \overline{\beta_R} + \overline{\beta_t}). \tag{2.1.11}$$

Neglecting β_g and β_R [1], which means that the viscosity is small enough to be neglected for the mean movement and that the radiation is isotropic, Eq. (2.1.11) can finally be expressed as :

$$\overline{\rho}\frac{d\mathbf{u}}{dt} = -\overline{\rho}\nabla\Phi - \nabla(\overline{p_g} + \overline{p_R} + \overline{p_t}) + \nabla\cdot\overline{\beta_t}. \tag{2.1.12}$$

2.1.3 Poisson equation

The Poisson equation is given by :

$$\nabla^2\Phi = 4\pi G\rho$$

and its mean version simply reads :

$$\nabla^2\Phi = 4\pi G\overline{\rho} \tag{2.1.13}$$

taking into account the fact that the convective fluctuation of the gravitational potential is neglected.

[1]This assumption is justified by the high Reynolds number of stellar turbulence ([Houdek and Dupret, 2015])

2.1.4 Equation of turbulent kinetic energy conservation

One can wonder what would be the equation of turbulent kinetic energy conservation. To obtain it, we first multiply Eq. (2.1.11) by the mean velocity $\mathbf{u}$ to obtain the mean equation of kinetic energy conservation. We also use a relation similar to Eq. (2.1.10) and we get :

$$\begin{aligned} \frac{1}{2}\overline{\rho}\frac{d\mathbf{u}^2}{dt} &= -\overline{\rho}\mathbf{u}\cdot\nabla\varPhi - \nabla\overline{p}\cdot\mathbf{u} + [\nabla\cdot(\overline{\beta_g}+\overline{\beta_R}+\overline{\beta_t})]\cdot\mathbf{u} \\ \Leftrightarrow \frac{1}{2}\frac{\partial(\overline{\rho}\mathbf{u}^2)}{\partial t} + \frac{1}{2}\nabla\cdot(\overline{\rho}\mathbf{u}^2\mathbf{u}) &= -\overline{\rho}\mathbf{u}\cdot\nabla\varPhi - \nabla\overline{p}\cdot\mathbf{u} + [\nabla\cdot(\overline{\beta_g}+\overline{\beta_R}+\overline{\beta_t})]\cdot\mathbf{u} \qquad (2.1.14) \end{aligned}$$

where we define $\overline{p} = \overline{p_g} + \overline{p_R} + \overline{p_t}$ to simplify the notations.

After that, we take the product of the equation of momentum (2.1.8) and the velocity vector $\mathbf{v}$ to obtain the equation of kinetic energy conservation :

$$\frac{1}{2}\frac{\partial(\rho\mathbf{v}^2)}{\partial t} + \frac{1}{2}\nabla\cdot(\rho\mathbf{v}^2\mathbf{v}) = -\rho\mathbf{v}\cdot\nabla\varPhi - \nabla\cdot(P_g+P_R)\cdot\mathbf{v}. \qquad (2.1.15)$$

One uses the decomposition of $\mathbf{v}$ introduced above and after some algebraic manipulations the average of the LHS (left-hand side) of the previous equation becomes :

$$\frac{1}{2}\frac{\partial(\rho\mathbf{v}^2)}{\partial t} + \frac{1}{2}\nabla\cdot(\rho\mathbf{v}^2\mathbf{v}) = \frac{1}{2}\frac{\partial(\overline{\rho}\mathbf{u})}{\partial t} + \frac{1}{2}\frac{\partial(\overline{\rho\mathbf{V}^2})}{\partial t} + \frac{1}{2}\nabla\cdot(\overline{\rho}\mathbf{u}^2\mathbf{u} + \overline{\rho\mathbf{V}^2}\mathbf{u} + \overline{\rho\mathbf{V}^2\mathbf{V}}) + \nabla\cdot(\overline{\rho\mathbf{V}\mathbf{V}}\mathbf{u}). \qquad (2.1.16)$$

We then take the difference between this result and the LHS of Eq. (2.1.14) which gives :

$$\frac{1}{2}\frac{\partial(\overline{\rho\mathbf{V}^2})}{\partial t} + \frac{1}{2}\nabla\cdot(\overline{\rho\mathbf{V}^2}\mathbf{u} + \overline{\rho\mathbf{V}^2\mathbf{V}}) + \nabla\cdot(\overline{\rho\mathbf{V}\mathbf{V}}\mathbf{u}).$$

On the other hand, the average of the RHS (right-hand side) of Eq. (2.1.15) can be written as:

$$-\rho\mathbf{v}\cdot\nabla\varPhi - \nabla\cdot(P_g+P_R)\cdot\mathbf{v} = -\overline{\rho}\mathbf{u}\cdot\nabla\varPhi - \overline{\nabla\cdot(P_g+P_R)}\cdot\mathbf{u} - \overline{[\nabla\cdot(P_g+P_R)]\cdot\mathbf{V}}. \qquad (2.1.17)$$

We subtract this result from the RHS of the Eq. (2.1.14) using the definition of the Reynolds stress tensor ($\overline{\rho\mathbf{V}\mathbf{V}} = \overline{p_t}\mathbf{I} - \overline{\beta_t}$) and we obtain :

$$-\overline{[\nabla\cdot(P_g+P_R)]\cdot\mathbf{V}} + [\nabla\cdot(\overline{\rho\mathbf{V}\mathbf{V}})]\cdot\mathbf{u}.$$

By combining the two sides of the equation we easily get :

$$\frac{1}{2}\frac{\partial(\overline{\rho\mathbf{V}^2})}{\partial t} + \frac{1}{2}\nabla\cdot(\overline{\rho\mathbf{V}^2}\mathbf{u} + \overline{\rho\mathbf{V}^2\mathbf{V}}) = -\overline{[\nabla\cdot(P_g+P_R)]\cdot\mathbf{V}} + \underbrace{[\nabla\cdot(\overline{\rho\mathbf{V}\mathbf{V}})]\cdot\mathbf{u} - \nabla\cdot(\overline{\rho\mathbf{V}\mathbf{V}}\mathbf{u})}_{\mathbf{A}}. \qquad (2.1.18)$$

Some terms in this equation deserve to be further developed. The term $\mathbf{A}$ can be rewritten as $-\overline{\rho\mathbf{V}\mathbf{V}}\otimes\nabla\mathbf{u}$. Indeed, we have using the summation convention on the repeated indices :

$$\partial_i(\overline{\rho V_i V_j})u_i - \partial_i(\overline{\rho V_i V_j}u_i) = -\overline{\rho V_i V_j}\,\partial_i u_i. \qquad (2.1.19)$$

The first term on the RHS of Eq. (2.1.18) can be decomposed as follows :

$$\begin{aligned} \overline{[\nabla\cdot(P_g+P_R)]\cdot\mathbf{V}} &= \overline{[\nabla\cdot(p_g\mathbf{I}-\beta_g+p_R\mathbf{I}-\beta_R)]\cdot\mathbf{V}} \\ &= \overline{\nabla(p_g+p_R)\mathbf{V}} - \overline{[\nabla\cdot(\beta_g+\beta_R)]\cdot\mathbf{V}} \\ &= \overline{\nabla(p_g+p_R)\cdot\mathbf{V}} - \nabla\cdot\overline{[(\beta_g+\beta_R)\cdot\mathbf{V}]} + \overline{(\beta_g+\beta_R)\otimes\nabla\mathbf{V}} \end{aligned}$$

where we used a relation similar to Eq. (2.1.19) for the last step. Finally, we can show using the equation of continuity that

$$\frac{1}{2}\overline{\rho}\frac{d}{dt}\left(\frac{\overline{\rho\mathbf{V}^2}}{\overline{\rho}}\right) = \frac{\frac{1}{2}\overline{\rho}^2\frac{d\left(\overline{\rho\mathbf{V}^2}\right)}{dt} - \frac{1}{2}\overline{\rho}\overline{\rho\mathbf{V}^2}\frac{d\overline{\rho}}{dt}}{\overline{\rho}^2}$$
$$= \frac{1}{2}\frac{\partial(\overline{\rho\mathbf{V}^2})}{\partial t} + \frac{1}{2}\mathbf{u}\cdot\nabla(\overline{\rho\mathbf{V}^2}) - \frac{1}{2}\frac{d\ln\overline{\rho}}{dt}\overline{\rho\mathbf{V}^2}$$
$$= \frac{1}{2}\frac{\partial(\overline{\rho\mathbf{V}^2})}{\partial t} + \frac{1}{2}\nabla\cdot(\mathbf{u}\overline{\rho\mathbf{V}^2}). \tag{2.1.20}$$

Inserting Eq. (2.1.20) in Eq. (2.1.18) we finally obtain the equation of turbulent kinetic energy conservation :

$$\overline{\rho}\frac{d}{dt}\left(\frac{1}{2}\frac{\overline{\rho\mathbf{V}^2}}{\overline{\rho}}\right) = -\overline{(\beta_g+\beta_R)\otimes\nabla\mathbf{V}} - \overline{\mathbf{V}\cdot\nabla(p_g+p_R)} - \overline{\rho\mathbf{V}\mathbf{V}}\otimes\nabla\mathbf{u}$$
$$-\frac{1}{2}\nabla\cdot(\overline{\rho\mathbf{V}^2\mathbf{V}}) + \nabla\cdot\overline{[(\beta_g+\beta_R)\cdot\mathbf{V}]}.$$

Several remarks merit to be made concerning this equation, one can indeed note that :

- the second term on the RHS, $\overline{\mathbf{V}\cdot\nabla(p_g+p_R)}$, represents the pressure work ;
- the third term in the RHS can be decomposed following the definition of the Reynolds stress tensor as $\overline{\rho\mathbf{V}\mathbf{V}}\otimes\nabla\mathbf{u} = (\overline{p_t}\mathbf{I} - \overline{\beta_t})\otimes\nabla\mathbf{u} = \overline{p_t}\nabla\cdot\mathbf{u} - \overline{\beta_t}\otimes\nabla\mathbf{u}$ where the last term represents the rate of transformation of the kinetic energy of the mean flow into turbulent kinetic energy ;
- the fourth term represents the flux (or the divergence) of turbulent kinetic energy and is often negligible in the MLT ;
- the last term can be neglected [Ledoux and Walraven, 1958]

If we write $(\beta_g+\beta_R)\otimes\nabla\mathbf{V} = \rho\epsilon_2$ and using the simplifications from above we obtain :

$$\overline{\rho}\frac{d}{dt}\left(\frac{1}{2}\frac{\overline{\rho\mathbf{V}^2}}{\overline{\rho}}\right) = -\overline{\rho\epsilon_2} - \overline{\mathbf{V}\cdot\nabla(p_g+p_R)} - \overline{\rho\mathbf{V}\mathbf{V}}\otimes\nabla\mathbf{u}. \tag{2.1.21}$$

In a model at equilibrium, we can easily see that the previous equation reduces to :

$$\overline{\mathbf{V}\cdot\nabla(p_g+p_R) + \rho\epsilon_2} = 0.$$

We will see that the left hand side of this equation is also appearing in further developments of the total energy conservation equation. In fact, it can be considered as the rate of dissipation of turbulent kinetic energy into heat. This quantity has a direct impact on the excitation or damping rate of modes as it appears in the integral of work (see Section 2.6.5).

2.1.5 Equation of energy conservation

The equation of energy conservation can be written as :

$$\frac{\partial(\rho U)}{\partial t} + \nabla\cdot(\rho U\mathbf{v}) + (P_g+P_R)\otimes\nabla\mathbf{v} = \rho\epsilon - \nabla\cdot\mathbf{F}_R \tag{2.1.22}$$

where U is the internal energy, ϵ is the rate of energy generation by nuclear reactions and $\mathbf{F}_R$ is the radiative flux.

We then take the average of Eq. (2.1.22) and this gives :

$$\underbrace{\frac{\partial(\overline{\rho U})}{\partial t}}_{\textbf{(I)}} + \underbrace{\nabla \cdot (\overline{\rho U \mathbf{v}})}_{\textbf{(II)}} + \underbrace{\overline{(P_g + P_R) \otimes \nabla \mathbf{v}}}_{\textbf{(III)}} = \overline{\rho\epsilon} - \nabla \cdot \overline{\mathbf{F}}_R. \tag{2.1.23}$$

For each term, we will decompose the velocity into its two parts and do some algebra. The first term **(I)** becomes :

$$\frac{\partial(\overline{\rho U})}{\partial t} = \overline{\rho}\frac{\partial \overline{U}}{\partial t} + \overline{U}\frac{\partial \overline{\rho}}{\partial t} + \frac{\partial \overline{\Delta\rho\Delta U}}{\partial t}$$

where the third term in this relation is small enough to be neglected.

Term **(II)** of Eq. (2.1.23) can be written as follows :

$$\begin{aligned}
\nabla \cdot (\overline{U\rho\mathbf{v}}) &= \nabla \cdot (\overline{U\rho\mathbf{u}}) + \nabla \cdot (\overline{U\rho\mathbf{V}}) \\
&= \overline{\rho}\mathbf{u} \cdot \nabla\overline{U} + \overline{U}\nabla \cdot \overline{\rho}\mathbf{u} + \nabla \cdot (\overline{U\rho\mathbf{V}}) \\
&= \overline{\rho}\mathbf{u} \cdot \nabla\overline{U} - \overline{U}\frac{\partial\overline{\rho}}{\partial t} + \nabla \cdot (\overline{U\rho\mathbf{V}})
\end{aligned}$$

where we use the equation of continuity for the last step.

The third term **(III)** of Eq. (2.1.23) can be expressed as :

$$\begin{aligned}
\overline{(P_g + P_R) \otimes \nabla\mathbf{v}} &= \overline{p_{th}\nabla \cdot \mathbf{v}} - \overline{\beta \otimes \nabla\mathbf{v}} \\
&= \overline{p_{th}}\nabla \cdot \mathbf{u} + \overline{p_{th}\nabla \cdot \mathbf{V}} - \overline{\beta} \otimes \nabla\mathbf{u} - \overline{\beta \otimes \nabla\mathbf{V}}
\end{aligned}$$

where $p_{th} = p_g + p_R$ and $\beta = \beta_g + \beta_R$.

By combining the different terms and using the definition of $\rho\epsilon_2$ introduced above we obtain:

$$\overline{\rho}\frac{d\overline{U}}{dt} + \overline{(p_g + p_R)}\nabla \cdot \mathbf{u} = \overline{\rho\epsilon} + \overline{\rho\epsilon_2} - \nabla \cdot \overline{\mathbf{F}}_R - \nabla \cdot (\overline{U\rho\mathbf{V}}) - \overline{p_{th}\nabla \cdot \mathbf{V}} + \overline{(\beta_g + \beta_R)} \otimes \nabla\mathbf{u}. \tag{2.1.24}$$

In this equation we can neglect the last term on the RHS because the viscosity in the mean flow is again assumed to be negligible. Therefore Eq. (2.1.24) can be rewritten as follows :

$$\overline{\rho}\frac{d\overline{U}}{dt} + \overline{(p_g + p_R)}\nabla \cdot \mathbf{u} = -\nabla \cdot (\overline{\mathbf{F}}_R + \overline{\mathbf{F}}_c) + \overline{\rho\epsilon} + \overline{\rho\epsilon_2} + \overline{\mathbf{V} \cdot \nabla(p_g + p_R)} \tag{2.1.25}$$

where $\overline{\mathbf{F}}_c = \overline{(p_g + p_R + \rho U)\mathbf{V}} = \overline{\rho\Delta H\mathbf{V}}$ is the total flux of energy transported by convection (also called the convective flux) and H is the enthalpy. However, one can also express the convective flux in a different way using the fact that the variation of the enthalpy writes :

$$\begin{aligned}
\Delta H &= T\Delta s + \frac{\Delta p_{th}}{\rho} \\
&\simeq c_p\Delta T.
\end{aligned}$$

And so the convective flux can be written as :

$$\begin{aligned}
\mathbf{F}_c &\simeq \overline{c_p\rho\Delta T\mathbf{V}} \\
&\simeq c_p\overline{\rho T}\overline{\frac{\Delta T}{\overline{T}}\mathbf{V}} \\
&\simeq \overline{\rho T\Delta s\mathbf{V}}.
\end{aligned} \tag{2.1.26}$$

where we use for the last step a thermodynamic relation $\Delta s\overline{T} = c_p \Delta T$.

It can also be interesting to consider the mean equation of energy conservation using the entropy s instead of the internal energy U. One uses the first principle of thermodynamics which tells us that :

$$Tds = dU - \frac{p_g + p_R}{\rho^2} d\rho.$$

The previous equation can be written in another way by taking its average and using the mean continuity equation (Eq. (2.1.6)) :

$$\overline{\rho}\frac{d\overline{U}}{dt} = \overline{\rho}\overline{T}\frac{d\overline{s}}{dt} - \frac{\overline{p_g + p_R}}{\overline{\rho}}\overline{\rho}\nabla\cdot\mathbf{u}.$$

Injecting this result in Eq. (2.1.25), we can now write the final form of the mean equation of energy conservation which now depends on the entropy and not on the internal energy any more as :

$$\overline{\rho}\overline{T}\frac{d\overline{s}}{dt} = -\nabla\cdot(\overline{\mathbf{F}}_R + \overline{\mathbf{F}}_c) + \overline{\rho\epsilon} + \overline{\rho\epsilon_2} + \overline{\mathbf{V}\cdot\nabla(p_g + p_R)}. \tag{2.1.27}$$

One can note as already mentioned in the previous section that the term $\overline{\rho\epsilon_2 + \mathbf{V}\cdot\nabla(p_g + p_R)}$ appears in Eq. (2.1.27) as well as in the equation of turbulent kinetic energy conservation (Eq. (2.1.21)).

2.2 Equations for convection

In order to find the equations for convection, one has to take the difference between the classical hydrodynamic equations (Eqs. (2.1.5), (2.1.8), (2.1.22)) and the mean equations computed in the previous Section 2.1.

2.2.1 Equation of mass conservation

As mentioned above, we subtract in this case Eq. (2.1.6) from Eq. (2.1.5). Let us recall that any variable y (such as ρ) or the velocity $\mathbf{v}$ can be split into two components. We then obtain after some algebra :

$$\overline{\rho}\frac{d}{dt}\left(\frac{\Delta\rho}{\overline{\rho}}\right) + \nabla\cdot(\rho\mathbf{V}) = 0. \tag{2.2.1}$$

2.2.2 Equation of energy conservation

We now want to compute the equation of energy conservation for the convection. In order to do that, one takes the difference between Eq. (2.1.22) and its mean counterpart given by :

$$\frac{\partial\overline{\rho}\overline{U}}{\partial t} + \nabla\cdot(\overline{\rho U\mathbf{v}}) + \overline{(P_g + P_R)\otimes\nabla\mathbf{v}} = \overline{\rho\epsilon} - \nabla\cdot\overline{\mathbf{F}}_R. \tag{2.2.2}$$

We then split $\mathbf{v} = \mathbf{u} + \mathbf{V}$ in all terms. We also take into account the definition of $\rho\epsilon_2 = (\beta_g + \beta_R)\otimes\nabla\mathbf{V}$. One notes that the term $\Delta(\beta_g + \beta_R)\otimes\nabla\mathbf{u}$ can be once more neglected. Indeed, as already explained previously, we assume that the viscosity of the mean fluid (thus when we encounter the mean velocity $\mathbf{u}$) is not large enough to be kept in our developments. The difference between Eq. (2.1.22) and Eq. (2.2.2) gives :

$$\begin{aligned}
&\frac{\partial}{\partial t}(\rho U - \overline{\rho}\overline{U}) + \nabla\cdot[(\rho U - \overline{\rho U})\mathbf{u}] + \nabla\cdot(\rho U\mathbf{V} - \overline{\rho U\mathbf{V}}) \\
&+ p_{th}\nabla\cdot\mathbf{V} - \overline{p_{th}\nabla\cdot\mathbf{V}} + (\Delta p_g + \Delta p_R)\nabla\cdot\mathbf{u} \\
=&\rho\epsilon - \overline{\rho\epsilon} + \rho\epsilon_2 - \overline{\rho\epsilon_2} - \nabla\cdot\Delta\mathbf{F}_R.
\end{aligned}$$

The previous expression can also be written as :

$$\begin{aligned}
&\overline{\rho}\frac{d}{dt}\left(\frac{\rho U}{\overline{\rho}}-\overline{U}\right)+\nabla\cdot(\rho U\mathbf{V}-\overline{\rho U\mathbf{V}})\\
&+p_{th}\nabla\cdot\mathbf{V}-\overline{p_{th}\nabla\cdot\mathbf{V}}+(\mathit{\Delta} p_g+\mathit{\Delta} p_R)\nabla\cdot\mathbf{u}\\
=&\rho\epsilon-\overline{\rho\epsilon}+\rho\epsilon_2-\overline{\rho\epsilon_2}-\nabla\cdot\mathit{\Delta}\mathbf{F}_R.
\end{aligned}\tag{2.2.3}$$

Indeed, we can show that :

$$\begin{aligned}
\overline{\rho}\frac{d}{dt}\left(\frac{\rho U}{\overline{\rho}}-\overline{U}\right)&=\overline{\rho}\frac{d}{dt}\left(\frac{\rho U}{\overline{\rho}}\right)-\overline{\rho}\frac{d\overline{U}}{dt}\\
&=\rho\frac{dU}{dt}+U\overline{\rho}\frac{d}{dt}\left(\frac{\rho}{\overline{\rho}}\right)-\overline{\rho}\frac{d\overline{U}}{dt}\\
&=\rho\frac{dU}{dt}-U\nabla\cdot(\rho\mathbf{V})-\overline{\rho}\frac{d\overline{U}}{dt}\\
&=\frac{\partial}{\partial t}(\rho U-\overline{\rho}\overline{U})+\nabla\cdot[(\rho U-\overline{\rho U})\mathbf{u}].
\end{aligned}\tag{2.2.4}$$

To obtain this expression, we used Eq. (2.2.1) to show that $\frac{d}{dt}(\frac{\rho}{\overline{\rho}})=\frac{d}{dt}\left(\frac{\mathit{\Delta}\rho}{\overline{\rho}}\right)=-\frac{\nabla\cdot(\rho\mathbf{V})}{\overline{\rho}}$. We also used the Boussinesq approximation which states that the density fluctuations can be neglected except where they are coupled with terms related to the gravitational acceleration in the buoyancy force. In practice, we can neglect $\mathit{\Delta}\rho$ in the continuity equation as it is not linked to the buoyancy (see Eq. (2.2.1)) and we get that $\nabla\cdot(\rho\mathbf{V})=0$ or similarly $\nabla\cdot\mathbf{V}=0$.

Instead of the internal energy U, we can express this time the different equations in terms of the enthalpy H where $H=U+\frac{p_{th}}{\rho}$. We inject this in the Eq. (2.2.3) and we find after some algebra :

$$\begin{aligned}
&\overline{\rho}\frac{d}{dt}\left(\frac{\rho U}{\overline{\rho}}-\overline{U}\right)+\nabla\cdot(\rho H\mathbf{V}-\overline{\rho H\mathbf{V}})\\
&-\mathbf{V}\cdot\nabla p_{th}+\overline{\mathbf{V}\cdot\nabla p_{th}}+(\mathit{\Delta} p_g+\mathit{\Delta} p_R)\nabla\cdot\mathbf{u}\\
=&\rho\epsilon-\overline{\rho\epsilon}+\rho\epsilon_2-\overline{\rho\epsilon_2}-\nabla\cdot\mathit{\Delta}\mathbf{F}_R.
\end{aligned}\tag{2.2.5}$$

The first term on the LHS deserves to be developed more completely than in Eq. (2.2.4). One can show, keeping $\nabla\cdot(\rho\mathbf{V})$ this time (avoiding the Boussinesq approximation to be more accurate) and using the first principle of thermodynamics, that :

$$\begin{aligned}
\overline{\rho}\frac{d}{dt}\left(\frac{\rho U}{\overline{\rho}}-\overline{U}\right)&=\rho\frac{dU}{dt}-U\nabla\cdot(\rho\mathbf{V})-\overline{\rho}\frac{d\overline{U}}{dt}\\
&=\rho T\frac{ds}{dt}+\frac{p_{th}}{\rho}\frac{d\rho}{dt}-\overline{\rho T}\frac{d\overline{s}}{dt}-\frac{\overline{p_{th}}}{\overline{\rho}}\frac{d\overline{\rho}}{dt}-U\nabla\cdot(\rho\mathbf{V})\\
&=\rho T\frac{ds}{dt}-\overline{\rho T}\frac{d\overline{s}}{dt}+p_{th}\frac{d\ln\rho}{dt}-\overline{p_{th}}\frac{d\ln\rho}{dt}-U\nabla\cdot(\rho\mathbf{V})-\frac{p_{th}}{\rho}\nabla\cdot(\rho\mathbf{V})
\end{aligned}\tag{2.2.6}$$

where we use for the last step the following relation :

$$\begin{aligned}
\frac{p_{th}}{\rho}\frac{d\rho}{dt}-\frac{\overline{p_{th}}}{\overline{\rho}}\frac{d\overline{\rho}}{dt}-\frac{\overline{p_{th}}}{\rho}\frac{d\rho}{dt}+\frac{\overline{p_{th}}}{\rho}\frac{d\rho}{dt}&=\mathit{\Delta} p_{th}\frac{d\ln\rho}{dt}+\overline{p_{th}}\left(\frac{d\ln\rho}{dt}-\frac{d\ln\overline{\rho}}{dt}\right)\\
&=\mathit{\Delta} p_{th}\frac{d\ln\rho}{dt}+\overline{p_{th}}\frac{d\ln(\frac{\rho}{\overline{\rho}})}{dt}\\
&=\mathit{\Delta} p_{th}\frac{d\ln\rho}{dt}-\frac{p_{th}}{\rho}\nabla\cdot(\rho\mathbf{V}).
\end{aligned}$$

We then use the definition of the enthalpy and the Boussinesq approximation so that the pressure fluctuations can be neglected (e.g. $\Delta p = 0$). Eq. (2.2.6) then becomes :

$$\overline{\rho}\frac{d}{dt}\left(\frac{\rho U}{\overline{\rho}} - \overline{U}\right) = \Delta(\rho T)\frac{d\overline{s}}{dt} + \overline{\rho T}\frac{d\Delta s}{dt} - H\nabla\cdot(\rho\mathbf{V}).$$

This result is then injected in Eq. (2.2.5) and neglecting again the pressure fluctuations we obtain :

$$\Delta(\rho T)\frac{d\overline{s}}{dt} + \overline{\rho T}\frac{d\Delta s}{dt} \underbrace{-H\nabla\cdot(\rho\mathbf{V}) + \nabla\cdot(\rho H\mathbf{V} - \overline{\rho H\mathbf{V}}) - \mathbf{V}\cdot\nabla p_{th} + \overline{\mathbf{V}\cdot\nabla p_{th}}}_{\mathbf{A}}$$
$$= \rho\epsilon - \overline{\rho\epsilon} + \rho\epsilon_2 - \overline{\rho\epsilon_2} - \nabla\cdot\Delta\mathbf{F}_R.$$

The set of terms here above called $\mathbf{A}$ can be simplified as follows :

$$\begin{aligned}\mathbf{A} &= (\rho\nabla H - \nabla p_{th})\cdot\mathbf{V} - \overline{(\rho\nabla H - \nabla p_{th})\cdot\mathbf{V}} \\ &= (\rho T\nabla s)\cdot\mathbf{V} - \overline{(\rho T\nabla s)\cdot\mathbf{V}}\end{aligned}$$

where for the last step we use the fact that

$$Tds = dH - \frac{1}{\rho}dp_{th} \Rightarrow \rho T\nabla s = \rho\nabla H - \nabla p_{th}.$$

After all these developments and simplifications, the energy equation for the turbulence can be expressed as :

$$\Delta(\rho T)\frac{d\overline{s}}{dt} + \overline{\rho T}\frac{d\Delta s}{dt} + (\rho T\nabla s)\cdot\mathbf{V} - \overline{(\rho T\nabla s)\cdot\mathbf{V}} - \rho\epsilon_2 + \overline{\rho\epsilon_2} = \rho\epsilon - \overline{\rho\epsilon} - \nabla\cdot\Delta\mathbf{F}_R. \quad (2.2.7)$$

The expression found for the energy conservation is not easy to solve at all and many terms are not well understood. For this reason, in a similar way as we will do for the equation of momentum for the convection, we are going to linearise and crudely approximate the energy equation. This approximation is of course reducing the validity of our treatment and shadows multiple important phenomena such as the cascade of energy. This huge approximation consists in taking as closure term for the energy equation the following expression :

$$-\overline{\rho}\overline{T}\mathbf{V}\cdot\nabla\overline{s} + \left((\rho T\nabla s)\cdot\mathbf{V} - \overline{(\rho T\nabla s)\cdot\mathbf{V}}\right) - (\rho\epsilon_2 - \overline{\rho\epsilon_2}) = \overline{\rho}\overline{T}\frac{\Delta s}{\tau_c} \quad (2.2.8)$$

Using this assumption in Eq. (2.2.7), the energy equation becomes :

$$\frac{\Delta(\rho T)}{\overline{\rho T}}\frac{d\overline{s}}{dt} + \frac{d\Delta s}{dt} + \mathbf{V}\cdot\nabla\overline{s} = \frac{(\rho\epsilon - \overline{\rho\epsilon} - \nabla\cdot\Delta\mathbf{F}_R)}{\overline{\rho T}} - \frac{\Delta s}{\tau_c}.$$

This expression can be even more simplified by looking more closely at $\rho\epsilon - \overline{\rho\epsilon} - \nabla\cdot\Delta\mathbf{F}_R$. In that respect, we should keep in mind that we are interested only in the convective envelope where there is no nuclear reactions taking place. Since ϵ represents the rate of energy generation of nuclear reactions, in these outer regions located far from the nuclear core, we can consider that $\epsilon = 0$. We only need to evaluate the quantity $\nabla\cdot\Delta\mathbf{F}_R = \nabla\cdot\mathbf{F}_R - \nabla\cdot\overline{\mathbf{F}}_R$. Under some assumptions, we know that the radiative flux can be written as :

$$\mathbf{F}_R = -\frac{4ac}{3}\frac{T^3}{\kappa\rho}\nabla T$$

where κ is the opacity coefficient. Using this expression of the radiative flux we can write[2] :

$$\nabla \cdot \mathbf{F}_R - \nabla \cdot \overline{\mathbf{F}}_R = \frac{4ac}{3} \frac{\overline{T}^3}{\overline{\kappa\rho}} \frac{\Delta T}{\mathcal{L}^2} \tag{2.2.9}$$

where $\mathcal{L}$ is the typical length of the eddies. This quantity is linked to the mixing length l through the relation $\mathcal{L}^2 = (2/9)l^2$. However, this relation between $\mathcal{L}$ and l is only valid in the framework of the ML1 (see Section 2.4.1) In addition, we can define :

$$\omega_R = \frac{1}{\tau_R} = \frac{4ac}{3} \frac{\overline{T}^3}{c_p\overline{\kappa\rho}^2\mathcal{L}^2} \tag{2.2.10}$$

where τ_R is the characteristic time of energy loss through radiation of the turbulent elements. Using $\sigma = ac/4$ (where σ is the Stefan-Boltzmann constant) in this relation we can also write :

$$\tau_R = \frac{3c_p\overline{\kappa\rho}^2\mathcal{L}^2}{16\sigma\overline{T}^3} \tag{2.2.11}$$

Moreover, the equation of state $p = p(\rho, T)$ which describes the system is written as :

$$\frac{\Delta T}{\overline{T}} = Q_p \frac{\Delta\rho}{\overline{\rho}} \tag{2.2.12}$$

where we neglect the pressure fluctuations because of the Boussinesq approximation. Using the first principle of thermodynamics, we also know that $c_p\Delta T = \overline{T}\Delta s$ and so we finally have :

$$\nabla \cdot \Delta\mathbf{F}_R = -\omega_R \Delta s \overline{\rho T}. \tag{2.2.13}$$

At the end, after having linearised different terms we can write the energy equation for the turbulence as :

$$\frac{\Delta(\rho T)}{\overline{\rho T}} \frac{d\overline{s}}{dt} + \frac{d\Delta\rho}{dt} + \mathbf{V} \cdot \nabla\overline{s} = -\frac{\omega_R\,\tau_c + 1}{\tau_c}\Delta s. \tag{2.2.14}$$

This result can however be improved compared to what was done by [Grigahcène et al., 2005] in his work. Indeed, as it was suggested in [Dupret et al., 2006], a free parameter Ω can be introduced in the closure term of energy conservation. This parameter has an important physical meaning which will be explained in a following section (see Section 3.2). For now, let's just assume that this parameter varies with depth. To take it into account in our treatment, we multiply the RHS of Eq. (2.2.8) and Eq. (2.2.13) by $1/\Omega$. This yields the two new following equations for the closure terms :

$$\begin{aligned} &\frac{1}{\Omega}\nabla \cdot \Delta\mathbf{F}_R = -\omega_R \Delta s \overline{\rho T}, \\ &\frac{1}{\Omega}\overline{\rho}\overline{T}\frac{\Delta s}{\tau_c} = -\overline{\rho}\overline{T}\mathbf{V} \cdot \nabla\overline{s} + \Big((\rho T \nabla s) \cdot \mathbf{V} - \overline{(\rho T \nabla s) \cdot \mathbf{V}}\Big) - (\rho\epsilon_2 - \overline{\rho\epsilon_2}). \end{aligned} \tag{2.2.15}$$

With these new considerations, the energy equation for the turbulence (Eq. (2.2.14)) can now be written as :

$$\frac{\Delta(\rho T)}{\overline{\rho T}} \frac{d\overline{s}}{dt} + \frac{d\Delta s}{dt} + \mathbf{V} \cdot \nabla\overline{s} = -\frac{\omega_R\tau_c + 1}{\Omega\,\tau_c}\Delta s. \tag{2.2.16}$$

In what follows, this version of the treatment of the convection will be preferentially applied as it gives a more accurate vision of the convection.

[2]We make here a dimensional analysis.

2.2.3 Equation of momentum conservation

The difference between Eq. (2.1.8) and Eq. (2.1.9) gives after splitting all the variables in their two parts :

$$\frac{\partial \rho \mathbf{V}}{\partial t} + \frac{\partial \Delta\rho \mathbf{u}}{\partial t} + \nabla\cdot(\Delta\rho\mathbf{u}\mathbf{u}) + \nabla\cdot(\rho\mathbf{u}\mathbf{V} + \rho\mathbf{V}\mathbf{u}) = -\Delta\rho\nabla\varphi - \nabla\cdot[\Delta(P_g + P_R) + (\rho\mathbf{V}\mathbf{V} - \overline{\rho\mathbf{V}\mathbf{V}})]. \tag{2.2.17}$$

One can see that :

$$\begin{aligned}\overline{\rho}\frac{d}{dt}\left(\frac{\rho\mathbf{V}}{\overline{\rho}}\right) &= \frac{d(\rho\mathbf{V})}{dt} - \rho\mathbf{V}\frac{1}{\overline{\rho}}\frac{d\overline{\rho}}{dt} \\ &= \frac{\partial(\rho\mathbf{V})}{\partial t} + \mathbf{u}\cdot\nabla(\rho\mathbf{V}) + \rho\mathbf{V}\nabla\cdot\mathbf{u} \\ &= \frac{\partial(\rho\mathbf{V})}{\partial t} + \nabla\cdot(\mathbf{u}\rho\mathbf{V})\end{aligned}$$

where we used the continuity equation. This result is then injected in Eq. (2.2.17) and after some algebra we obtain :

$$\begin{aligned}\overline{\rho}\frac{d}{dt}\left(\frac{\rho\mathbf{V}}{\overline{\rho}}\right) =& -\Delta\rho\nabla\varphi - \nabla\cdot(P_g + P_R + \rho\mathbf{V}\mathbf{V}) + \nabla\cdot(\overline{P_g + P_R + \rho\mathbf{V}\mathbf{V}}) \\ & - \frac{\partial\Delta\rho\mathbf{u}}{\partial t} - \nabla\cdot(\Delta\rho\mathbf{u}\mathbf{u}) - \nabla\cdot(\rho\mathbf{V}\mathbf{u}).\end{aligned}$$

One can then develop the last three terms on the RHS in order to obtain an easier expression of the equation of momentum. One gets using Eq. (2.1.12) :

$$\begin{aligned}\overline{\rho}\frac{d}{dt}\left(\frac{\rho\mathbf{V}}{\overline{\rho}}\right) =& -\rho\mathbf{V}\cdot\nabla\mathbf{u} + \frac{\Delta\rho}{\overline{\rho}}\nabla\overline{p} - \nabla\Delta p \\ & - \frac{\Delta\rho}{\overline{\rho}}\nabla\cdot(\overline{\beta_g} + \overline{\beta_R} + \overline{\beta_t}) + \nabla\cdot(\Delta\beta_g + \Delta\beta_R + \Delta\beta_t).\end{aligned} \tag{2.2.18}$$

In order to simplify the problem we will once more make some assumptions. As we want to linearise the equation of momentum for convection written here above, we will simply assume ([Unno, 1967]) that :

$$\frac{\Delta\rho}{\overline{\rho}}\nabla\cdot(\overline{\beta_g} + \overline{\beta_R} + \overline{\beta_t}) - \nabla\cdot(\Delta\beta_g + \Delta\beta_R + \Delta\beta_t) = \Lambda\frac{\overline{\rho}\mathbf{V}}{\tau_c} \tag{2.2.19}$$

where Λ is a dimensionless parameter and τ_c is the typical lifetime of a convective element. By reducing these two complicated terms (composed themselves of different terms) into one simple term we indirectly neglect important properties of the convection such as the cascade of the energy coming from transfer of energy at different scales. Finally, if we neglect $\Delta\rho$ in the expression of $\frac{d}{dt}(\frac{\rho\mathbf{V}}{\overline{\rho}})$, the equation of momentum conservation for the convection can be written:

$$\overline{\rho}\frac{d\mathbf{V}}{dt} = \frac{\Delta\rho}{\overline{\rho}}\nabla\overline{p} - \nabla\Delta p - \rho\mathbf{V}\cdot\nabla\mathbf{u} - \Lambda\frac{\overline{\rho}\mathbf{V}}{\tau_c}. \tag{2.2.20}$$

In this equation, we see that the first term on the RHS corresponds to the buoyancy force accelerating the convective element. It is the main driver of convection. The last term on the RHS is on the contrary acting as a brake of the element due to its interaction with the surrounding medium. One can see that this term is proportional to the velocity just as in viscous braking. The typical lifetime of a convective element τ_c appears at the denominator giving to this term the units of an acceleration (per unit volume) which is coherent with its given meaning.

In the same way as it was done for the equation of energy conservation, we will again introduce in our equations the parameter Ω. This parameter will give us a greater possibility in a following section (VOIR 3D) to fit 3D simulations and thus to improve the description of the convection. In this case, we multiply the RHS of the closure term Eq. (2.2.19) by Ω and so the equation of momentum conservation for the convection (Eq. (2.2.20)) becomes :

$$\overline{\rho}\frac{d\mathbf{V}}{dt} = \frac{\Delta\rho}{\overline{\rho}}\nabla\overline{p} - \nabla\Delta p - \rho\mathbf{V}\cdot\nabla\mathbf{u} - \Omega\Lambda\frac{\overline{\rho}\mathbf{V}}{\tau_c}. \tag{2.2.21}$$

Again, in what follows we will adopt this version of the equation of momentum conservation rather than Eq. (2.2.20) to be as consistent as possible with our goal of representing convection more accurately.

2.3 Mixing Length Theory (MLT)

Describing convection in stars rapidly becomes challenging and approximations are abundantly needed in order to be able to find a proper description of this phenomenon. Surprisingly, it is sometimes possible to model convection with a rather simple theory : the mixing length theory. The core idea is to describe the wide variety of motions caused by convection using a quantity called the mixing length representing the movement of imaginary convective cells. This theory is highly phenomenological and is often neglecting the complexity of turbulent movements in stars (this is the reason why we will try to improve it, based on ideas introduced by [Grigahcène et al., 2005] and based on 3D hydrodynamical models). This model is mainly used for its simplicity to implement but its accuracy remains nonetheless doubtful.

Usually, the mixing length is denoted l and is parametrized as follows :

$$\begin{aligned} l &= \alpha H_p \\ &= -\alpha\left(\frac{d\ln p}{dr}\right)^{-1} \end{aligned}$$

with α being the mixing length parameter and H_p the pressure scale-height[3]. During the movement over the mixing length of a convective cell, energy can be lost through radiative processes for example. The mixing length theory takes into account this loss thanks to the dimensionless quantity γ called the convective efficiency and defined as :

$$\gamma = \frac{\nabla - \nabla'}{\nabla' - \nabla_{ad}} = \frac{\tau_R}{\tau_c} \tag{2.3.1}$$

where $\nabla = \frac{d\ln T}{d\ln p}$ is the temperature gradient, $\nabla_{ad} = \left.\frac{d\ln T}{d\ln p}\right|_s$ is the adiabatic gradient, ∇' is the gradient seen through the convective element and τ_c, τ_R are the same as the ones defined in the previous section. The convective efficiency can be computed solving the following equation in the specific case of the mixing length theory :

$$\frac{9}{4}\gamma^3 + \gamma^2 + \gamma = \mathcal{A}(\nabla_{rad} - \nabla_{ad}) \tag{2.3.2}$$

[3]In the following Section 2.4 we will make use of the scale height again. We thus recall here its expression which is given by :

$$H_p = -\frac{dr}{d\ln p} = -p\left(\frac{dp}{dr}\right)^{-1}$$

The pressure scale height represents the distance over which the pressure decreases by a factor e

in which $\mathcal{A}$ is hiding different physical quantities :

$$\mathcal{A} = -\frac{\partial \ln \rho}{\partial \ln T}\frac{p}{2\rho}\left[\frac{\kappa c_p \rho^3 g l^2}{12acT^3 P}\right]^2 .$$

After solving this equation, the different gradients can then be deduced leading to the classical solutions of the MLT :

$$\begin{aligned} \gamma(\gamma+1) &= \mathcal{A}(\nabla - \nabla_{ad}), \\ F_c &= \frac{1}{4}\alpha^2 c_p \rho T \left(\frac{P_T p}{2P_\rho \rho}\right)^{1/2} \left(\frac{\gamma}{\gamma+1}(\nabla - \nabla_{ad})\right)^{3/2}, \\ p_t &= \frac{\alpha^2}{8}\frac{P_T p}{2P_\rho}\frac{\gamma}{\gamma+1}(\nabla - \nabla_{ad}) \end{aligned} \tag{2.3.3}$$

with F_c being the convective flux and p_t the turbulent pressure. In these expressions, $P_T = \frac{\partial \ln p}{\partial \ln T}\Big|_\rho$ and $P_\rho = \frac{\partial \ln p}{\partial \ln \rho}\Big|_T$.

2.4 Stationary solutions of the equations for convection

We have in Section 2.2 computed the different equations for convection. This set of equations has no analytical solution and this is the reason why the MLT is most of the time used as mentioned in the previous section. However, the MLT is not representing the reality correctly, it provides in many instances a local and time-independent treatment of the convection which is not enough if we want to have an accurate description of the convection in pulsating stars.

Nevertheless, this rather simple theory provides equations that are much easier to solve and we are going to show in this section that our set of equations obtained previously gives back the MLT in the stationary case (i.e. at equilibrium) with a cubic equation as in Section 2.3.

To avoid misunderstandings, we recall here what is our meaning of an equilibrium state (or stationary state); at equilibrium we assume that there is no mean motion of the medium meaning that $\mathbf{u} = 0$. Furthermore, the mean structure of the star is assumed to be independent of time implying that material time derivatives of the different star properties are all equal to zero. Finally we assume that the convection is stationary.

In this case, the equations for convection (Eqs. (2.2.1), (2.2.21), (2.2.16) and (2.2.12)) obtained in the previous Section 2.2 and therein are simplified. For example, the continuity equation becomes :

$$\nabla \cdot (\rho \mathbf{V}) = 0.$$

The equation of momentum conservation is :

$$\frac{\Delta\rho}{\overline{\rho}} - \nabla \Delta p - \Omega \Lambda \frac{\overline{\rho}\mathbf{V}}{\tau_c} = 0 \tag{2.4.1}$$

and the equation of energy conservation writes :

$$\mathbf{V} \cdot \nabla \overline{s} = -\frac{\tau_c/\tau_R + 1}{\Omega \tau_c}\Delta s. \tag{2.4.2}$$

Using the convective efficiency γ, the equation of energy conservation is also given by :

$$\mathbf{V} \cdot \nabla \overline{s} = -\frac{\gamma+1}{\gamma}\frac{1}{\tau_c}\Delta s. \tag{2.4.3}$$

The equation of state remains the same as before and is again written :

$$\frac{\Delta T}{\overline{T}} = Q_p \frac{\Delta \rho}{\overline{\rho}}.$$

In what follows, several approximations are going to be made in order to get back to the MLT at the end :

(a) Firstly, the Boussinesq approximation is again used which means that $\nabla \cdot \mathbf{V} = 0$. As a consequence, we can assume that the different coefficients of the system are constant or in other words independent of the radial distance r. Indeed, because of the Boussinesq approximation, the relative variations of the convective quantities are small compared to the variations of the variables of the mean model.

(b) Under these approximations, the geometry of the problem can be simplified. Instead of having to consider a spherical geometry, one can assume a plane geometry (with x and y being the horizontal coordinates and r the distance from the centre of the star towards its surface) with plane waves as potential solutions for the equations written above. And so we can write the possible solutions as :

$$\begin{aligned} \mathbf{V} &= \mathbf{V}_a \exp(i\mathbf{k} \cdot \mathbf{r}) \\ \Delta y &= \Delta y_a \exp(i\mathbf{k} \cdot \mathbf{r}) \end{aligned} \tag{2.4.4}$$

where $\mathbf{V}_a$ and Δy_a are constants characterizing the amplitude of the fluctuations and $\mathbf{k}$ is the wave vector.

(c) The quotient of the horizontal component k_h and the vertical component k_r is constant and given by :

$$\frac{k_r^2}{k_h^2} = \frac{1}{A} \tag{2.4.5}$$

where A is an anisotropy parameter and because all horizontal directions are equiprobable we have $k_x = k_h \cos\varphi$ and $k_y = k_h \sin\varphi$ where φ is an uniform probability variable. In conclusion, we have a vectorial wave vector drawing a cone with an axis along the vertical and whose aperture is determined by the parameter A. This gives the following relation :

$$\begin{aligned} k^2 &= k_h^2 + k_r^2 \\ &= \frac{A+1}{A} k_h^2 \\ &= (A+1) k_r^2. \end{aligned} \tag{2.4.6}$$

Equilibrium solutions that satisfy the approximations can be found. Injecting the plane wave solution for the velocity (Eq. (2.4.4)) in the equation deduced from the first approximation (a) ($\nabla \cdot \mathbf{V} = 0$), we obtain for a given $\mathbf{k}$:

$$\mathbf{V}_a \cdot \mathbf{k} = 0. \tag{2.4.7}$$

One can notice that in the case of the plane waves approximation, some differential operations such as the divergence or the gradient are equivalent to more simple algebraic operations. For example, taking the divergence of $\mathbf{V}$ is nothing but multiplying $\mathbf{V}$ by $i\mathbf{k}$, in other words we have $\nabla \cdot \mathbf{V} = i\mathbf{k} \cdot \mathbf{V}$. In the same idea, we have $\nabla(\Delta X) = i\mathbf{k}\Delta X$.

As first step of our calculations, we multiply Eq. (2.4.1) by $\mathbf{k}$ (which is the same as taking the divergence of this equation, as explained above) :

$$\begin{aligned}\frac{\Delta\rho}{\overline{\rho}}\nabla\overline{p}\cdot\mathbf{k}-\nabla\Delta p\cdot\mathbf{k}-\Omega\Lambda\frac{\overline{\rho}\mathbf{V}\cdot\mathbf{k}}{\tau_c}&=0\\ \Leftrightarrow\frac{\Delta\rho}{\overline{\rho}}\nabla\overline{p}\cdot\mathbf{k}-\nabla\Delta p\cdot\mathbf{k}&=0\\ \Leftrightarrow\frac{\Delta\rho}{\overline{\rho}}\frac{d\overline{p}}{dr}k_r-ik^2\Delta p&=0\end{aligned}$$

where we use Eq. (2.4.7) and the fact that the pressure has only a component along the radial direction $\mathbf{e}_r$. Expressing $\Delta\rho$ and Δp in terms of plane waves (Eq. (2.4.4)) we then obtain :

$$\Delta p_a=-i\frac{\Delta\rho_a}{\overline{\rho}}\frac{d\overline{p}}{dr}\frac{k_r}{k^2}.$$

We then use this result to eliminate Δp_a in Eq. (2.4.1). Taking the j^{th} component of Eq. (2.4.1) and using typical solution expressions (Eqs. (2.4.4)) we have :

$$\begin{aligned}\frac{\Omega\Lambda\overline{\rho}}{\tau_c}V_{a,j}\exp(i\mathbf{k}\cdot\mathbf{r})&=\frac{\Delta\rho_a}{\overline{\rho}}\exp(i\mathbf{k}\cdot\mathbf{r})\frac{d\overline{p}}{dr}\delta_{rj}-\nabla_j(\Delta p_a\exp(i\mathbf{k}\cdot\mathbf{r}))\\ \Leftrightarrow\frac{\Omega\Lambda\overline{\rho}}{\tau_c}V_{a,j}&=\frac{\Delta\rho_a}{\overline{\rho}}\frac{d\overline{p}}{dr}\delta_{rj}-k_j\frac{\Delta\rho_a}{\overline{\rho}}\frac{d\overline{p}}{dr}\frac{k_r}{k^2}\\ \Leftrightarrow\frac{\Omega\Lambda\overline{\rho}}{\tau_c}V_{a,j}&=\frac{\Delta\rho_a}{\overline{\rho}}\frac{d\overline{p}}{dr}\left(\delta_{rj}-\frac{k_rk_j}{k^2}\right).\end{aligned}\tag{2.4.8}$$

The convective velocity $\mathbf{V}$ can be expressed in a more general manner for each wave vector $\mathbf{k}$, using the previous relation we obtain :

$$\rho\mathbf{V}_{\mathbf{k}}=\frac{\tau_c}{\Omega\Lambda}\frac{\Delta\rho_a}{\overline{\rho}}\frac{d\overline{p}}{dr}\mathbf{b}\exp(i\mathbf{k}\cdot\mathbf{r}),\tag{2.4.9}$$

where $\mathbf{b}$ is given by :

$$\mathbf{b}=(-\frac{k_rk_x}{k^2},-\frac{k_rk_y}{k^2},\frac{k_h^2}{k^2}).$$

Indeed, if we replace j by x,y and r successively in Eq. (2.4.8) we retrieve Eq. (2.4.9). However, we are not interested in an expression for the turbulent velocity for each wave vector $\mathbf{k}$ but for a more general equation which is given by the superposition of the different modes. This solution can be expressed as :

$$\rho\mathbf{V}=\int\frac{\tau_c}{\Omega\Lambda}\frac{\Delta\rho_a}{\overline{\rho}}\frac{d\overline{p}}{dr}P(\mathbf{k})\mathbf{b}\exp(i\mathbf{k}\cdot\mathbf{r})d\mathbf{k}$$

where $P(\mathbf{k})$ is the distribution function of the wave vector as briefly introduced in the approximation (c). In particular we have :

$$\begin{aligned}V_r&=\frac{\tau_c}{\Omega\Lambda}\frac{1}{\rho}\frac{\Delta\rho_a}{\overline{\rho}}\frac{d\overline{p}}{dr}\frac{k_h^2}{k^2}\\ &=\frac{\tau_c}{\Omega\Lambda}\frac{1}{\rho}\frac{\Delta\rho_a}{\overline{\rho}}\frac{d\overline{p}}{dr}\frac{A}{A+1}\end{aligned}\tag{2.4.10}$$

where we used Eq. (2.4.6) the last equation. We can also look closer at the parameter A defined above and try to understand its meaning. To do that, one can look at the following ratio where we take the average over all wave vectors (using Eqs. (2.4.8) and (2.4.5)) :

$$\frac{\langle(V_{A,x})^2\rangle}{\langle(V_{A,r})^2\rangle}=\frac{\frac{\langle k_r^2k_x^2\rangle}{k^4}}{\frac{\langle k_h^4\rangle}{k^4}}=\frac{\langle k_x^2\rangle\,k_r^2}{k_h^4}=\frac{k_h^2}{2}\frac{k_r^2}{k_h^4}=\frac{1}{2A},\tag{2.4.11}$$

using the fact that

$$\left\langle k_x^2 \right\rangle = \left\langle k_h^2 \cos^2\varphi \right\rangle = \frac{k_h^2}{2\pi} \oint \cos^2\varphi \, d\varphi = \frac{k_h^2}{2}.$$

From Eq. (2.4.11) one can see that A is characterising the anisotropy of the convection. If $A = 1/2$, both the x (horizontal component) and the radial component of the turbulent velocity will have on average the same value while for $A > 1/2$, the horizontal component will be smaller than the vertical one.

From thermodynamics we know that :

$$\frac{dT}{T} = \frac{ds}{c_p} + \nabla_{ad} \frac{dp_{th}}{p_{th}}$$

where ∇_{ad} is the adiabatic gradient and $p_{th} = p_g + p_R$. We can thus write :

$$\begin{aligned} \frac{ds}{dr} &= c_p \left[\frac{dT}{dr} \frac{1}{T} - \nabla_{ad} \frac{dp_{th}}{dr} \frac{1}{p_{th}} \right] \\ &= c_p \frac{d\ln p}{dr} \left[\frac{d\ln T}{d\ln p} - \nabla_{ad} \frac{d\ln p_{th}}{d\ln p} \right] \\ &= c_p \frac{d\ln p}{dr} \left[\nabla - \nabla_{ad} \frac{d\ln p_{th}}{d\ln p} \right]. \end{aligned} \tag{2.4.12}$$

Taking the average of Eq. (2.4.12) we obtain :

$$\frac{d\overline{s}}{dr} = c_p \frac{d\ln \overline{p}}{dr} \left[\overline{\nabla} - \overline{\nabla}_{ad} \frac{d\ln \overline{p_{th}}}{d\ln \overline{p}} \right]. \tag{2.4.13}$$

There is another quantity that is worth mentioning (and that will be used later) at this point which is the velocity of the convective elements but this time expressed directly from the definition of the mixing length l :

$$l = V\,\tau_c \Rightarrow V^2 = \frac{l^2}{\tau_c^2}. \tag{2.4.14}$$

where l is the mixing length which corresponds to the distance travelled by an element before it can no longer be differentiated from its surrounding medium In order to obtain it, we will first determine the expression of $1/\tau_c^2$. For that, we use the definition of the velocity we have already introduced previously (Eq. (2.4.10)) combined with the expression obtained for Δs[4] which gives the following relation :

$$V = k_V \Delta s \tag{2.4.15}$$

where k_V is just a factor introduced to lighter the notation. It is in fact proportional to τ_c and can be written as $k_V = k_{V_0} \tau_c$ where

$$\begin{aligned} k_{V_0} &= \frac{1}{\Omega \Lambda \rho Q_p c_p} \frac{d\overline{p}}{dr} \frac{A}{A+1} \\ &= -\frac{g}{Q_p c_p} \frac{A}{A+1} \frac{1}{\Omega \Lambda}. \end{aligned}$$

[4] This relation was established in Section 2.2.2 and is given by :

$$\Delta s = c_p Q_p \frac{\Delta\rho}{\overline{\rho}}$$

In addition to what was just done, the velocity can also be expressed using this time Eq. (2.4.3) which gives :

$$V(\overline{\nabla} - \overline{\nabla}_{ad}) = k_E \Delta s \tag{2.4.16}$$

where k_E is again a factor introduced to reduce the notation, which is proportional to $\frac{\gamma+1}{\gamma}\frac{1}{\tau_c}$ or in other words $k_E = k_{E_0}\frac{\gamma+1}{\gamma}\frac{1}{\tau_c} = k_{E_0}\left(\frac{1}{\tau_R} + \frac{1}{\tau_c}\right)$ where

$$\begin{aligned} k_{E_0} &= -\frac{1}{\Omega c_p}\frac{dr}{d\ln\overline{p}} \\ &= \frac{H_p}{\Omega c_p}. \end{aligned}$$

We can then eliminate V from Eqs. (2.4.15)(2.4.16) and isolate $1/\tau_c^2$:

$$\begin{aligned} k_E \Delta s &= k_V \Delta s(\overline{\nabla} - \overline{\nabla}_{ad}) \\ \Rightarrow k_{E_0}\frac{\gamma+1}{\gamma}\frac{1}{\tau_c} &= k_{V_0}\tau_c(\overline{\nabla} - \overline{\nabla}_{ad}) \\ \Rightarrow \frac{1}{\tau_c^2} &= \frac{k_{V_o}}{k_{E_0}}\frac{\gamma}{\gamma+1}(\overline{\nabla} - \overline{\nabla}_{ad}). \end{aligned}$$

Using this result to compute $V^2 = l^2/\tau_c^2$ we finally obtain for the expression of the velocity the following equation :

$$V^2 = \frac{l^2}{\tau_c^2} = \frac{k_{V_0}}{k_{E_0}} l^2 \frac{\gamma}{\gamma+1}(\overline{\nabla} - \overline{\nabla}_{ad})$$

or if we replace k_{V_0} and k_{E_0} by their respective value :

$$V^2 = -\frac{g}{Q_p H_p}\frac{A}{A+1}\frac{1}{\Lambda} l^2 \frac{\gamma}{\gamma+1}(\overline{\nabla} - \overline{\nabla}_{ad}) \tag{2.4.17}$$

This equation will be useful in later developments when we will introduce a new set of parameters describing another version of the MLT (see Section 2.4.1).

Our goal now is to rewrite Eq. (2.4.2) using the different relations we have obtained in this section. First of all, we use the dimensionless quantity $\gamma = \frac{\tau_R}{\tau_c}$ defined in the previous section as the convective efficiency. Injecting Eqs. (2.4.13) and (2.4.10) in Eq. (2.4.2) we get :

$$\frac{\tau_c}{\Omega\Lambda}\frac{\Delta\rho_a}{\rho\,\rho_a}\frac{d\overline{p}}{dr}\frac{A}{A+1}c_p\left[\overline{\nabla} - \overline{\nabla}_{ad}\frac{d\ln\overline{p_{th}}}{d\ln\overline{p}}\right]\frac{d\ln\overline{p}}{dr} = -\frac{\tau_c/\tau_R+1}{\Omega\,\tau_c}c_p Q_p\frac{\Delta\rho}{\overline{\rho}}. \tag{2.4.18}$$

In order to simplify the RHS we can show that :

$$\frac{\tau_c/\tau_R+1}{\tau_c^2} = \frac{\tau_c+\tau_R}{\tau_R\,\tau_c^2} = \frac{\tau_R/\gamma+\tau_R}{\tau_R\,\tau_R^2/\gamma^2} = \frac{\gamma(1+\gamma)}{\tau_R^2}.$$

With this result, Eq. (2.4.18) can be written as follows :

$$\begin{aligned} \frac{\gamma(1+\gamma)}{\Omega\,\tau_R^2} &= -\frac{\Delta\rho_a}{\Omega\,\Lambda\,\rho\,\rho_a}\frac{d\overline{p}}{dr}\frac{A}{A+1}\left[\overline{\nabla} - \overline{\nabla}_{ad}\frac{d\ln\overline{p_{th}}}{d\ln\overline{p}}\right]\frac{d\ln\overline{p}}{dr}\frac{\overline{\rho}}{Q_p\Delta\,\rho} \\ \Leftrightarrow \gamma(1+\gamma) &= -\frac{A}{A+1}\left(\frac{d\ln\overline{p}}{dr}\right)^2\frac{\overline{p}\,\tau_R^2}{\Lambda\,\overline{\rho}\,Q_p}\left[\overline{\nabla} - \overline{\nabla}_{ad}\frac{d\ln\overline{p_{th}}}{d\ln\overline{p}}\right]. \end{aligned} \tag{2.4.19}$$

An interesting remark deserves to be addressed here concerning the parameter Ω. Indeed, we see that in the previous equation and in Eq. (2.4.17), this parameter has disappeared. As a result (or rather thanks to our precautious introduction of the parameter into the different closure terms), the meaning of the convective efficiency γ remains the same i.e. it remains solution of the quadratic equation and we can also see that the convective velocities are not affected by Ω.

In order to make the mixing length l appears in the convective flux, we can look at an alternative definition for it compared to the one proposed earlier. First of all, we assume that the total flux is the sum of the radiative flux and the convective flux ($\mathbf{F} = \mathbf{F}_c + \mathbf{F}_R$) where the total flux can be written as :

$$\mathbf{F} = -\frac{4ac}{3}\frac{\overline{T}^4}{\overline{\kappa}\,\overline{\rho}}\nabla(\ln\overline{p})\,\overline{\nabla}_R$$

where $\overline{\nabla}_R$, the radiative gradient, corresponds to the temperature gradient that the star would have if all the energy was transported by radiation. The radiative flux is given by :

$$\mathbf{F}_R = -\frac{4ac}{3}\frac{\overline{T}^4}{\overline{\kappa}\,\overline{\rho}}\nabla(\ln\overline{p})\,\overline{\nabla}.$$

Using the assumption made above we can establish the convective flux by subtracting the radiative flux to the total one which gives :

$$\mathbf{F}_c = -\frac{4ac}{3}\frac{\overline{T}^4}{\overline{\kappa}\,\overline{\rho}}(\overline{\nabla}_R - \overline{\nabla})\nabla(\ln\overline{p}). \tag{2.4.20}$$

In Section 2.1.5, we had found another way to write the convective flux using Eq. (2.1.26) :

$$\mathbf{F}_c = \overline{\rho}\,\overline{T}\,\overline{\Delta s\mathbf{V}}.$$

Replacing $\overline{\Delta s\mathbf{V}}$ by its value obtained after some manipulations[5] of Eq. (2.4.2), the expression of the convective flux can be written differently :

$$\mathbf{F}_c = -\overline{\rho}\,\overline{T}\frac{\Omega\,\tau_c}{\tau_c/\tau_R + 1}\overline{(\mathbf{V}\cdot\nabla\overline{s})\mathbf{V}}.$$

Looking at the vertical component of this flux one can write :

$$F_{c,r} = -\frac{1}{2}\overline{\rho}\,\overline{T}\frac{\Omega\,\tau_c}{\tau_c/\tau_R + 1}\frac{d\overline{s}}{dz}(V_{a,r})^2. \tag{2.4.21}$$

This expression can be slightly modified in anticipation of the future use we will make of the convective flux. In this respect, we use Eq. (2.4.14) to get rid of one $V_{a,r}$, we use the definition of γ and we substitute the vertical gradient of the mean entropy by its value computed before. The new expression of the convective flux is given by :

$$\begin{aligned} F_{c,r} &= -\frac{1}{2}\overline{\rho}\overline{T}\Omega\, l\frac{d\overline{s}}{dz}\frac{\gamma}{\gamma+1}V_{a,r} \\ &= -\frac{1}{2}\frac{\overline{\rho}\overline{T}\Omega\, c_p}{H_p}lV_{a,r}\frac{\gamma}{\gamma+1}(\overline{\nabla} - \overline{\nabla}_{ad}). \end{aligned} \tag{2.4.22}$$

[5] We multiply both sides of Eq. (2.4.2) by $\mathbf{V}$ and then take the average so that we obtain :

$$\overline{\Delta s\mathbf{V}} = -\frac{\Omega\,\tau_c}{\tau_c/\tau_R + 1}\overline{(\mathbf{V}\cdot\nabla\overline{s})\mathbf{V}}.$$

We can then compare Eq. (2.4.20) and Eq. (2.4.21) using Eq. (2.2.10) and Eq. (2.4.13). Finally, we have :

$$\begin{aligned}
\frac{4ac}{3}\frac{\overline{T}^4}{\overline{\kappa}\,\overline{\rho}}(\overline{\nabla}_R-\overline{\nabla})\nabla(\ln\overline{p}) &= \frac{1}{2}\overline{\rho}\overline{T}\frac{\varOmega\,\tau_c}{\tau_c/\tau_R+1}\frac{d\overline{s}}{dz}(V_{a,r})^2\\
\Leftrightarrow \tau_R^{-1}(\overline{\nabla}_R-\overline{\nabla})\frac{d\ln\overline{p}}{dr}\mathcal{L}^2 c_p\overline{\kappa}\overline{\rho} &= \frac{1}{2}\overline{\rho}\frac{\varOmega\,\tau_c}{\tau_c/\tau_R+1}\frac{d\overline{s}}{dz}(V_{a,r})^2\\
\Leftrightarrow \tau_R^{-1}(\overline{\nabla}_R-\overline{\nabla})\mathcal{L}^2 &= \frac{1}{2}\frac{\varOmega\,\tau_c}{\tau_c/\tau_R+1}\left[\overline{\nabla}-\overline{\nabla}_{ad}\frac{d\ln\overline{p}_{th}}{d\ln\overline{p}}\right](V_{a,r})^2\\
\Leftrightarrow 2(\overline{\nabla}_R-\overline{\nabla})\left(\frac{\mathcal{L}}{l}\right)^2 &= \frac{\varOmega\,\tau_R}{\tau_c(\tau_c/\tau_R+1)}\left[\overline{\nabla}-\overline{\nabla}_{ad}\frac{d\ln\overline{p}_{th}}{d\ln\overline{p}}\right]\\
\Leftrightarrow 2(\overline{\nabla}_R-\overline{\nabla})\left(\frac{\mathcal{L}}{l}\right)^2 &= \frac{\varOmega\,\gamma^2}{\gamma+1}\left[\overline{\nabla}-\overline{\nabla}_{ad}\frac{d\ln\overline{p}_{th}}{d\ln\overline{p}}\right] \qquad (2.4.23)
\end{aligned}$$

where we use for the last step the fact that :

$$\frac{\gamma^2}{\gamma+1}=\frac{\tau_R}{\tau_c(\tau_c/\tau_R+1)}.$$

One can then combine Eq. (2.4.23) and Eq. (2.4.19) in order to eliminate the temperature gradient $\overline{\nabla}$ and the new equation can be written as follows :

$$\frac{1}{2}\varOmega\left(\frac{l}{\mathcal{L}}\right)^2\gamma^3+\gamma(\gamma+1)=-\frac{A}{A+1}\left(\frac{d\ln\overline{p}}{dr}\right)^2\frac{\overline{p}\tau_R^2}{\varLambda\overline{\rho}Q_p}\left[\overline{\nabla}_R-\overline{\nabla}_{ad}\frac{d\ln\overline{p}_{th}}{d\ln\overline{p}}\right]. \qquad (2.4.24)$$

In practice, the LHS of this relation is known (knowing the different measurable variables $r, P, T, L, ...$) and the only unknown is γ. Once γ is determined, we inject its value in Eq. (2.4.19) and we can then deduce the value of the mean temperature gradient $\overline{\nabla}$.

2.4.1 ML1 & ML2

When using the appropriate values for the different parameters, the cubic equation (Eq. (2.4.24)) which is based on our treatment of the convection in the stationary case gives back the cubic we had presented in the frame of the classical MLT. These physical parameters are namely $\varOmega$, $\varLambda$, A and $\mathcal{L}^2/l^2$. However, a more generalised set of parameters is often used by other authors using a different version of the MLT than our (see [Tassoul et al., 1990]) consisting of three new numerical parameters a, b and c. Before explaining the reason why different versions of this theory are used and in what they differ from each other, we will deduce the relations that exist between "our" parameters and the new ones. To do that, we can compare the equation we have found for the square of the velocity and the one presented in [Tassoul et al., 1990] (Eq. (36)). In their work, they had established the following relation for the average speed of a convective cell[6] :

$$V^2=-a\frac{l^2g}{Q_pH_p}\frac{\gamma}{\gamma+1}(\overline{\nabla}-\overline{\nabla}_{ad})$$

while previously we had obtained for the same quantity (Eq. (2.4.17)) the expression :

$$V^2=-\frac{A}{A+1}\frac{1}{\varLambda}\frac{l^2g}{Q_pH_p}\frac{\gamma}{\gamma+1}(\overline{\nabla}-\overline{\nabla}_{ad}).$$

[6] With some quantities adapted to match to ours

Comparing these two equations, we can express our parameters as the "new" one a in the resulting way :

$$a = \frac{A}{A+1}\frac{1}{\Lambda}. \tag{2.4.25}$$

In like manner, to see the link between b and our parameter(s), we use the equation of the convective flux as described in their work (Eq. (37)) :

$$F_c = -\frac{b\overline{\rho}Vc_p\overline{T}l}{H_p}\frac{\gamma}{\gamma+1}(\overline{\nabla} - \overline{\nabla}_{ad})$$

and we compare it to the one we have computed formerly (Eq. (2.4.22)) :

$$F_c = -\frac{1}{2}\frac{\Omega\overline{\rho}Vc_p\overline{T}l}{H_p}\frac{\gamma}{\gamma+1}(\overline{\nabla} - \overline{\nabla}_{ad}).$$

From this comparison we directly deduce that $b = \Omega/2$. Finally, for the last parameter c we use this time the definition of the radiative time scale introduced in their article (Eq. (38)) which is given by :

$$\tau_R = \frac{c_p\overline{\rho}^2 l^2 \overline{\kappa}}{c\sigma\overline{T}^3}.$$

In our case, we had defined τ_R in Eq. (2.2.11) as :

$$\tau_R = \frac{3\mathcal{L}^2 c_p\overline{\rho}^2\overline{\kappa}}{16\sigma\overline{T}^3}$$

And so we find that :

$$\frac{16}{3c} = \frac{\mathcal{L}^2}{l^2}. \tag{2.4.26}$$

As mentioned earlier, different versions of the mixing-length theory exist and are commonly used. This is not so surprising knowing the big limitations of this theory and thus the possible adaptations to one specific case or another. For white dwarfs (and subdwarfs) modelling, the first version of the MLT which is often refereed to as the ML1 is the one developed by [Böhm-Vitense, 1958] and that we are using in this work. The second flavour of the MLT is named ML2 and originate from the work of [Bohm and Cassinelli, 1971]. In both versions, the mixing length is defined as $l = H_p$ (i.e $\alpha = 1$) but they differ in the values given to the set of parameters a, b and c and by extension on some physical phenomena as these parameters are related to physical quantities. To retrieve our version of the MLT, we take the following values for the parameters : $a = 1/8$, $b = 1/2$, $c = 24$ and $A = 1/2$ (isotropic turbulence) which gives us back $\Omega = 1$, $\Lambda = 8/3$, $\mathcal{L}^2/l^2 = 2/9$. In the ML2 version, they chose $a = 1$, $b = 2$, $c = 16$ which gives $\Omega = 4$, $\Lambda = A/A+1 = 1/3$ if $A = 1/2$ and $\mathcal{L}^2/l^2 = 1/3$. Physically, the ML2 version estimates a higher convective efficiency than ML1 version thanks to a reduction of the horizontal energy loss rate. There exists also a third version of the MLT, the ML3 for which the convective efficiency is even greater than in ML2. In this theory, the mixing length is equal to $l = 2H_p$.

2.5 Perturbation of the mean structure

This section will be dedicated to the study of the perturbation of the equations describing the mean structure of stars as presented in Section 2.1. In fact, in the present section we are going to establish the equations to be solved to model the stellar oscillations. Again, interesting terms connecting convection and pulsation will appear in the different equations and their knowledge will give us valuable information on how pulsation and convection adapt to each other.

But first, we will recall some key elements of the small perturbation theory which is going to be used abundantly in this section. Most of the time we will make use of the Lagrangian perturbation noted "δ" which represents the difference between the instantaneous value of the quantity studied and its equilibrium value for a given material element such that for a given quantity y we have : $y = y_0 + \delta y$. In other words, we follow the movement in the space of an elementary piece of the star. The other type of perturbation is called the Eulerian perturbation and is often expressed with a " $'$ ". In this case, it represents the difference between the instantaneous value of the quantity and its equilibrium value for a fixed spatial position in the star (i.e. independently of the movement). These two types of perturbation are not independent of each other and there exists a relation linking them. Indeed, for a given quantity y we can show that (neglecting terms of order higher than one):

$$\delta y = y' + \delta \mathbf{r} \cdot \nabla y.$$

In the context of small perturbation theory, the amplitude of the oscillations is considered to be a perturbation of the equilibrium state. Moreover, we assume that this variation is small enough in order to linearise the equations neglecting terms involving products of perturbations. In general, we can express the Lagrangian perturbation of a given quantity y by :

$$\delta y(\mathbf{r}, t) = \delta y(r) \exp(i\sigma t) Y_\ell^m(\theta, \varphi) \tag{2.5.1}$$

where we used the method of separation of variables with the real part of σ noted σ_R representing the angular frequency while the opposite of the imaginary part $(-\sigma_i)$ is representing the growth rate of the mode and Y_ℓ^m being the spherical harmonic (which depends on the angular variables only). At the end, our set of differential equations will be simplified to a eigenvalue problem which is easier to solve.

2.5.1 Perturbed equation of momentum conservation

In a previous section, we have obtained the mean equation of motion, Eq. (2.1.12), given by :

$$\begin{aligned} \overline{\rho}\frac{d\mathbf{u}}{dt} &= -\overline{\rho}\nabla\Phi - \nabla(\overline{p_g} + \overline{p_R} + \overline{p_t}) + \nabla \cdot \overline{\beta_t} \\ &= -\overline{\rho}\nabla\Phi - \nabla\overline{p} + \nabla \cdot \overline{\beta_t} \end{aligned} \tag{2.5.2}$$

where we recall the simplified notation for the pressure $p = p_g + p_R + p_t$. At equilibrium, we have $\frac{d\mathbf{u}}{dt} = 0$ and so the equation of motion becomes :

$$0 = -\overline{\rho}\nabla\Phi_0 - \nabla\overline{p}_0 + \nabla \cdot \overline{\beta_{t0}} \tag{2.5.3}$$

where the quantities at equilibrium are marked with a 0 as subscript. One notes that the mean velocity $\mathbf{u}$ can be written in terms of the partial derivative of the perturbation of the position field $\mathbf{r}$ such that :

$$\mathbf{u} = \frac{d\mathbf{r}}{dt} = \frac{d\mathbf{r}_0 + \delta\mathbf{r}}{dt} = \frac{d\delta\mathbf{r}}{dt} \simeq \frac{\partial\delta\mathbf{r}}{\partial t}$$

where we neglect the term of second order $\mathbf{u} \cdot \nabla\delta\mathbf{r}$ in consistency with our linear approximation theory. In order to obtain the perturbed equation of motion we then subtract Eq. (2.5.3) from Eq. (2.5.2) and using the new definition of $\mathbf{u}$ we obtain :

$$\begin{aligned} \overline{\rho}\frac{\partial^2\delta\mathbf{r}}{\partial t^2} &= -\overline{\rho}\nabla\Phi + \overline{\rho}_0\nabla\Phi_0 - \nabla\overline{p} + \nabla\overline{p}_0 + \nabla \cdot \overline{\beta_t} - \nabla \cdot \overline{\beta_{t0}} \\ &= -\delta(\overline{\rho}\nabla\Phi) - \delta(\nabla\overline{p}) + \delta(\nabla \cdot \overline{\beta_t}). \end{aligned} \tag{2.5.4}$$

In addition, the two first terms in the RHS of this equation can be written in a slightly different way. One can show that for any quantity X there exists the following relation :

$$\delta(\nabla X) = \nabla(\delta X) - \nabla X \cdot \nabla \delta \mathbf{r}. \tag{2.5.5}$$

If we apply this relation to our case we obtain :

$$\begin{aligned}\delta(\overline{\rho}\nabla\Phi) &= \delta\overline{\rho}\nabla\Phi + \overline{\rho}\delta(\nabla\Phi)\\ &= \delta\overline{\rho}\nabla\Phi + \overline{\rho}(\nabla(\delta\Phi) - \nabla\Phi\cdot\nabla\delta\mathbf{r}).\end{aligned}$$

The second term on the RHS of Eq. (2.5.4) can also be written :

$$\delta(\nabla\overline{p}) = \nabla\delta\overline{p} - \nabla\overline{p}\cdot\nabla\delta\mathbf{r}.$$

Gathering all the terms in Eq. (2.5.4) we obtain the following relation :

$$\overline{\rho}\frac{\partial^2\delta\mathbf{r}}{\partial t^2} = -\delta\overline{\rho}\nabla\Phi - \overline{\rho}\nabla\delta\Phi + \overline{\rho}\nabla\Phi\cdot\nabla\delta\mathbf{r} - \nabla\delta\overline{p} + \nabla\overline{p}\cdot\nabla\delta\mathbf{r} + \delta(\nabla\cdot\overline{\beta_t}).$$

We then develop the LHS of this equation using Eq. (2.5.1) and so we can establish the following expression :

$$-\sigma^2\overline{\rho}\delta\mathbf{r} = -\delta\overline{\rho}\nabla\Phi - \overline{\rho}\nabla\delta\Phi - \nabla\delta\overline{p} + \delta(\nabla\cdot\overline{\beta_t}) + (\overline{\rho}\nabla\Phi + \nabla\overline{p})\cdot\nabla\delta\mathbf{r}. \tag{2.5.6}$$

The last term of this equation can be written in a different way using this time Eq. (2.5.2). Indeed, at equilibrium the time derivative of the mean velocity **u** vanishes and so we obtain :

$$(\overline{\rho}\nabla\Phi + \nabla\overline{p})\cdot\nabla\delta\mathbf{r} = (\nabla\cdot\overline{\beta_t})\cdot\nabla\delta\mathbf{r}$$

where we multiplied both sides of the equation by $\nabla\delta\mathbf{r}$. We inject this result in Eq. (2.5.6) which then becomes :

$$-\sigma^2\overline{\rho}\delta\mathbf{r} = -\delta\overline{\rho}\nabla\Phi - \overline{\rho}\nabla\delta\Phi - \nabla\delta\overline{p} + \delta(\nabla\cdot\overline{\beta_t}) + (\nabla\cdot\overline{\beta_t})\cdot\nabla\delta\mathbf{r}. \tag{2.5.7}$$

In what follows, we will again use the separation of variables where we separate in three independent terms the radial coordinate r, the angular coordinates (θ,φ) and the time dependence t. To be able to use this technique, we need to use a specific notation for the perturbation of the turbulent viscosity $\delta(\nabla\cdot\overline{\beta_t})$ noted :

$$\delta(\nabla\cdot\overline{\beta_t}) = \left(-\Xi_R^r(r)Y_l^m(\theta,\varphi), -\Xi_R^h(r)\frac{\partial Y_l^m(\theta,\varphi)}{\partial\theta}, -\frac{\Xi_R^h(r)}{\sin\theta}\frac{\partial Y_l^m(\theta,\varphi)}{\partial\varphi}\right).$$

It can also be shown that the divergence of the Reynolds tensor is given by :

$$\nabla\cdot\overline{\beta_t} = -\frac{2A-1}{A}\frac{\overline{p}_t}{r}\mathbf{e}_r. \tag{2.5.8}$$

One can also be interested in computing the radial and transverse component of Eq. (2.5.7) keeping in mind the notation introduced for the perturbation of the turbulent viscosity. To compute these components, we first recall here the definition of some differential operators in spherical coordinates which are of interest. As such, the gradient of a scalar quantity y is denoted:

$$\nabla y = \frac{\partial y}{\partial r}\mathbf{e}_r + \frac{1}{r}\frac{\partial y}{\partial\theta}\mathbf{e}_\theta + \frac{1}{r\sin\theta}\frac{\partial y}{\partial\varphi}\mathbf{e}_\varphi.$$

The gradient of a vectorial field (turbulent velocity $\mathbf{V}$ for example) in spherical coordinates has a more complicated form. Indeed, we write :

$$\nabla \mathbf{V} = \begin{bmatrix} \frac{\partial V_r}{\partial r} & \frac{1}{r}\frac{\partial V_r}{\partial \theta} - \frac{V_\theta}{r} & \frac{1}{r\sin\theta}\frac{\partial V_r}{\partial \varphi} - \frac{V_\varphi}{r} \\ \frac{\partial V_\theta}{\partial r} & \frac{1}{r}\frac{\partial V_\theta}{\partial \theta} + \frac{V_r}{r} & \frac{1}{r\sin\theta}\frac{\partial V_\theta}{\partial \varphi} - \frac{V_\varphi \cot\theta}{r} \\ \frac{\partial V_\varphi}{\partial r} & \frac{1}{r}\frac{\partial V_\varphi}{\partial \theta} & \frac{1}{r\sin\theta}\frac{\partial V_\varphi}{\partial \varphi} + \frac{V_r}{r} + \frac{V_\theta \cot\theta}{r} \end{bmatrix}.$$

To compute the two components, we first need to look at the last term on the RHS of Eq. (2.5.7) using the definition of the gradient of a vectorial field. The i^{th} component of this term is given by :

$$\begin{aligned} \Big[(\nabla \cdot \overline{\beta_t}) \cdot \nabla \delta \mathbf{r}\Big]_i &= \nabla \cdot \overline{\beta_t}_j \partial_i \xi_j \\ &= -\frac{2A-1}{A}\frac{\overline{p}_t}{r}\partial_i \xi_r . \end{aligned}$$

For the radial component, we take $i = r$ and we obtain the following relation :

$$-\frac{2A-1}{A}\frac{\overline{p}_t}{r}\frac{\partial \xi_r}{\partial r}$$

while for the transverse component we will have to look at the two cases where $i = \theta$ and $i = \varphi$. In the first case we obtain :

$$-\frac{2A-1}{A}\frac{\overline{p}_t}{r}\left(\frac{1}{r}\frac{\partial \xi_r}{\partial \theta} - \frac{\xi_\theta}{r}\right)$$

and in the second case we have :

$$-\frac{2A-1}{A}\frac{\overline{p}_t}{r}\left(\frac{1}{r\sin\theta}\frac{\partial \xi_r}{\partial \varphi} - \frac{\xi_\varphi}{r}\right).$$

One can then use the previous operators and the different definitions introduced above to compute the **radial** component of Eq. (2.5.7) :

$$\sigma^2 \xi_r = \frac{d\delta\Phi}{dr} + \frac{\delta\overline{\rho}}{\overline{\rho}}\frac{d\Phi}{dr} + \frac{1}{\overline{\rho}}\left[\frac{d\delta\overline{p}}{dr} + \Xi^r_R(r) + \left(\frac{2A-1}{A}\frac{\overline{p}_t}{r}\right)\frac{d\xi_r}{dr}\right]. \tag{2.5.9}$$

To find this expression, one also needs to use the separation of variables with adequate notations for the perturbation of the mean pressure, perturbation of the gravitational potential, perturbation of the mean density and of the displacement vector. These perturbed quantities are noted as follows :

$$\begin{aligned} \delta\overline{p} &= \delta\overline{p}(r) Y_\ell^m(\theta,\varphi) \\ \delta\Phi &= \delta\Phi(r) Y_\ell^m(\theta,\varphi) \\ \delta\overline{\rho} &= \delta\overline{\rho}(r) Y_\ell^m(\theta,\varphi). \end{aligned}$$

and

$$\delta\mathbf{r} = \left(\xi_r(r) Y_\ell^m(\theta,\varphi), \xi_h(r)\frac{\partial Y_\ell^m(\theta,\varphi)}{\partial\theta}, \frac{\xi_h(r)}{\sin\theta}\frac{\partial Y_\ell^m(\theta,\varphi)}{\partial\varphi}\right)$$

where ξ_h is the horizontal vector displacement from which we can retrieve ξ_φ and ξ_θ. Indeed, we have the following two relations :

$$\begin{aligned} \xi_\theta(r) &= \xi_h(r)\frac{\partial Y_\ell^m(\theta,\varphi)}{\partial\theta} \\ \xi_\varphi(r) &= \frac{\xi_h(r)}{\sin\theta}\frac{\partial Y_\ell^m(\theta,\varphi)}{\partial\varphi}. \end{aligned}$$

One remarks that the second term on the RHS of Eq. (2.5.9) can be modified and written as $g = \frac{d\Phi}{dr}$ which is nothing else than the gravitational acceleration.

For the **transverse** component, taking into account all definitions presented above we directly obtain the following equation :

$$\sigma^2 \xi_h = \frac{1}{r}\left[\delta\Phi + \frac{\delta\overline{p}}{\overline{\rho}} + \frac{\Xi_R^h(r)r}{\overline{\rho}} + \frac{2A-1}{A}\frac{\overline{p}_t}{r}\left(\frac{\xi_r}{r} - \frac{\xi_h}{r}\right)\right]. \tag{2.5.10}$$

2.5.2 Perturbed equation of mass conservation

In order to obtain the perturbed equation of mass conservation, we start from the mean equation of continuity Eq. (2.1.7) which writes :

$$\frac{d\overline{\rho}}{dt} + \overline{\rho}\nabla\cdot\mathbf{u} = 0. \tag{2.5.11}$$

Substituting $\mathbf{u}$ by its approximate definition in Eq. (2.5.11) we obtain :

$$\begin{aligned}
&\frac{d\overline{\rho}}{dt} + \overline{\rho}\nabla\cdot\left(\frac{\partial\delta\mathbf{r}}{\partial t}\right) = 0 \\
\Leftrightarrow &\frac{d\overline{\rho}}{dt} + \overline{\rho}\frac{\partial}{\partial t}(\nabla\cdot\delta\mathbf{r}) = 0 \\
\Leftrightarrow &\frac{d\overline{\rho}}{dt} + \overline{\rho}\frac{d}{dt}(\nabla\cdot\delta\mathbf{r}) = 0
\end{aligned}$$

neglecting again in the last step a term of second order. We then integrate both terms of this equation from t_0 (at t_0 we have $\rho = \rho_0$) to t . The first term yields :

$$\begin{aligned}
\int_{t_0}^{t}\frac{1}{\overline{\rho}}\frac{d\overline{\rho}}{dt}dt &= \ln\overline{\rho} - \ln\overline{\rho}_0 \\
&= \delta\ln\overline{\rho} \\
&\simeq \frac{\delta\overline{\rho}}{\overline{\rho}}.
\end{aligned} \tag{2.5.12}$$

For the second term one shows that :

$$\int_{t_0}^{t}\frac{d}{dt}(\nabla\cdot\delta\mathbf{r})dt = \nabla\cdot\delta\mathbf{r}(t) - \nabla\cdot\delta\mathbf{r}(t_0) = \nabla\cdot\delta\mathbf{r}(t).$$

Indeed, as $\nabla\cdot\delta\mathbf{r}(t_0)$ is a constant whose value is arbitrary, we choose it equal to zero. The reason for that choice is simple : as perturbed quantities are on average null (meaning that $\delta\overline{\rho}/\overline{\rho} = 0$ and $\nabla\cdot\delta\mathbf{r}(t) = 0$ on average), if we want to satisfy the integrated equation in this case we need to chose the constant as such. At the end, we obtain the following equation :

$$\frac{\delta\overline{\rho}}{\overline{\rho}} + \nabla\cdot\delta\mathbf{r} = 0. \tag{2.5.13}$$

Because the mean model has a spherical symmetry, the displacement vector can be decomposed into the three following components : $\delta\mathbf{r} = \xi_r\mathbf{e}_r + \xi_\theta\mathbf{e}_\theta + \xi_\varphi\mathbf{e}_\varphi$ where $(\mathbf{e}_r, \mathbf{e}_\theta, \mathbf{e}_\varphi)$ forms a canonical orthogonal base. With the divergence expressed in spherical coordinates we can write Eq. (2.5.13) as :

$$\frac{\delta\overline{\rho}}{\rho} + \frac{1}{r^2}\frac{\partial}{\partial r}(r^2\xi_r) + \frac{1}{r\sin\theta}\frac{\partial}{\partial\theta}(\sin\theta\,\xi_\theta) + \frac{1}{r\sin\theta}\frac{\partial\xi_\varphi}{\partial\varphi} = 0.$$

Replacing ξ_θ and ξ_φ by their respective values found earlier and noticing that we have the Legendre operator $\mathcal{L}^2$ [7] that appears with $\mathcal{L}^2 Y_\ell^m(\theta,\varphi) = \ell(\ell+1)Y_\ell^m(\theta,\varphi)$ where ℓ is an integer number, we can write the perturbed equation of mass conservation as :

$$\frac{\delta\overline{\rho}}{\overline{\rho}} + \frac{1}{r^2}\frac{\partial}{\partial r}(r^2\xi_r) = \ell(\ell+1)\frac{\xi_h}{r}. \tag{2.5.14}$$

2.5.3 Perturbed Poisson equation

In this case, we make use of the Eulerian perturbation instead of the Lagrangian one. This offers us the possibility to use the fact that the Eulerian perturbation and the ∇^2 operator are commuting. At the end, the perturbed equation of Poisson is given by :

$$\nabla^2\Phi' = 4\pi G\rho'$$

where "$'$" denotes the Eulerian perturbation. Developing the LHS we obtain a more detailed expression :

$$\frac{1}{r^2}\frac{d}{dr}\left(r^2\frac{d\Phi'}{dr}\right) - \frac{\ell(\ell+1)}{r^2}\Phi' = 4\pi G\rho'. \tag{2.5.15}$$

2.5.4 Perturbed equation of energy conservation

The next logical step is to compute the perturbed equation of energy conservation. To do so, we divide both sides of Eq. (2.1.27) by the mean density $\overline{\rho}$ which gives :

$$\overline{T}\frac{d\overline{s}}{dt} = \overline{\epsilon} - \frac{1}{\overline{\rho}}\nabla\cdot(\overline{\mathbf{F}}_R + \overline{\mathbf{F}}_c) + \left(\overline{\epsilon_2} + \frac{1}{\overline{\rho}}\overline{\mathbf{V}\cdot\nabla p_{th}}\right).$$

At equilibrium (which implies that the time derivatives of the physical quantities are equal to zero), this equation can be written as :

$$0 = \overline{\epsilon}_0 - \frac{1}{\overline{\rho}}\nabla\cdot\left(\overline{\mathbf{F}}_R + \overline{\mathbf{F}}_c\right)_0 + \left(\overline{\epsilon_2} + \frac{1}{\overline{\rho}}\overline{\mathbf{V}\cdot\nabla p_{th}}\right)_0$$

where the zero represents the value at equilibrium. After that, we subtract the second equation from the first one and we take for the LHS of the result the Lagrangian perturbation while for the RHS we take the Eulerian perturbation. We are allowed to do that because we assumed that $d\overline{s}_0/dt = 0$. We can then write :

$$\overline{T}\delta\left(\frac{d\overline{s}}{dt}\right) = \overline{\epsilon}' - \left(\frac{1}{\overline{\rho}}\nabla\cdot(\overline{\mathbf{F}}_R + \overline{\mathbf{F}}_c)\right)' + \left(\overline{\epsilon_2} + \frac{1}{\overline{\rho}}\overline{\mathbf{V}\cdot\nabla p_{th}}\right)'. \tag{2.5.16}$$

One can develop the LHS of the previous equation using one of the properties of the Lagrangian perturbation[8] and the fact that the perturbation of the mean entropy is given by : $\delta\overline{s} = \delta\overline{s}(r)\exp(i\sigma t)Y_\ell^m(\theta,\varphi)$. And so this term can now be expressed as :

$$\overline{T}\delta\left(\frac{d\overline{s}}{dt}\right) = i\sigma\overline{T}\delta\overline{s}.$$

[7] We recall here that the Legendre operator is $\mathcal{L}^2 = -\frac{1}{\sin\theta}\frac{\partial}{\partial\theta}\left(\sin\theta\frac{\partial}{\partial\theta}\right) - \frac{1}{\sin^2\theta}\frac{\partial^2}{\partial\varphi^2} = -r^2\nabla_h^2$.

[8] This property states that for any quantity X we have :

$$\delta\left(\frac{dX}{dt}\right) = \frac{\partial\delta X}{\partial t}.$$

We can also modify the second term on the RHS using this time properties of the Eulerian perturbation :

$$\begin{aligned}\left(\frac{1}{\overline{\rho}}\nabla\cdot(\overline{\mathbf{F}}_R+\overline{\mathbf{F}}_c)\right)' &= \left(\frac{1}{\overline{\rho}}\right)'\nabla\cdot(\overline{\mathbf{F}}_R+\overline{\mathbf{F}}_c)+\frac{1}{\overline{\rho}}\Big(\nabla\cdot(\overline{\mathbf{F}}_R+\overline{\mathbf{F}}_c)\Big)' \\ &= -\frac{\rho'}{\overline{\rho}^2}\nabla\cdot(\overline{\mathbf{F}}_R+\overline{\mathbf{F}}_c)+\frac{\nabla\cdot(\overline{\mathbf{F}}_R+\overline{\mathbf{F}}_c)'}{\overline{\rho}}.\end{aligned}$$

Combining these two developments we can rewrite Eq. (2.5.16) :

$$i\sigma\overline{T}\delta\overline{s}=\frac{\rho'}{\overline{\rho}^2}\nabla\cdot(\overline{\mathbf{F}}_R+\overline{\mathbf{F}}_c)-\frac{\nabla\cdot(\overline{\mathbf{F}}_R+\overline{\mathbf{F}}_c)'}{\overline{\rho}}+\overline{\epsilon}'+\left(\overline{\epsilon_2}+\frac{1}{\overline{\rho}}\overline{\mathbf{V}\cdot\nabla p_{th}}\right)'. \qquad (2.5.17)$$

In this equation, one term deserves to be further developed. Indeed, in the second term on the RHS, the divergence can be divided into two parts (one radial and one horizontal component) :

$$\frac{\nabla\cdot(\overline{\mathbf{F}}_R+\overline{\mathbf{F}}_c)'}{\overline{\rho}}=\underbrace{\frac{1}{4\pi r^2\overline{\rho}}\frac{\partial}{\partial r}\Big(4\pi r^2(F'_{R,r}+F'_{c,r})\Big)}_{\mathbf{A}}+\underbrace{\frac{1}{\overline{\rho}}\nabla_h\cdot(\overline{\mathbf{F}}_R+\overline{\mathbf{F}}_c)'}_{\mathbf{B}}. \qquad (2.5.18)$$

First of all, let us look at **A** using the definition of the total luminosity L and the link that exists between Eulerian and Lagrangian perturbations[9] :

$$\begin{aligned}\frac{1}{4\pi r^2\overline{\rho}}\frac{\partial}{\partial r}\Big(4\pi r^2(F'_{R,r}+F'_{c,r})\Big) &= \frac{1}{4\pi r^2\overline{\rho}}\frac{\partial}{\partial r}(L') \\ &= \frac{1}{4\pi r^2\overline{\rho}}\frac{\partial}{\partial r}\left(\delta L-\frac{dL}{dr}\xi_r\right) \\ &= \frac{d\delta L}{dm}-\frac{dL}{dm}\frac{d\xi_r}{dr}-\frac{1}{4\pi r^2\overline{\rho}}\xi_r\frac{d^2L}{dr^2} \qquad (2.5.19)\end{aligned}$$

where we also use the fact that $4\pi r^2\overline{\rho}dr=dm$ where dm is an infinitesimal mass element. In practice, if we consider the star at equilibrium, we can write :

$$\overline{\epsilon}-\frac{1}{\overline{\rho}}\nabla\cdot(\overline{\mathbf{F}}_R+\overline{\mathbf{F}}_c)=0.$$

Therefore, we can say that :

$$\frac{1}{4\pi r^2\overline{\rho}}\frac{dL}{dr}=\frac{dL}{dm}=\overline{\epsilon}. \qquad (2.5.20)$$

At equilibrium, the variation of luminosity of a shell of mass m is given by the rate of production of energy. We then derive both sides of this equation with respect to the radial coordinate r which gives the following relation :

$$\begin{aligned}\frac{1}{4\pi r^2\overline{\rho}}\frac{d^2L}{dr^2} &= \frac{d\overline{\epsilon}}{dr}+\overline{\epsilon}\frac{d\ln\overline{\rho}}{dr}+\frac{2\overline{\epsilon}}{r} \\ &= \overline{\epsilon}\left[\frac{d\ln\overline{\epsilon}}{dr}+\frac{d\ln\overline{\rho}}{dr}+\frac{2}{r}\right].\end{aligned}$$

Both sides of this expression are then multiplied by the radial displacement component ξ_r so that we retrieve the third term on the RHS of Eq. (2.5.19):

$$\frac{1}{4\pi r^2\overline{\rho}}\frac{d^2L}{dr^2}\xi_r=\overline{\epsilon}\left[\frac{d\ln\overline{\epsilon}}{dr}+\frac{d\ln\overline{\rho}}{dr}+\frac{2}{r}\right]\xi_r.$$

[9] Indeed, it can be shown that for any scalar quantity X we have $\delta X=X'+dX/dr\,\xi_r$. For any vectorial quantity $\mathbf{V}$ depending only on the radial variable r the formula becomes : $\delta\mathbf{V}=\mathbf{V}'+dV_r/dr\,\xi_r\mathbf{e}_r+V_r/r\,\xi_\theta\mathbf{e}_\theta+V_r/r\,\xi_\varphi\mathbf{e}_\varphi$.

After these multiple calculations we can go back to Eq. (2.5.19) and write the term **A** as :

$$\begin{aligned}\frac{1}{4\pi r^2\overline{\rho}}\frac{\partial}{\partial r}\left(4\pi r^2(F'_{R,r}+F'_{c,r})\right) &= \frac{d\delta L}{dm}-\frac{dL}{dm}\frac{d\xi_r}{dr}-\overline{\epsilon}\left[\frac{d\ln\overline{\epsilon}}{dr}+\frac{d\ln\overline{\rho}}{dr}+\frac{2}{r}\right]\xi_r\\ &= \frac{d\delta L}{dm}-\overline{\epsilon}\left[\frac{d\xi_r}{dr}+\frac{2}{r}\xi_r+\left(\frac{d\ln\overline{\epsilon}}{dr}+\frac{d\ln\overline{\rho}}{dr}\right)\xi_r\right]\\ &= \frac{d\delta L}{dm}-\overline{\epsilon}\left[\frac{1}{r^2}\frac{d}{dr}(r^2\xi_r)+\left(\frac{d\ln\overline{\epsilon}}{dr}+\frac{d\ln\overline{\rho}}{dr}\right)\xi_r\right].\end{aligned}$$

In addition, if we use again the relation (2.5.20), we can show that :

$$\begin{aligned}\frac{\rho'}{\overline{\rho}^2}\nabla\cdot(\overline{\mathbf{F}}_R+\overline{\mathbf{F}}_c) &= \frac{\rho'}{\overline{\rho}}\epsilon\\ &= \epsilon\left(\frac{\delta\rho}{\overline{\rho}}-\frac{d\ln\overline{\rho}}{dr}\xi_r\right)\end{aligned}$$

which is the first term on the RHS of Eq. (2.5.17).

From now on, only the term **B** of Eq. (2.5.18) needs to be developed. First of all, we can separate in two terms the divergence of the perturbation of the convective flux and the one of the radiative flux :

$$\begin{aligned}\frac{\nabla_h\cdot(\overline{\mathbf{F}}_R+\overline{\mathbf{F}}_c)'}{\overline{\rho}} &= \frac{\nabla_h\cdot\overline{\mathbf{F}}'_c}{\overline{\rho}}+\frac{\nabla_h\cdot\overline{\mathbf{F}}'_R}{\overline{\rho}}\\ &= \frac{1}{\overline{\rho}}\nabla_h\cdot\left[\delta\overline{\mathbf{F}}_c-\frac{dF_{c,r}}{dr}\xi_r\mathbf{e}_r-\frac{F_{c,r}}{r}(\xi_\theta\mathbf{e}_\theta+\xi_\varphi\mathbf{e}_\varphi)\right]+\frac{\nabla_h\cdot\overline{\mathbf{F}}'_R}{\overline{\rho}}\end{aligned}\tag{2.5.21}$$

where we use again the relation between a Lagrangian and an Eulerian perturbation for a vectorial quantity (see footnote 9). Assuming the following expression for the perturbation of the convective flux :

$$\delta\overline{\mathbf{F}}_c=\left(\delta F_{c,r}(r)Y_\ell^m(\theta,\varphi)\mathbf{e}_r+\delta F_{c,h}(r)(r\nabla_h)Y_\ell^m(\theta,\varphi)\right)$$

with the displacement vector being written in spherical coordinates as :

$$\xi=\xi_r(r)Y_\ell^m(\theta,\varphi)\mathbf{e}_r+\xi_h(r)(r\nabla_h)Y_\ell^m(\theta,\varphi),$$

one can express the first term on the RHS of Eq. (2.5.21) as :

$$\begin{aligned}\frac{1}{\overline{\rho}}\nabla_h\cdot\delta\overline{\mathbf{F}}_c &= \frac{1}{\overline{\rho}}\nabla_h\cdot\delta F_{c,h}(r)(r\nabla_h)Y_\ell^m(\theta,\varphi)\\ &= \frac{1}{\overline{\rho}r}\delta F_{c,h}(r)r^2\nabla_h^2Y_\ell^m(\theta,\varphi)\\ &= -\frac{1}{\overline{\rho}r}\delta F_{c,h}(r)\mathcal{L}^2Y_\ell^m(\theta,\varphi)\\ &= -\frac{\ell(\ell+1)}{\overline{\rho}r}\delta F_{c,h}(r).\end{aligned}$$

The second term on the RHS of Eq. (2.5.21) is simply equal to zero because in this case we take the horizontal divergence of a quantity depending only on the radial variable r. Finally, the third term can be expressed as :

$$\begin{aligned}\frac{1}{\overline{\rho}}\nabla_h\cdot\frac{F_{c,r}}{r}(\xi_\theta\mathbf{e}_\theta+\xi_\varphi\mathbf{e}_\varphi) &= \frac{1}{\overline{\rho}r^2}r^2\nabla_h^2F_{c,r}\xi_h(r)Y_\ell^m(\theta,\varphi)\\ &= -\frac{\ell(\ell+1)}{\overline{\rho}r}F_{c,r}(r)\frac{\xi_h}{r}.\end{aligned}$$

In total, combining these three terms we can write :

$$\frac{\nabla_h \cdot (\overline{\mathbf{F}}_R + \overline{\mathbf{F}}_c)'}{\overline{\rho}} = -\frac{\ell(\ell+1)}{\overline{\rho} r}\left(\delta F_{c,h}(r) - F_{c,r}(r)\frac{\xi_h}{r}\right) + \frac{\nabla_h \cdot \overline{\mathbf{F}}_R'}{\overline{\rho}}. \tag{2.5.22}$$

Now one can focus on the last term which contains the perturbation of the mean radiative flux. To do that, we recall here the expression of $\overline{\mathbf{F}}_R$ in the diffusion approximation which is given by:

$$\overline{\mathbf{F}}_R = -\frac{4ac\overline{T}^3}{3\overline{\kappa\rho}}\nabla\overline{T}.$$

Therefore, we get :

$$\begin{aligned}
\frac{\nabla_h \cdot \overline{\mathbf{F}}_R'}{\overline{\rho}} &= -\frac{4ac\overline{T}^3}{3\overline{\kappa}\,\overline{\rho}^2}\nabla_h^2 T' \\
&= \frac{4ac\overline{T}^3}{3\overline{\kappa}\,\overline{\rho}^2 r^2}\mathcal{L}^2 T' \\
&= \ell(\ell+1)\frac{4ac\overline{T}^3}{3\overline{\kappa}\,\overline{\rho}^2 r^2}\left(\delta T - \frac{dT}{dr}\xi_r\right).
\end{aligned} \tag{2.5.23}$$

We can now fully express Eq. (2.5.22) as :

$$\frac{\nabla_h \cdot (\overline{\mathbf{F}}_R + \overline{\mathbf{F}}_c)'}{\overline{\rho}} = -\frac{\ell(\ell+1)}{\overline{\rho} r}\left(\delta F_{c,h}(r) - F_{c,r}(r)\frac{\xi_h}{r}\right) + \ell(\ell+1)\frac{4ac\overline{T}^3}{3\overline{\kappa}\,\overline{\rho}^2 r^2}\left(\delta T - \frac{dT}{dr}\xi_r\right). \tag{2.5.24}$$

In addition of all this, we can write the radiative luminosity and the convective luminosity as :

$$\begin{aligned}
L_R &= -\frac{4ac\overline{T}^3}{3\overline{\kappa\rho} r^2}4\pi r^4 \overline{\rho}\frac{d\overline{T}}{dr} \\
L_c &= 4\pi r^2 F_{c,r}.
\end{aligned}$$

Injecting these definitions in Eq. (2.5.24) and then gathering all the terms in Eq. (2.5.17) we obtain finally the perturbed equation of energy conservation :

$$\begin{aligned}
i\sigma\overline{T}\delta\overline{s} = &- \frac{d\delta(L_c + L_R)}{dm} + \epsilon\left[\frac{\delta\epsilon}{\epsilon} + \ell(\ell+1)\frac{\xi_h}{r}\right] \\
&+ \frac{\ell(\ell+1)}{4\pi r^3\overline{\rho}}\left[L_R\left(\frac{\delta T}{r\frac{dT}{dr}} - \frac{\xi_h}{r}\right) - L_c\frac{\xi_h}{r}\right] \\
&+ \frac{\ell(\ell+1)}{\overline{\rho} r}\delta F_{c,h} + \delta\left[\overline{\epsilon}_2 + \frac{1}{\overline{\rho}}\overline{\mathbf{V}\cdot\nabla p_{th}}\right].
\end{aligned} \tag{2.5.25}$$

To end this Section with, we can compute additional perturbed quantities such as the perturbation of the radiative luminosity $L_R = 4\pi r^2 F_R$. Indeed, we can show that the Lagrangian perturbation is written as :

$$\delta L_R = 4\pi r^2 \delta F_R + 8\pi r F_R \delta r$$

using the fact that $\delta r^2 = dr^2/dr\,\delta r = 2r\delta r$. One can divide both sides by the radiative luminosity itself and this gives :

$$\frac{\delta L_R}{L_R} = \frac{\delta F_R}{F_R} + 2\frac{\delta r}{r}. \tag{2.5.26}$$

However, we can write the radiative flux as $F_R = -\mathit{\Lambda}\frac{dT}{dr}$ where $\mathit{\Lambda} = \frac{4acT^3}{3\kappa\rho}$ and so we have :

$$\frac{\delta F_R}{F_R} = \frac{\delta\mathit{\Lambda}}{\mathit{\Lambda}} + \frac{\delta(dT/dr)}{dT/dr}.$$

The two terms on the RHS of this equation can be expressed as :

$$\frac{\delta \Lambda}{\Lambda} = 3\frac{\delta T}{T} - \frac{\delta \kappa}{\kappa} - \frac{\delta \rho}{\rho},$$
$$\delta(dT/dr) = \frac{dT'}{dr} + \frac{d^2T}{dr^2}\xi_r = \frac{d\delta T}{dr} - \frac{dT}{dr}\frac{d\xi_r}{dr}$$

respectively. Injecting these results in Eq. (2.5.26) we can write the perturbed expression of the radiative luminosity as :

$$\frac{\delta L_R}{L_R} = 2\frac{\xi_r}{r} + 3\frac{\delta T}{T} - \frac{\delta \kappa}{\kappa} - \frac{\delta \rho}{\rho} + \frac{d\delta T/dr}{dT/dr} - \frac{d\xi_r}{dr}. \tag{2.5.27}$$

2.6 Perturbation of the convection

It is now necessary to look closer at some terms coming from the convection and especially to their perturbation. Such terms are the convective flux or the turbulent pressure, to name only them, which are quantities directly coming from convective effects taken into account in our treatment.

In practice, we first perturb the equations for the convective fluctuations that have been established in Section 2.2. We then assume that these perturbed equations have solutions of the following form : $\delta(\Delta X) = \delta(\Delta X)_k \exp(i\mathbf{k}\cdot\mathbf{r})\exp(i\sigma t)$.

2.6.1 Equation of mass conservation

Using this formalism we directly see that the simplified equation for convection $\nabla \cdot \mathbf{V} = 0$ becomes when perturbed :

$$\mathbf{k}\cdot\delta\mathbf{V} = 0.$$

2.6.2 Equation of energy conservation

The first step consists in taking the perturbation of the energy equation for turbulence (Eq. (2.2.16)). Besides, one can then develop a little bit some of the terms in this expression which gives at the end :

$$\delta\left(\frac{\Delta(\rho T)}{\overline{\rho T}}\right)\frac{d\overline{s}}{dt} + \frac{\Delta(\rho T)}{\overline{\rho T}}\frac{d\delta\overline{s}}{dt} + \frac{d\delta\Delta s}{dt} + \delta\mathbf{V}\cdot\nabla\overline{s} + \mathbf{V}\cdot(\delta\nabla\overline{s}) = -\frac{\omega_R\delta\Delta s}{\Omega} - \frac{\delta\omega_R\Delta s}{\Omega} - \delta\left(\frac{\Delta s}{\Omega\tau_c}\right).$$

The first term on the LHS of this equation is in general considered to be null because we assume that the mean structure of the star is at thermal equilibrium meaning that $d\overline{s}/dt = 0$. Taking this into account, the perturbed equation of energy conservation for turbulence writes :

$$\left(\frac{\Delta\rho}{\overline{\rho}} + \frac{\Delta T}{\overline{T}}\right)\frac{d\delta\overline{s}}{dt} + \frac{d\delta\Delta s}{dt} + \delta\mathbf{V}\cdot\nabla\overline{s} + \mathbf{V}\cdot(\delta\nabla\overline{s}) + \frac{\omega_R\delta\Delta s}{\Omega} + \frac{\delta\omega_R\Delta s}{\Omega} + \delta\left(\frac{\Delta s}{\Omega\tau_c}\right) = 0. \tag{2.6.1}$$

We can now express and develop each term one by one. To do that, we first multiply both sides by $\Omega\tau_c/\Delta s$ for a reason that will be presented soon after. In addition, we use useful relations obtained at equilibrium coming from previous sections. After some manipulations, we obtain :

- for the first term :

$$\begin{aligned}\frac{\Omega\,\tau_c}{\Delta s}\left(\frac{\Delta\rho}{\overline{\rho}}+\frac{\Delta T}{\overline{T}}\right)\frac{d\delta\overline{s}}{dt} &= i\sigma\Omega\left(\frac{\tau_c}{\Delta s}\frac{\Delta\rho}{\overline{\rho}}+\frac{\tau_c}{\Delta s}\frac{\Delta T}{\overline{T}}\right)\delta\overline{s}\\ &= i\sigma\Omega\,\tau_c\left(\frac{\Delta\rho}{\overline{\rho}}\frac{\overline{\rho}}{\Delta\rho\, c_pQ_p}+\frac{\Delta T}{\overline{T}}\frac{\overline{T}}{c_p\Delta T}\right)\delta\overline{s}\\ &= i\sigma\Omega\,\tau_c\frac{Q_p+1}{Q_p}\frac{\delta\overline{s}}{c_p}\end{aligned}$$

where we use the relation $\Delta s = c_p\Delta T/\overline{T} = c_pQ_p\Delta\rho/\overline{\rho}$.

- for the second term we simply have :

$$\frac{\Omega\,\tau_c}{\Delta s}\frac{d\delta\Delta s}{dt} = i\sigma\Omega\,\tau_c\frac{\delta\Delta s}{\Delta s}.$$

- the third term is given by :

$$\begin{aligned}\frac{\Omega\,\tau_c}{\Delta s}(\delta\mathbf{V}\cdot\nabla\overline{s}) &= \frac{\Omega\,\tau_c}{\Delta s}\frac{\delta\mathbf{V}}{\mathbf{V}}\mathbf{V}\cdot\nabla\overline{s}\\ &= -\frac{\Omega\,\tau_c}{\Delta s}\frac{\delta\mathbf{V}}{\mathbf{V}}\left(\frac{\tau_c/\tau_R+1}{\Omega\,\tau_c}\Delta s\right)\\ &= -\frac{\delta V_r}{V_r}(\tau_c\omega_R+1)\end{aligned}$$

using the equation of energy conservation at equilibrium Eq. (2.4.2) and taking only the radial component.

- the fourth term deserves some additional manipulations, we start with :

$$\frac{\Omega\,\tau_c}{\Delta s}\mathbf{V}\cdot(\delta\nabla\overline{s}) = \frac{\Omega\,\tau_c}{\Delta s}\left[\mathbf{V}\cdot\nabla(\delta\overline{s})-\mathbf{V}\cdot\frac{d\overline{s}}{dr}\nabla\xi_r\right] \tag{2.6.2}$$

where we use a relation already used in previous developments (Eq. (2.5.5)) which applied in this case states that $\delta\nabla\overline{s} = \nabla(\delta\overline{s}) - d\overline{s}/dr\nabla\xi_r$ and $\nabla\overline{s} = d\overline{s}/dr\,\mathbf{e}_r$. After that, one can multiply the first term on the RHS of this equation by V_r/V_r and by the radial component of $\nabla\overline{s}/\nabla\overline{s}$ giving the following result :

$$\begin{aligned}\frac{\Omega\,\tau_c}{\Delta s}\mathbf{V}\cdot\nabla(\delta\overline{s})\frac{V_r}{V_r}\frac{d\overline{s}}{dr}\left(\frac{d\overline{s}}{dr}\right)^{-1} &= \frac{\Omega\,\tau_c}{\Delta s}\frac{\mathbf{V}}{V_r}\cdot\nabla(\delta\overline{s})V_r\cdot\frac{d\overline{s}}{dr}\left(\frac{d\overline{s}}{dr}\right)^{-1}\\ &= -(\tau_c\omega_R+1)\left(\frac{d\overline{s}}{dr}\right)^{-1}\frac{\mathbf{V}}{V_r}\cdot\nabla(\delta\overline{s})\end{aligned}$$

where we use again Eq. (2.4.2) to eliminate Δs. The same method is utilized for the second term on the RHS which can be expressed as :

$$\frac{\Omega\,\tau_c}{\Delta s}\mathbf{V}\cdot\frac{d\overline{s}}{dr}\nabla\xi_r = -(\tau_c\omega_R+1)\frac{\mathbf{V}}{V_r}\cdot\nabla\xi_r.$$

Eq. (2.6.2) can ultimately be reformulated as :

$$\frac{\Omega\,\tau_c}{\Delta s}\mathbf{V}\cdot(\delta\nabla\overline{s}) = -(\tau_c\omega_R+1)\left[\left(\frac{d\overline{s}}{dr}\right)^{-1}\frac{\mathbf{V}}{V_r}\cdot\nabla(\delta\overline{s})-\frac{\mathbf{V}}{V_r}\cdot\nabla\xi_r\right].$$

- the fifth and sixth terms do not change a lot and can be written as :

$$\frac{\Omega\tau_c}{\Delta s}\frac{\omega_R\delta\Delta s}{\Omega} + \frac{\Omega\tau_c}{\Delta s}\frac{\delta\omega_R\Delta s}{\Omega} = \tau_c\omega_R\frac{\delta\Delta s}{\Delta s} + \tau_c\omega_R\frac{\delta\omega_R}{\omega_R}.$$

- for the last term, one should pay attention to the meaning of it. In fact, $\Delta s/\Omega\tau_c$ was already introduced in a previous section and represents the closure approximation for the energy equation which we have used in our treatment of the convection (see Eq. (2.2.15)). Under this rather simple ratio hides multiple complicated terms representing some important phenomena: the way the whole turbulent cascade of energy dissipation reacts to the oscillations just to name one. It thus seems necessary to keep an eye on how we take the perturbation of this term and one should remember the very crude approximations that were made to obtain it at the beginning. Keeping all these considerations in mind, we assume that the perturbation of this term is given by[10] :

$$\begin{aligned}\delta\left(\frac{\Delta s}{\Omega\tau_c}\right) &= \frac{\delta\Delta s}{\Omega\tau_c} - \Delta s\frac{\delta(\Omega\tau_c)}{\Omega^2\tau_c^2} \\ &= \frac{\Delta s}{\Omega\tau_c}\left(\frac{\delta\Delta s}{\Delta s} - \frac{\delta\tau_c}{\tau_c} - \frac{\delta\Omega}{\Omega}\right) \\ &\simeq \frac{\Delta s}{\Omega\tau_c}\left(\frac{\delta\Delta s}{\Delta s} - \frac{\delta\tau_c}{\tau_c}\right). \end{aligned} \tag{2.6.3}$$

Now, we clearly understand why all the terms were multiplied by $\Omega\tau_c/\Delta s$ leaving $\delta\Delta s/\Delta s$ and $\delta\tau_c/\tau_c$ without any factor before them. Besides, the perturbation of Ω was arbitrary neglected in the last step of our development because we do not know how to express it. This approximation shows again the limit of this theory. Indeed, there is a priori no reason why we should not take into consideration the perturbation of this parameter.

Often, as it was proposed by [Grigahcène et al., 2005], another expression for the perturbation of this closure term can be adopted in order to avoid some non-physical spatial oscillations occurring with the expression for the perturbation given in Eq. (2.6.3). This includes the introduction of a new free parameter β such that the perturbation can be written as :

$$\delta\left(\frac{\Delta s}{\Omega\tau_c}\right) = \frac{\Delta s}{\Omega\tau_c}\left((1+\beta\sigma\tau_c)\frac{\delta\Delta s}{\Delta s} - \frac{\delta\tau_c}{\tau_c}\right). \tag{2.6.4}$$

In practice (see Section 3.2), with a value of the order of unity for β, one reproduces the reality more accurately allowing some phase lags to occur between the oscillations and how the turbulence cascade adapts to them. Again, the perturbation of β is considered as negligible without any physical justification. However, for the sake of simplicity, we will continue to use in the following theoretical developments Eq. (2.6.3) instead of Eq. (2.6.4) for which we should modify and add the parameter β at different places.

After all these developments we can finally write Eq. (2.6.1) as :

$$\begin{aligned}(i\sigma\Omega\tau_c + \omega_R\tau_c + 1)\left(\frac{\delta\Delta s}{\Delta s}\right) &= -\,i\sigma\Omega\tau_c\frac{Q_p+1}{Q_p}\frac{\delta\bar{s}}{c_p} + (\omega_R\tau_c+1)\left[\frac{\delta V_r}{V_r} - \frac{\mathbf{V}}{V_r}\cdot\nabla\xi_r + \left(\frac{d\bar{s}}{dr}\right)^{-1}\nabla\delta\bar{s}\cdot\frac{\mathbf{V}}{V_r}\right] \\ &+ \frac{\delta\tau_c}{\tau_c} - \omega_R\tau_c\frac{\delta\omega_R}{\omega_R}. \end{aligned} \tag{2.6.5}$$

[10] It appears clear that by doing so, we neglect and do not look at all at the perturbation of a multitude of terms much more complicated than Δs and τ_c.

Using the following notations :

$$C = \frac{\omega_R\tau_c + 1}{i\sigma\Omega\tau_c + \omega_R\tau_c + 1},$$
$$D = \frac{1}{i\sigma\Omega\tau_c + \omega_R\tau_c + 1}$$

and isolating $\delta\Delta s/\Delta s$ in Eq. (2.6.5) we obtain :

$$\frac{\delta\Delta s}{\Delta s} = D\left\{-i\sigma\Omega\tau_c\frac{Q_p+1}{Q_p}\frac{\delta\overline{s}}{c_p} + (\omega_R\tau_c+1)\left[\frac{\delta V_r}{V_r} + \frac{\mathbf{V}\cdot\nabla\delta\overline{s}}{V_r(d\overline{s}/dr)} - \frac{\mathbf{V}}{V_r}\cdot\nabla\xi_r\right] + \left(\frac{\delta\tau_c}{\tau_c} - \omega_R\tau_c\frac{\delta\omega_R}{\omega_R}\right)\right\}. \tag{2.6.6}$$

We can then multiply this equation by V_j/V_r and take the average :

$$\begin{aligned}\frac{\overline{\delta\Delta s V_j}}{\Delta s V_r} =& D\left\{-i\sigma\Omega\tau_c\frac{Q_p+1}{Q_p}\frac{\delta\overline{s}}{c_p} + \frac{\delta\tau_c}{\tau_c} - \omega_R\tau_c\frac{\delta\omega_R}{\omega_R}\right\}\frac{\overline{V_rV_j}}{V_r^2} \\ &+C\left\{\left[\left(\frac{d\overline{s}}{dr}\right)^{-1}\nabla_k\delta\overline{s} - \nabla_k\xi_r\right]\frac{\overline{V_jV_k}}{V_r^2} + \frac{\overline{V_j\delta V_r}}{V_r^2}\right\}\end{aligned} \tag{2.6.7}$$

using the usual Einstein summation convention for indices appearing more than once. Finally, if we take the radial component $(j, k = r)$ the equation above can be written as :

$$\begin{aligned}\frac{\overline{\delta\Delta s}}{\Delta s} =& D\left\{-i\sigma\Omega\tau_c\frac{Q_p+1}{Q_p}\frac{\delta\overline{s}}{c_p} + \frac{\delta\tau_c}{\tau_c} - \omega_R\tau_c\frac{\delta\omega_R}{\omega_R}\right\} \\ &+C\left\{\left[\left(\frac{d\overline{s}}{dr}\right)^{-1}\frac{d\delta\overline{s}}{dr} - \frac{d\xi_r}{dr}\right] + \frac{\overline{\delta V_r}}{V_r}\right\}.\end{aligned} \tag{2.6.8}$$

2.6.3 Equation of momentum conservation

The next step of our treatment is to determine the perturbed version of the equation of momentum conservation for the convection and ultimately a relation for the perturbed turbulent velocity. Therefore, we perturb Eq. (2.2.21) which gives[11] :

$$i\sigma\overline{\rho}\delta\mathbf{V} = \delta\left(\frac{\Delta\rho}{\overline{\rho}}\right)\nabla\overline{p} + \frac{\Delta\rho}{\overline{\rho}}\delta(\nabla\overline{p}) - \delta(\nabla\Delta p) - \rho\mathbf{V}\cdot\delta\nabla\mathbf{u} - \frac{\Omega\Lambda\overline{\rho}\mathbf{V}}{\tau_c}\left(\frac{\delta\overline{\rho}}{\overline{\rho}} - \frac{\delta\tau_c}{\tau_c}\right) - \frac{\Omega\Lambda\overline{\rho}\delta\mathbf{V}}{\tau_c}$$

where we use the fact that the average of $d\mathbf{V}/dt = 0$ and that $\nabla\mathbf{u} = 0$ because we assume that the average of the mean component of the velocity $\mathbf{u}$ is null and that only the perturbation of it is different from zero. We then take the divergence of this equation or in other words we multiply this equation by $\mathbf{k}$ the wave vector number. In addition, we use the following notation:

$$B = \frac{i\sigma\tau_c + \Omega\Lambda}{\Omega\Lambda}$$

and relations already used before applied in this case to the mean pressure : $\delta\nabla\overline{p} = \nabla\delta\overline{p} - d\overline{p}/dr\nabla\xi_r$ and $\nabla\overline{p} = d\overline{p}/dr\,\mathbf{e}_r$. At the end, we obtain for a given $\mathbf{k}$:

$$\begin{aligned}B\frac{\delta V_j}{V_r} =& \frac{A+1}{A}\frac{\delta(\Delta\rho/\overline{\rho})}{\Delta\rho/\overline{\rho}}K_{jr} + \frac{A+1}{A}\left[\left(\frac{d\overline{p}}{dr}\right)^{-1}\nabla_i\delta\overline{p} - \nabla_i\xi_r\right]K_{ji} \\ &- \frac{i\sigma\tau_c}{\Omega\Lambda}\frac{V_i}{V_r}\nabla_i\xi_l K_{lj} - \left(\frac{\delta\overline{\rho}}{\overline{\rho}} - \frac{\delta\tau_c}{\tau_c}\right)\frac{V_j}{V_r}\end{aligned} \tag{2.6.9}$$

[11] We again assume the perturbation of Ω to be small enough to be neglected without any physical justification.

where

$$K_{ji} = \delta_{ji} - \frac{k_j k_i}{k^2},$$
$$K_{jr} = \frac{A}{A+1}\frac{V_j(\mathbf{k})}{V_r}.$$

Contrary to the first relation for K_{ji} which is just a definition, the second relation is not trivial at all. Indeed, it can be deduced using on one side Eq. (2.4.8) in which we isolate $V_j(\mathbf{k})$ and using the first relation for $K_{rj} = \delta_{rj} - \frac{k_r k_j}{k^2}$. This gives :

$$V_j(\mathbf{k}) = \frac{\tau_c}{\Omega\Lambda}\frac{\Delta\rho}{\rho^2}\frac{d\overline{p}}{dr}K_{rj}.$$

On the other side, we integrate Eq. (2.4.8) over all $\mathbf{k}$ and we obtain :

$$V_r = \frac{A}{A+1}\frac{1}{\rho}\frac{\tau_c}{\Omega\Lambda}\frac{\Delta\rho_a}{\overline{\rho}}\frac{d\overline{p}}{dr}.$$

Comparing both results we indeed retrieve our second relation for K_{jr}. For the next step, we want to eliminate from Eq. (2.6.9) the term where the perturbation of the turbulent density component appears. To do that, we use the following relation of thermodynamics (neglecting Δp as it was already done before) :

$$\frac{\Delta\rho}{\overline{\rho}} = \frac{1}{Q_p}\frac{\Delta s}{c_p}.$$

Knowing this, we easily show that :

$$\begin{aligned}
\delta\left(\frac{\Delta\rho}{\overline{\rho}}\right) &= \delta\left(\frac{1}{Q_p}\frac{\Delta s}{c_p}\right) \\
&= -Q_p^{-2}\delta Q_p\frac{\Delta s}{c_p} + \delta\Delta s\frac{1}{c_p Q_p} - c_p^{-2}\delta c_p\frac{\Delta s}{Q_p} \\
&= \frac{1}{Q_p}\frac{\Delta s}{c_p}\left(\frac{\delta\Delta s}{\Delta s} - \frac{\delta Q_p}{Q_p} - \frac{\delta c_p}{c_p}\right) \\
&= \frac{\Delta\rho}{\overline{\rho}}\left(\frac{\delta\Delta s}{\Delta s} - \frac{\delta Q_p}{Q_p} - \frac{\delta c_p}{c_p}\right).
\end{aligned}$$

One can then eliminate from this equation the perturbation of the convective entropy using Eq. (2.6.6). This result is then injected in Eq. (2.6.9) and yields :

$$\begin{aligned}
B\frac{\delta V_j}{V_r} = \frac{V_j}{V_r}&\left\{-\frac{\delta Q_p}{Q_p} - \frac{\delta c_p}{c_p} - \frac{\delta\rho}{\overline{\rho}} + \frac{\delta\tau_c}{\tau_c} + D\left[-i\sigma\Omega\tau_c\frac{Q_p+1}{Q_p}\frac{\delta\overline{s}}{c_p} + \frac{\delta\tau_c}{\tau_c} - \omega_R\tau_c\frac{\delta\omega_R}{\omega_R}\right.\right. \\
&\left.\left. + (\omega_R\tau_c+1)\left(\frac{\delta V_r}{V_r} + \frac{V_k}{V_r}\left(\frac{\nabla_k\delta\overline{s}}{d\overline{s}/dr} - \nabla_k\xi_r\right)\right)\right]\right\} \\
&+ \frac{A+1}{A}\left[\left(\frac{d\overline{p}}{dr}\right)^{-1}\nabla_i\delta\overline{p} - \nabla_i\xi_r\right]K_{ji} - \frac{i\sigma\tau_c}{\Omega\Lambda}\frac{V_i}{V_r}\nabla_i\xi_l K_{lj}.
\end{aligned} \tag{2.6.10}$$

This equation expresses the turbulent velocity perturbation. As it can be seen clearly, this expression is quite long and complicated. In order to simplify its writing one can introduce several notations, these are :

$$\begin{aligned}
\mathcal{J}_{jk} &= \nabla_j \delta r_k, \\
\mathcal{S}_k &= \left(\frac{d\overline{s}}{dr}\right)^{-1} \nabla_k \delta\overline{s} - \mathcal{J}_{kr}, \\
\mathcal{P}_k &= \left(\frac{d\overline{p}}{dr}\right)^{-1} \nabla_k \delta\overline{p} - \mathcal{J}_{kr}, \\
\mathcal{A} &= -\frac{\delta Q_p}{Q_p} - \frac{\delta c_p}{c_p} - \frac{\delta\rho}{\overline{\rho}} + \frac{\delta\tau_c}{\tau_c} + D\left[-i\sigma\Omega\tau_c \frac{Q_p+1}{Q_p}\frac{\delta\overline{s}}{c_p} + \frac{\delta\tau_c}{\tau_c} - \omega_R\tau_c\frac{\delta\omega_R}{\omega_R}\right].
\end{aligned}$$

With these new definitions we can rewrite Eq. (2.6.10) as :

$$B\frac{\delta V_j}{V_r} = \left\{\mathcal{A} + C\frac{\delta V_r}{V_r} + C\mathcal{S}_k\frac{V_k}{V_r}\right\}\frac{V_j}{V_r} + \frac{A+1}{A}\mathcal{P}_k K_{jk} - (B-1)\mathcal{J}_{kl}\frac{V_k}{V_r}K_{jl}. \tag{2.6.11}$$

In this equation, hidden in the simplified notation $\mathcal{A}$ lies important perturbation terms such as the convective time τ_c and the inverse of the radiative time ω_R. To acquire the complete expression of their perturbation, we use their respective definition. For the convective lifetime, we perturb Eq. (2.4.14)[12] which gives :

$$\delta\tau_c = \frac{\delta l}{l}\frac{l}{\sqrt{\overline{V}_r^2}} - \frac{\overline{\delta V_r}}{V_r}\frac{l}{\sqrt{\overline{V}_r^2}},$$

dividing both sides by τ_c we obtain :

$$\frac{\delta\tau_c}{\tau_c} = \frac{\delta l}{l} - \frac{\overline{\delta V_r}}{V_r}. \tag{2.6.12}$$

For the radiative lifetime we perturb Eq. (2.2.10) which is given by :

$$\begin{aligned}
\omega_R &= \frac{1}{\tau_R} = \frac{4ac}{3}\frac{\overline{T}^3}{c_p\overline{\kappa}\overline{\rho}^2}\mathcal{L}^2 \\
\Rightarrow \frac{\delta\omega_R}{\omega_R} &= 3\frac{\delta T}{T} - \frac{\delta c_p}{c_p} - \frac{\delta\kappa}{\kappa} - 2\frac{\delta\rho}{\rho} - 2\frac{\delta l}{l}.
\end{aligned} \tag{2.6.13}$$

These two new perturbation terms can be injected in Eq. (2.6.11). An additional computation can be done in order to find the average radial turbulent velocity perturbation. To do that, we multiply Eq. (2.6.11) by $\frac{V_k V_l}{V_r^2}$ recalling here that we integrate the solutions over all values of k_θ and k_ϕ ($k_\theta^2 + k_\phi^2 = Ak_r^2$ with A being the anisotropy factor) and we then take the horizontal average. After all these manipulations we obtain for the radial turbulent velocity (taking $j = r$) perturbation the following equation :

$$\begin{aligned}
\frac{\overline{\delta V_r}}{V_r} =& \frac{1}{B + (i\sigma\Omega\tau_c + 1)D}\left\{-\frac{\delta c_p}{c_p} - \frac{\delta Q_p}{Q_p} - \frac{\delta\rho}{\rho} + \frac{d\delta p}{p} - \frac{d\xi_r}{dr} - i\sigma\Omega\tau_c D\frac{Q_p+1}{Q_p}\frac{\delta s}{c_p}\right. \\
&+ C\left[\frac{d\delta s}{ds} - \frac{d\xi_r}{dr}\right] - \frac{A}{A+1}\frac{i\sigma\tau_c}{\Omega\Lambda}\left(\frac{d\xi_r}{dr} + \frac{1}{A}\frac{\xi_r}{r} - \frac{\ell(\ell+1)}{2A}\frac{\xi_h}{r}\right) \\
&\left.-\omega_R\tau_c D\left(3\frac{\delta T}{T} - \frac{\delta c_p}{c_p} - \frac{\delta\kappa}{\kappa} - 2\frac{\delta\rho}{\rho}\right) + (i\sigma\Omega\tau_c + 3\omega_R\tau_c + 2)D\frac{\delta l}{l}\right\}.
\end{aligned} \tag{2.6.14}$$

[12]In our case, this equation is $\tau_c = l/\sqrt{\overline{V}_r^2}$ where l is the usual mixing length.

2.6.4 Perturbation of some important quantities

Convective flux

The perturbation of the convective flux appears at different places but we have not yet determined its complete expression. We recall here the definition introduced for the convective flux (Eq. (2.1.26)) :

$$\mathbf{F}_c = \overline{\rho}\overline{T}\overline{\Delta s \mathbf{V}}.$$

Perturbing this equation we obtain :

$$\delta \mathbf{F}_c = \overline{\mathbf{F}_c}\left(\frac{\delta\rho}{\overline{\rho}} + \frac{\delta\overline{T}}{\overline{T}}\right) + \overline{\rho}\overline{T}\left(\overline{\delta\Delta s\mathbf{V}} + \overline{\Delta s\delta\mathbf{V}}\right).$$

One can also be interested in the radial component of the perturbation of the convective flux $\delta F_{c,r}/F_{c,r}$. The previous relation becomes in this case :

$$\frac{\delta F_{c,r}}{F_{c,r}} = \left(\frac{\delta\rho}{\overline{\rho}} + \frac{\delta\overline{T}}{\overline{T}}\right) + \frac{\overline{\delta\Delta s}}{\Delta s} + \frac{\overline{\delta V_r}}{V_r}. \tag{2.6.15}$$

Several terms of this equation have already been computed beforehand. Using Eqs. (2.6.6), (2.6.12) and (2.6.13) we have :

$$\begin{aligned}\frac{\delta F_{c,r}}{F_{c,r}} =& \frac{\delta\rho}{\rho} + \frac{\delta T}{T} - i\sigma\Omega\tau_c D\frac{Q_p+1}{Q_p}\frac{\delta s}{c_p} + C\left[\frac{d\delta s}{ds} - \frac{d\xi_r}{dr}\right]\\ &- \omega_R\tau_c D\left(3\frac{\delta T}{t} - \frac{\delta c_p}{c_p} - \frac{\delta\kappa}{\kappa} - 2\frac{\delta\rho}{\rho}\right)\\ &+ (i\sigma\Omega\tau_c + 2\omega_R\tau_c + 1)D\frac{\overline{\delta V_r}}{V_r} + (2\omega_R\tau_c + 1)D\frac{\delta l}{l}.\end{aligned}$$

Turbulent pressure

As shown in a previous section, the turbulent pressure is given by $\overline{p}_t = \overline{\rho V_r^2}$. Perturbing this relation we obtain the perturbed turbulent pressure :

$$\frac{\delta\overline{p}_t}{\overline{p}_t} = \frac{\delta\overline{\rho}}{\overline{\rho}} + 2\frac{\overline{\delta V_r}}{V_r}.$$

Mixing length

Throughout our developments, we have seen the mixing length l appearing in various equations and more especially its perturbation. However, there exist multiple ways to express the perturbation of l depending on the flavour of the MLT (which is a crude approximation of the convection) chosen. Most of the time, just by the definition given to the mixing length (see Section 2.3) the perturbed mixing length is given by :

$$\frac{\delta l}{l} = \frac{\delta H_p}{H_p}. \tag{2.6.16}$$

Nevertheless, one should take into account that in some particular cases where the life-time τ_c of the convective elements is much longer than the typical time-scale of pulsation (considering a frozen convection) the perturbation of the mixing length becomes negligible. The previous definition of the perturbation of the mixing length is not able to reproduce this particular case leading to a new definition of the perturbation of this quantity :

$$\frac{\delta l}{l} = \frac{1}{1+(\sigma\tau_c)^2}\frac{\delta H_p}{H_p}.$$

This relation gives back the previous expression Eq. (2.6.16) when we consider $\sigma\tau_c << 1$. And we also find as intended that in the case of a large τ_c, the perturbation of the mixing length $\delta l/l$ tends to 0.

Rate of dissipation of turbulent kinetic energy into heat

To end with, one can focus on the perturbation of this important term appearing both in the perturbed equation of energy conservation Eq. (2.5.25) and in the equation of turbulent kinetic energy conservation Eq. (2.1.21) :

$$\delta\left(\overline{\epsilon_2 + \mathbf{V}\cdot\frac{\nabla p_{th}}{\rho}}\right). \tag{2.6.17}$$

We can perturb Eq. (2.1.21) so that we obtain after some algebra :

$$\begin{aligned}\delta\left(\overline{\epsilon_2 + \mathbf{V}\cdot\frac{\nabla p_{th}}{\rho}}\right) &= -i\sigma\rho\delta\left(\frac{\overline{\rho\mathbf{V}^2}}{2\rho}\right) - i\sigma\overline{\rho\mathbf{V}\mathbf{V}}\otimes\nabla\xi \\ &= -i\sigma p_t\left[\frac{A+1}{2A}\left(\frac{\delta p_t}{p_t}-\frac{\delta\rho}{\rho}\right)+\frac{d\xi_r}{dr}+\frac{1}{2A}\left(2\frac{\xi_r}{r}-\ell(\ell+1)\frac{\xi_h}{r}\right)\right]\end{aligned} \tag{2.6.18}$$

2.6.5 Integral expressions

Now that we have found the expression of several important physical quantities and the different equations used in our treatment of the convection, we are interested in the role they play in the integral expressions for the frequencies. To start with, we multiply the radial component of the perturbed equation of movement describing the mean structure Eq. (2.5.9) by ξ_r^* (with the "*" meaning that we deal with the complex conjugate) and then we integrate it over the mass of the star. The expression to be computed is given by[13] :

$$\begin{aligned}\sigma^2\int_0^M|\xi_r|^2dm = \int_0^M \xi_r^*\frac{d\delta\Phi}{dr}dm + \int_0^M\xi_r^*\frac{1}{\rho}\frac{d\delta p}{dr}dm + \int_0^M\xi_r^* g\frac{\delta\rho}{\rho}dm \\ + \int_0^M\xi_r^*\frac{\Xi_R^r(r)}{\rho}dm + \frac{2A-1}{A}\int_0^M\xi_r^*\frac{p_t}{r\rho}\frac{d\xi_r}{dr}dm\end{aligned} \tag{2.6.19}$$

with $g=\frac{d\Phi}{dr}$. The two first terms on the RHS of this equation deserve some more attention. For both terms, one will prefer to integrate over the radius of the star instead of its mass using the relation linking both variables in the case of a model at equilibrium :

$$\frac{dm}{dr} = 4\pi\rho r^2.$$

[13] In the following developments for integral expressions, to avoid a too heavy notation we expressly omit the average notation on the mean quantities. The context should be clear enough to know whereas we face an average value or not.

Using the above relation and integrating by parts, the first term on the RHS becomes :

$$\begin{aligned}\int_0^R \xi_r^* \frac{d\delta\Phi}{dr} 4\pi\rho r^2 dr &= \left[\xi_r^* \delta\Phi 4\pi\rho r^2\right]_0^R - \int_0^R \delta\Phi \frac{d(\xi_r^* r^2 \rho)}{dr} 4\pi dr \\ &= -\int_0^R \delta\Phi \frac{d(\xi_r^* r^2)}{dr} 4\pi\rho dr - \int_0^R \delta\Phi \xi_r^* r^2 \frac{d\rho}{dr} 4\pi dr \\ &= -\int_0^M \delta\Phi \frac{d(\xi_r^* r^2)}{dr} \frac{1}{r^2} dm - \int_0^M \delta\Phi \frac{\xi_r^*}{\rho} \frac{d\rho}{dr} dm\end{aligned}$$

in which the density at the surface is assumed to be equal to zero. Recalling Eq. (2.5.14), the expression can be written as :

$$\int_0^M \xi_r^* \frac{d\delta\Phi}{dr} dm = -\ell(\ell+1) \int_0^M \frac{\xi_h^*}{r} \delta\Phi dm + \int_0^M \frac{\delta\rho^*}{\rho} \delta\Phi dm - \int_0^M \xi_r^* \frac{\delta\Phi}{\rho} \frac{d\rho}{dr} dm.$$

The same procedure is followed for the second term on the RHS of Eq. (2.6.19) :

$$\begin{aligned}\int_0^R \xi_r^* \frac{1}{\rho} \frac{d\delta p}{dr} 4\pi r^2 \rho dr &= \left[\xi_r^* \delta p 4\pi r^2\right]_0^R - \int_0^R \delta p 4\pi \frac{d(\xi_r^* r^2)}{dr} dr \\ &= -\int_0^M \delta p \frac{1}{r^2\rho} \frac{d(\xi_r^* r^2)}{dr} dm \\ &= -\ell(\ell+1) \int_0^M \frac{\xi_h^*}{r} \frac{\delta p}{\rho} dm + \int_0^M \frac{\delta\rho^*}{\rho} \frac{\delta p}{\rho} dm.\end{aligned}$$

Gathering these two expressions in Eq. (2.6.19) we obtain :

$$\begin{aligned}\sigma^2 \int_0^M |\xi_r|^2 dm = &-\ell(\ell+1) \int_0^M \frac{\xi_h^*}{r} \left(\delta\Phi + \frac{\delta p}{\rho}\right) dm + \int_0^M \frac{\delta\rho^*}{\rho} \left(\delta\Phi + \frac{\delta p}{\rho}\right) dm \\ &- \int_0^M \xi_r^* \frac{\delta\Phi}{\rho} \frac{d\rho}{dr} dm + \int_0^M \xi_r^* g \frac{\delta\rho}{\rho} dm \\ &+ \int_0^M \xi_r^* \frac{\Xi_R^r(r)}{\rho} dm + \frac{2A-1}{A} \int_0^M \xi_r^* \frac{p_t}{r\rho} \frac{d\xi_r}{dr} dm.\end{aligned} \tag{2.6.20}$$

After that, we can do something similar but this time using the horizontal component of the perturbed equation of movement Eq. (2.5.10) and multiplying both sides by $\ell(\ell+1)\xi_h^*$. The result is given by :

$$\ell(\ell+1)\sigma^2 \int_0^M |\xi_h|^2 dm = \ell(\ell+1) \int_0^M \frac{\xi_h^*}{r} \left(\delta\Phi + \frac{\delta p}{\rho}\right) + \ell(\ell+1) \int_0^M \frac{\xi_h^*}{\rho} \left[\Xi_R^h + \frac{2A+1}{A} \frac{p_t}{r^2} (\xi_r - \xi_h)\right] dm. \tag{2.6.21}$$

As next step, we make the sum of Eq. (2.6.20) and Eq. (2.6.21) and we get :

$$\begin{aligned}\sigma^2 \int_0^M (|\xi_r|^2 + \ell(\ell+1)|\xi_h|^2) dm = &\int_0^M \frac{\delta\rho^*}{\rho} \left(\delta\Phi + \frac{\delta p}{\rho}\right) dm - \int_0^M \xi_r^* \frac{\delta\Phi}{\rho} \frac{d\rho}{dr} dm \\ &+ \int_0^M \xi_r^* g \frac{\delta\rho}{\rho} dm + \int_0^M \frac{1}{\rho} \left[\xi_r^* \Xi_R^r + \ell(\ell+1)\xi_h^* \Xi_R^h\right] dm \\ &+ \frac{2A-1}{A} \int_0^M \frac{p_t}{\rho} \left[\frac{\xi_r^*}{r} \frac{d\xi_r}{dr} + \ell(\ell+1) \frac{\xi_h^*}{r^2} (\xi_r - \xi_h)\right] dm.\end{aligned} \tag{2.6.22}$$

This integral can be even more simplified using the two following relations :

$$\int_0^M \xi_r^* g \frac{\delta\rho}{\rho} dm = 2\,\Re\left(\int_0^M \xi_r^* g \frac{\delta\rho}{\rho} dm\right) - \int_0^M \frac{\delta\rho^*}{\rho} \xi_r g \, dm,$$

$$\delta\Phi = \Phi' + g\xi_r$$

with Φ' being the Eulerian perturbation of the gravitational potential and $\Re$ denoting the real part of a complex quantity. Considering those two relations, Eq. (2.6.22) can now be written :

$$\begin{aligned}\sigma^2 \int_0^M (|\xi_r|^2 + \ell(\ell+1)|\xi_h|^2)dm = &\int_0^M \left\{ \frac{\delta\rho^*}{\rho}\frac{\delta p}{\rho} + 2\,\Re\left(\xi_r^*\frac{\delta\rho}{\rho}g\right) + \frac{\rho'^*}{\rho}\Phi' - |\xi_r|^2 g \frac{d\ln p}{dr}\right\} dm \\ &+ \frac{2A-1}{A}\int_0^M \frac{p_t}{\rho}\left\{\frac{\xi_r^*}{r}\frac{d\xi_r}{dr} + \ell(\ell+1)\frac{\xi_h^*}{r}\left(\frac{\xi_r}{r} - \frac{\xi_h}{r}\right)\right\} dm \\ &+ \int_0^M \frac{1}{\rho}\left\{\xi_r^*\Xi_R^r + \ell(\ell+1)\xi_h^*\Xi_R^h\right\} dm. \qquad (2.6.23)\end{aligned}$$

As we want to take at the end the imaginary part of this relation, we first search for terms that would be purely real so that we could neglect them later. Among all the terms of Eq. (2.6.23) two are trivially real :

$$\int_0^M 2\,\Re\left(\xi_r^*\frac{\delta\rho}{\rho}g\right) dm \quad \text{and} \quad \int_0^M |\xi_r|^2 g\frac{d\ln p}{dr}dm$$

while a third term,

$$\int_0^M \frac{\rho'^*}{\rho}\Phi' dm$$

is purely real assuming that the density at the surface of the star is negligible. To show it, we replace ρ'^* in this integral by its value deduced from Eq. (2.5.15). Integrating by parts we obtain :

$$\begin{aligned}\int_0^M \frac{\rho'^*}{\rho}\Phi' dm &= \int_0^M \frac{1}{4\pi G\rho}\left[\frac{1}{r^2}\frac{d}{dr}\left(\frac{d\Phi'^*}{dr}r^2\right) - \frac{\ell(\ell+1)}{r^2}\Phi'^*\right]\Phi' dm \\ &= \int_0^R \frac{1}{G}\frac{d}{dr}\left(\frac{d\Phi'^*}{dr}r^2\right)\Phi' dr - \int_0^R \frac{\ell(\ell+1)}{G}\Phi'^*\Phi' dr \\ &= \left[\frac{r^2}{G}\frac{d\Phi'^*}{dr}\Phi'\right]_0^R - \int_0^R \frac{r^2}{G}\left|\frac{d\Phi'}{dr}\right|^2 dr - \int_0^R \frac{\ell(\ell+1)}{G}|\Phi'|^2 dr.\end{aligned}$$

In this last equation, using the appropriate boundary condition for the gravitational potential and taking into account the small density at the surface we can say that the first term on the RHS is real. As a consequence, the LHS is real.

Now we can look at the imaginary part of Eq. (2.6.23) remembering that $\sigma = \sigma_R + i\sigma_i$[14] and so that $\Im\left(\sigma^2\right) = 2\sigma_R\sigma_i$ with $\Im$ denoting the imaginary part of a complex quantity. One can write :

$$\begin{aligned}2\sigma_R\sigma_i \int_0^M (|\xi_r|^2 + \ell(\ell+1)|\xi_h|^2)dm = &\int_0^M \Im\left\{\frac{\delta\rho^*}{\rho}\frac{\delta p}{\rho} + \frac{1}{\rho}\left(\xi_r^*\Xi_R^r + \ell(\ell+1)\xi_h^*\Xi_R^h\right)\right\} dm \\ &+ \int_0^M \Im\left\{\frac{2A-1}{A}\frac{p_t}{\rho}\left[\frac{\xi_r^*}{r}\frac{d\xi_r}{dr} + \ell(\ell+1)\frac{\xi_h^*}{r}\left(\frac{\xi_r}{r} - \frac{\xi_h}{r}\right)\right]\right\}.\end{aligned}$$

Out of this result, one can see that the term $-\pi\int_0^M \Im\{\delta\rho^*\delta p/\rho^2\}dm$ is the work done by the system during one cycle of pulsation ([Dupret, 2018]). The study of this work integral in particular will show us the importance of some terms introduced in our treatment of the convection. First of all, we recall here that $\delta p = \delta p_{th} + \delta p_t$ where $p_{th} = p_g + p_R$ is the total pressure (gaseous

[14]To avoid any confusion, let's recall here that σ_i is representing the damping rate of a mode while $-\sigma_i$ corresponds to the growth rate of a mode. Depending on the author, one may find different notation for each of these terms.

and radiative) and p_t is the turbulent pressure. In addition, it can be shown using equations of state that :

$$\frac{\delta p_{th}}{\rho} = (\Gamma_3 - 1)T\delta s + \Gamma_1 \frac{\delta \rho}{\rho}\frac{p_{th}}{\rho}$$

in which Γ_3 represents the third adiabatic exponent and is defined as $\Gamma_3 - 1 = \left.\frac{\partial \ln T}{\partial \ln \rho}\right|_s$. Knowing this, we can write :

$$\begin{aligned}\Im\left(\frac{\delta\rho^*}{\rho}\frac{\delta p}{\rho}\right) &= \Im\left(\frac{\delta\rho^*}{\rho}\frac{\delta p_t}{\rho}\right) + \Im\left(\frac{\delta\rho^*}{\rho}(\Gamma_3 - 1)T\delta s\right) + \Im\left(\Gamma_1\left|\frac{\delta\rho}{\rho}\right|^2\frac{p_{th}}{\rho}\right)\\ &= \Im\left(\frac{\delta\rho^*}{\rho}\frac{\delta p_t}{\rho}\right) + (\Gamma_3 - 1)\Im\left(\frac{\delta\rho^*}{\rho}T\delta s\right)\end{aligned} \tag{2.6.24}$$

where the third term on the RHS in the first line is only composed of real quantities and thus has no imaginary part. In Section 2.5, we had determined the perturbed equation of energy conservation Eq. (2.5.25). If we only consider the radial case for ease, the equation of energy conservation becomes :

$$T\delta s = \frac{i}{\sigma}\left[\frac{d\delta(L_c + L_R)}{dm} - \delta\epsilon - \delta\left(\overline{\epsilon_2 + \mathbf{V}\cdot\frac{\nabla p_{th}}{\rho}}\right)\right].$$

This expression is then injected in Eq. (2.6.24) and gives :

$$\Im\left(\frac{\delta\rho^*}{\rho}\frac{\delta p}{\rho}\right) = \Im\left(\frac{\delta\rho^*}{\rho}\frac{\delta p_t}{\rho}\right) + (\Gamma_3 - 1)\Re\left(\frac{\delta\rho^*}{\rho}\frac{1}{\sigma}\left[\frac{d\delta(L_c + L_R)}{dm} - \delta\epsilon - \delta\left(\overline{\epsilon_2 + \mathbf{V}\cdot\frac{\nabla p_{th}}{\rho}}\right)\right]\right).$$

Using Eq. (2.6.18) and assuming $A = 1/2$ (isotropic turbulence) we see that :

$$\Re\left(\frac{\delta\rho^*}{\rho\sigma}\delta\left(\overline{\epsilon_2 + \mathbf{V}\cdot\frac{\nabla p_{th}}{\rho}}\right)\right) = \frac{3}{2}\Im\left(\frac{\delta\rho^*}{\rho}\frac{\delta p_t}{\rho}\right). \tag{2.6.25}$$

Gathering all the different terms we can write the work integral as follows :

$$W = -\pi\int_0^M \left\{\left(1 - \frac{3}{2}(\Gamma_3 - 1)\right)\Im\left(\frac{\delta\rho^*}{\rho}\frac{\delta p_t}{\rho}\right) + (\Gamma_3 - 1)\Re\left(\frac{\delta\rho^*}{\rho\sigma}\left[\frac{d\delta(L_c + L_R)}{dm} - \delta\epsilon\right]\right)\right\} dm. \tag{2.6.26}$$

The first part on the RHS is of huge interest for us. Indeed, hidden in this term we find the perturbation of turbulent pressure and the perturbation of dissipation rate of turbulent kinetic energy. Both appear with an opposite sign meaning that their action on the work integral is also opposite. As the work integral reflects the damping or growing rate of modes, we clearly understand that both the turbulent pressure and the dissipation rate are of huge importance if we want to know the stability of a mode.

An interesting situation deserves to be mention : if the gas is considered totally ionised with a negligible radiative pressure, the third adiabatic exponent becomes $\Gamma_3 - 1 \simeq 2/3$. In this particular but still realistic case, both effects are compensating each other perfectly. As a consequence, we do understand that if we take into account one the term, the others should also be included. In addition, the importance in the choice of Γ_3 and A is not negligible.

One additional remark is worth mentioning concerning this time the second part of the work integral ([Dupret, 2018]). In fact we can also express the second part as follows :

$$(\Gamma_3 - 1)\Re\left(\frac{\delta\rho^*}{\rho\sigma}\left[\frac{d\delta(L_c + L_R)}{dm} - \delta\epsilon\right]\right) = \Re\left(\frac{1}{\sigma}\left[\frac{d\delta(L_c + L_R)}{dm} - \delta\epsilon\right]\frac{\delta T^*}{T}\right) \tag{2.6.27}$$

using the succeeding thermodynamics relation : $(\Gamma_3 - 1)\delta\rho^*/\rho = \delta T^*/T - \delta s^*/c_v$. If one now looks at the work integral and takes into account the two expressions for the second part of it expressed just before, we can deduce that in order to have a vibrationally unstable mode ($W > 0$) both $\delta T^*/T$ and $(\delta\epsilon - d\delta L/dm)$ need to be in "phase". That is, during the hot phase of the oscillation $\delta T^*/T > 0$ (or in other words during the maximum of compression $\delta\rho^*/\rho > 0$) the star needs to accumulate heat $(\delta\epsilon - d\delta L/dm) > 0$. This situation is quite similar to the condition imposed to a thermodynamic cycle to be considered as a heat engine (the Carnot cycle is a good example). Indeed, for a cycle to be considered as a heat engine, heat must be provided to the gas during the hot phase (after the maximum of compression) and evacuated during the cold phase (after the maximum of expansion). Back in stars and more especially in the convective envelope of white dwarfs stars where the energy production from nuclear reactions can be neglected, this damping or excitation of modes can be understood easily by considering one layer of matter : at compression $\delta\rho^*/\rho$ is positive and so if $d\delta L/dm$ is positive it means that more energy will leave the top of the layer than what will come from the bottom of it. As a result, this layer will suffer a net energy loss and mode will be damped. On the contrary, if $d\delta L/dm$ is negative, more energy will enter than leave this portion of matter giving a net excess of energy leading to the possible excitation of the oscillations. In the case of white dwarfs, we will see later that it is in regions close to the base of the convection zone that the strongest effect on the excitation of the modes will be observed.

2.7 3D hydrodynamical stellar simulations

So far, the theory that has been presented and which is based on the relatively simplistic mixing length theory treats convection as a one-dimensional phenomenon. Although the predictions resulting from this theory have encounter some successes (as we will see in the following chapter), it is clear that the description of such a complex phenomenon that is convection with a one-dimensional model relying on so many approximations cannot give the most realistic results. Indeed, a better approach to describe convection which is by itself a non local, time-dependent and three-dimensional phenomenon would be the use 3D hydrodynamical simulations. For these reasons, we have also included in our study some models partially based on 3D simulations computed with the CO^5BOLD code (which was developed by [Freytag et al., 2012]) in the hope of finding more accurate predictions. In this section, we first give some explanations on the working of the CO^5BOLD code. After that, we will present some major differences between quantities obtained from 1D MLT models and 3D simulations computed with the CO^5BOLD code.

This code performs realistic simulations as it is able to reproduce what is observed relatively well. In fact, it takes into account a good description of the microphysics present in stars with the adequate equation of state and optical properties of the matter. As detailed in [Freytag et al., 2012][15], the hydrodynamics equations that are solved are written in terms of the mass density ρ, the three momentum densities $\rho v_1, \rho v_2, \rho v_3$ (the three subscripts represent the coordinate axes) and the total energy density per volume e_{tot}. These three equations are the mass conservation equation :

$$\frac{\partial \rho}{\partial t} + \frac{\partial \rho v_1}{\partial x_1} + \frac{\partial \rho v_2}{\partial x_2} + \frac{\partial \rho v_3}{\partial x_3} = 0,$$

[15] using its notation

the momentum equation :

$$\frac{\partial}{\partial t}\begin{pmatrix}\rho v_1\\ \rho v_2\\ \rho v_3\end{pmatrix}+\frac{\partial}{\partial x_1}\begin{pmatrix}\rho v_1 v_1+P\\ \rho v_2 v_1\\ \rho v_3 v_1\end{pmatrix}+\frac{\partial}{\partial x_2}\begin{pmatrix}\rho v_1 v_2\\ \rho v_2 v_2+P\\ \rho v_3 v_2\end{pmatrix}+\frac{\partial}{\partial x_3}\begin{pmatrix}\rho v_1 v_3\\ \rho v_2 v_3\\ \rho v_3 v_3+P\end{pmatrix}=\begin{pmatrix}\rho g_1\\ \rho g_2\\ \rho g_3\end{pmatrix}$$

and the energy equation :

$$\frac{\partial \rho e_{tot}}{\partial t}+\frac{\partial(\rho e_{tot}+P)v_1}{\partial x_1}+\frac{\partial(\rho e_{tot}+P)v_2}{\partial x_2}+\frac{\partial(\rho e_{tot}+P)v_3}{\partial x_3}+\frac{\partial F_{1rad}}{\partial x_1}+\frac{\partial F_{2rad}}{\partial x_2}+\frac{\partial F_{3rad}}{\partial x_3}=0$$

where $F_{1rad}, F_{2rad}, F_{3rad}$ are the radiative energy flux components, P is the sum of the gas and radiation pressures and is computed via an equation of state tabulated in the form $P = P(\rho, e_{int})$ with e_{int} the internal energy per unit mass. The radiative flux vector is obtained by solving the radiative transfer equation along a limited set of directions. In addition, the three previous equations are then solved by CO^5BOLD. The total energy density can be expressed differently using the equation for the total energy :

$$\rho e_{tot} = \rho e_{int} + \rho\frac{v_1^2+v_2^2+v_3^2}{2} + \rho\Phi$$

where Φ is the gravitational potential. The gravity field is given in our case by :

$$\begin{pmatrix}g_1\\ g_2\\ g_3\end{pmatrix} = -\begin{pmatrix}\frac{\partial}{\partial x_1}\\ \frac{\partial}{\partial x_2}\\ \frac{\partial}{\partial x_3}\end{pmatrix}\Phi.$$

Two different types of models can be considered: local models or global models. In our case, we will only focus on local models (box-in-a-star models) as these are already sufficient to solve our problem because we are only interested in a limited area. This simplifies the problem as we can neglect the effects of the spherical geometry and also the variations in gravity. Concerning the boundary conditions, several configurations are possible. While the side boundaries are as most of the time periodic, the top boundary is considered open to flows and lets material (or radiation) fall back into the model. For the bottom boundary, as in white dwarfs it is located deep in the convection zone where we know that the entropy of the material reaches an asymptotic value (as we will see a bit later, this idea was demonstrated by [Ludwig et al., 1999]), we can constrain with an open bottom the entropy of the ascending material and thus ensure a zero total mass flux.

As an example of result obtained at the end of a simulation, the final snapshot for a white dwarf of $T_{\mathsf{eff}} = 12\ 000$ K and $\log g = 8$ is presented in Fig. 2.1 (taken from [Tremblay, P.-E. et al., 2013]). A remark that is worth mentioning concerns the size of these convective cells. Indeed, we have already mentioned in a previous section that the Reynolds number is very large in the convection zone. This immense Reynolds number leads to a highly turbulent flow and in that case, the turbulent kinetic energy is dissipated into heat at the Komolgorov microscale ($\ell = H_p Re^{-3/4}$) which is of the order of the centimetre. With the current simulations, the spatial resolution is of course not good enough to be able to represent such small characteristics. Accordingly, the simulations usually follow the large-eddy approach to overcome this problem. In this approach, only the largest structures are considered while the dissipation of turbulent kinetic energy is taken into account by the numerical scheme (giving rise to unrealistic high value of the viscosity).

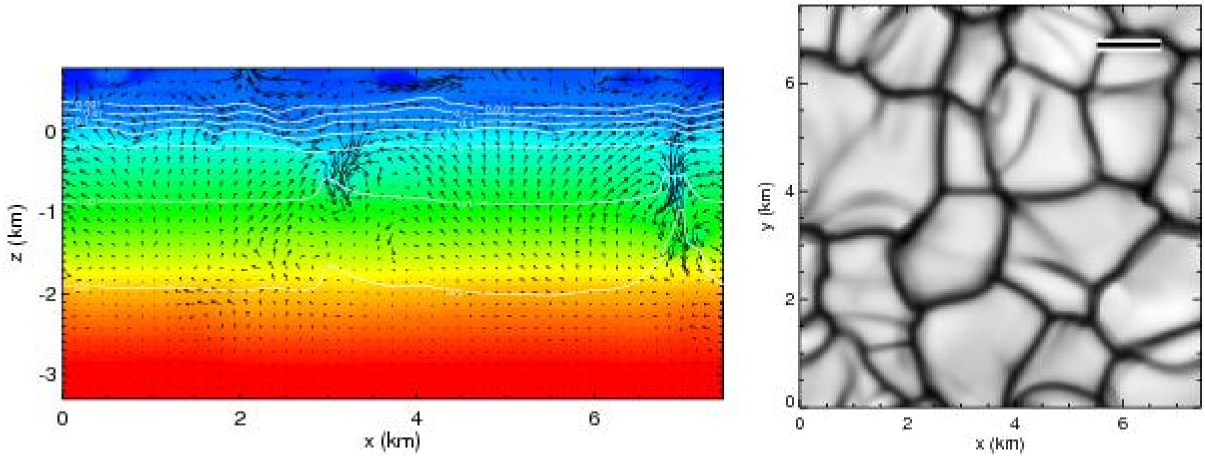

Figure 2.1: *Left panel:* slice in the horizontal-vertical xz plane with the temperatures colour coded from 14 000 K in red to 3 000 K in blue. The arrows represent the relative convective velocities. *Right panel:* Emergent continuum intensity at the top of the horizontal xy plane. Image taken from [Tremblay, P.-E. et al., 2013]

Now that we have briefly described the working of the CO^{5}BOLD code, we are going to look at some physical quantities that are of interest. But before, we should recall the definition of convective layers and where they can appear. To define a convective layer we use the Schwarzschild criterion which states that a layer is convectively unstable if

$$\nabla_{rad} > \nabla_{ad}$$

where $\nabla_{rad} = \frac{3\kappa pL}{16\pi acGmT^4}$ is the radiative gradient (the gradient required to transport the entire luminosity by radiation) and ∇_{ad} is the adiabatic gradient. When this condition is verified, the temperature gradient required to transport energy only by radiation is too steep and so convection takes place. The Schwarzschild criterion directly gives information on the regions where we can expect to find convective layers, namely in regions where the radiative gradient is large. More precisely, several quantities can lead to the creation of a convective envelope. For instance, in the superficial layers, as the opacity becomes larger one may expect a convective envelope to develop as κ directly appears in the expression of the radiative gradient. In addition to that, relatively cool stars are also good candidates to have a convective envelope. Indeed, as the temperature becomes smaller, the radiative gradient grows larger and so the Schwarzschild criterion is verified. This is exactly the case of ZZ Ceti white dwarfs which have a large opacity because of the recombination of H atoms and a low effective temperature.

Concerning some properties of the deep convection zone, we can look at the entropy which represents an interesting case and is one of the most important parameter as it uniquely determines the effective temperature of our 3D model [Ludwig et al., 1999]. In Fig. 2.2, the red solid line represents the mean entropy profile obtained from 3D simulations over constant geometrical depth. The local 3D values of the entropy in convective structures as a function of geometrical depth are represented by black dots. What is striking with the local values is the important fluctuations appearing at all depths. Besides, we clearly see that there is an asymptotic value which seems constant in the subsurface layers. The explanation for this was developed by [Ludwig et al., 1999] and consists in the following : in central regions of large ascending flows (as it is the case in the majority of the convection zone), the gas is thermally isolated from its surroundings and cannot be influenced by low entropy flows or radiative losses until it reaches the beginning of the radiative surface layers (the entropy is thus nearly constant and equal to

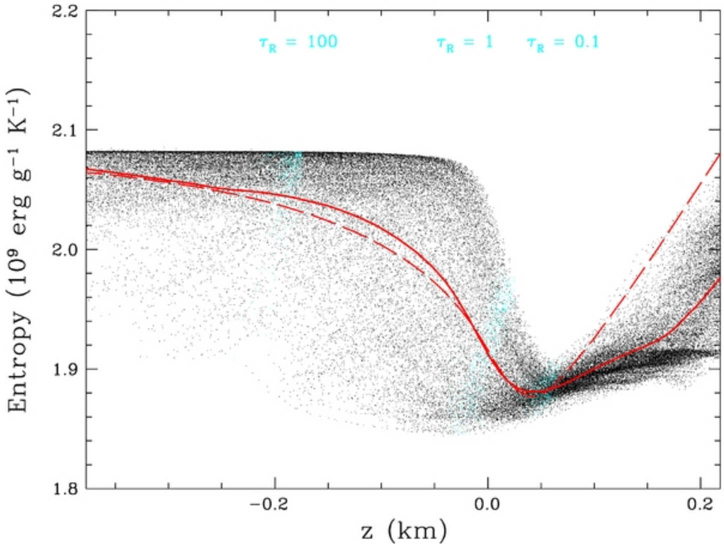

Figure 2.2: Depth dependence of the entropy in the solar surface layers as obtained from 3D simulations at $T_{\mathrm{eff}} = 10\ 025$ K and $\log g = 8$. Black dots represent the local 3D entropy values, the red solid line is the averaged entropy profile and the dashed red line is the 1D entropy with the MLT parametrization calibrated from 3D simulations. Image taken from [Tremblay et al., 2015].

the asymptotic value there). This asymptotic value is extremely powerful as it gives us valuable information coming directly from the bottom of the convection zone. This is not visible when considering averaged 3D values as we can see in Fig. 2.2 with the solid red line because the mean values take into account radiative losses for example. The red dashed line represents the entropy obtained from a 1D MLT model calibrated on 3D simulations, we see that its value is close to the one of the mean 3D values and more especially as we go towards the base of the convective zone.

Now that we have introduced 3D hydrodynamical simulations, we can illustrate some additional differences in the results obtained with them compared to those acquired from one-dimensional models. Fig. 2.3 (taken from [Tremblay et al., 2015]) shows the vertical rms velocity in function of the temperature (the surface is towards the left side). The red line is for 3D simulations at $\log g = 8$, the dotted black line represents 1D model calibrated for the Schwarzschild boundary (defined from the Schwarzschild criterion introduced in a previous paragraph) while the dashed blue line is for 1D model calibrated on the flux boundary. The position of the Schwarzschild boundary is indicated by open circles. But as we already know, at the base of the convection zone, the downwards flows of convective elements still have large inertia. In consequence, as they are also denser than the surrounding, they still possess an acceleration once the Schwarzschild boundary is passed. For that reason, a positive flux is also present below the convection zone and we can define the bottom of this region as the flux boundary (filled circles).

Finally, Fig. 2.4 shows the mean 3D convective flux profiles (solid red line) as well as the profiles obtained from 1D calibrated models (dotted black for a calibration matching Schwarzschild boundary and dashed blue for matching the flux boundary). We can see on this figure a negative flux (i.e. a flux going downwards) for 3D simulations. In fact, this flux is caused by downdrafts (which are warmer than the surrounding medium) still active after the flux boundary as their momentum remains non negligible. This "negative" flux remains nevertheless relatively small compared to the total flux and its effect on the structure rapidly becomes small.

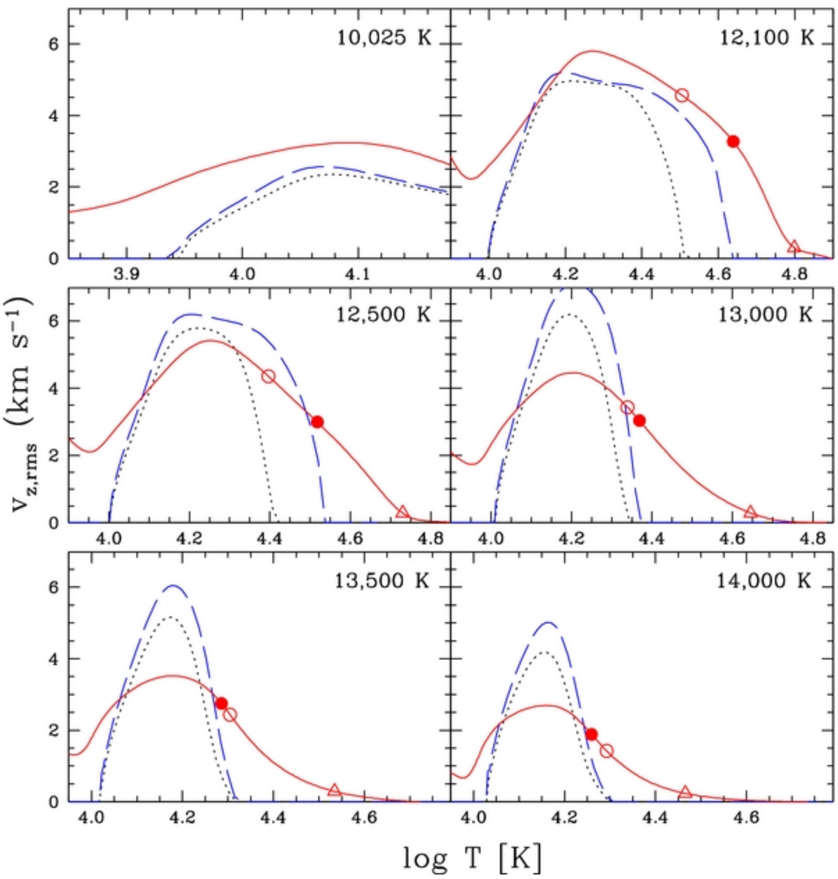

Figure 2.3: Vertical rms velocity for 3D simulations at $\log g = 8$ (solid red line) at different effective temperatures. The position of the Schwarzschild boundary is indicated by open circles while the position of the flux boundary is represented by filled circles. 1D model atmospheres calibrated for the Schwarzschild boundary (dotted black) and flux boundary (dashed blue) are also illustrated. Image taken from [Tremblay et al., 2015].

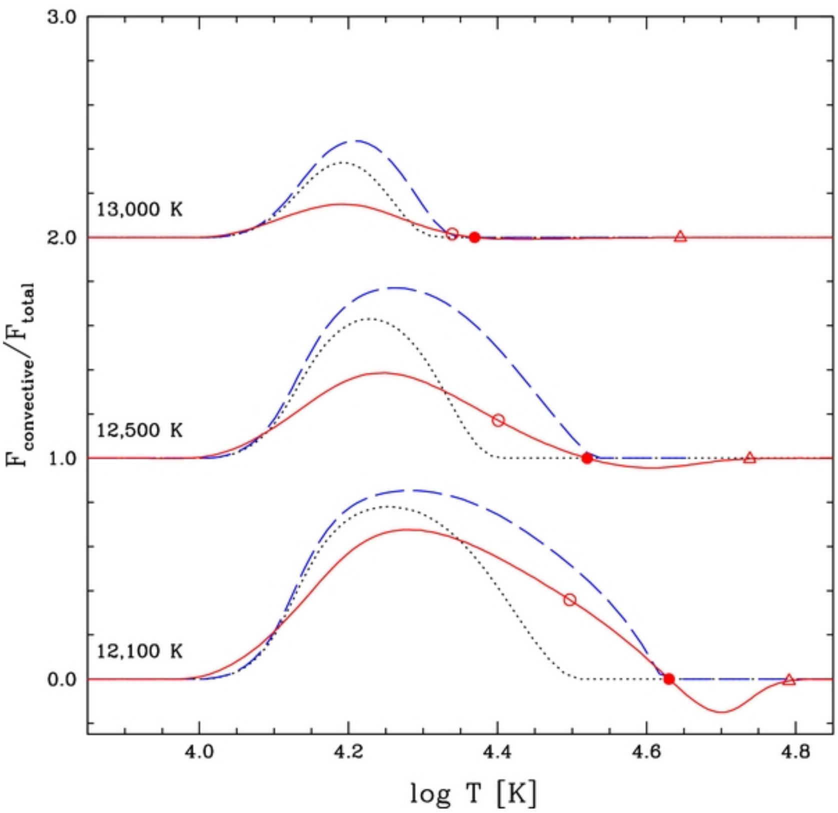

Figure 2.4: Ratio between the convective flux and the total flux as a function of the logarithm of the temperature at $\log g = 8$. The same colour code as in Fig. 2.3 is used. Image taken from [Tremblay et al., 2015].

Chapter 3

The instability strip of ZZ Ceti white dwarfs

In the previous chapter, a theory describing interaction between convection and pulsation has been presented based on the original idea of [Unno, 1967], which was developed by [Gabriel et al., 1974] and then improved by [Grigahcène et al., 2005]. In addition to their developments, we have introduced some new parameters in the closure equations (as suggested in [Dupret et al., 2006]) that are going to be useful when taking into account 3D hydrodynamic simulations. However, this theory is not perfect for different reasons : one of them and certainly the most relevant is that we are still working in the framework of the mixing-length theory. For that reason, we should not expect our local 1D models to give us a precise description of convection and thus on its influence on the pulsations as many phenomena have been since the beginning simplified or just ignored throughout the great number of approximations taken. Accordingly, we have in the last section of the previous chapter talked about the possible improvements using 3D hydrodynamical simulations and we are going to make use of them in this chapter.

More pragmatically, our aim in this work is to see whether the improvements that were brought to the theory are able to reproduce with a better fidelity the theoretical location of the ZZ Ceti white dwarfs instability strip (see Fig. 1.1). And more especially the red edge localization which seems more challenging to obtain theoretically. But first, we should justify our use of time-dependent convection (TDC) models. In fact, many authors have first tried to reproduce this instability trip using the frozen convection (FC) approximation where the convective flux variations due to pulsations are neglected (see [Winget et al., 1982] or [Starrfield et al., 1982] just to name these two) and it seems that even if it was a crude approximation, the results they obtained were not so far from the ones found using a more evolved time-dependent theory as in [Van Grootel, V. et al., 2012]. Still, as the typical pulsation periods[1] can be much greater (as it is the case at the blue edge) or of the same order (at the red edge) compared to the typical lifetimes of the convective elements τ_c as can be seen in Fig. 3.1, convection will most of the time have an impact on the pulsations and cannot be regarded as *frozen*. This clearly justifies the use of time-dependent convection treatment as we did.

In Fig. 3.2 we present for comparison purposes between FC and TDC treatments two eigenfunctions of a same mode, from the centre (left) to the surface (right) computed at the blue edge (T_{eff} = 12 000 K) : the left panel shows the real part of the entropy variations $\Re(\delta s)$ while on the right panel we present the work integral W. In Eq. (2.6.26) we obtained an integral expression relating the growth rate to the eigenfunctions. We define the work integral as the function obtained by replacing in this expression the integration over the full star by an

[1] In ZZ Ceti white dwarfs, the typical periods are between 100 and 1500 s [Van Grootel, V. et al., 2012]

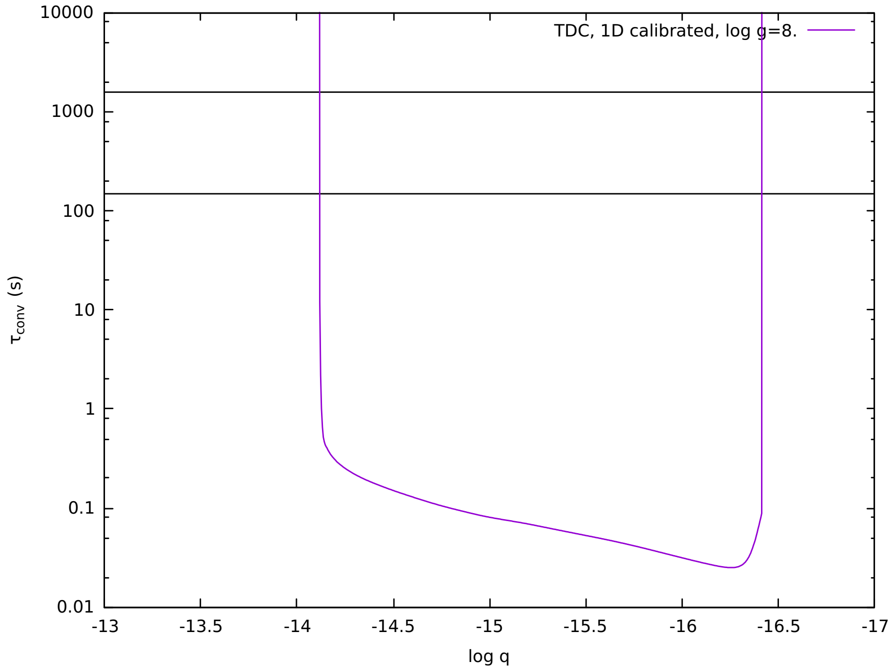

Figure 3.1: Convective lifetime τ_c of a $\log g = 8$ white dwarf model on the blue side ($T_{\text{eff}} = 11$ 500 K) as a function of the logarithm of the mass fraction $\log q = \log(1 - m(r)/M)$. The centre of the star on this scale is at $\log q = 0$. The two horizontal lines at 150s and 1600s represent the typical range of pulsation periods of such a model. The convection zone lies between $\log q =$ -14.1 and $\log q =$ -16.4 .

integration from the center to any layer. W(m) is thus the work performed by the sphere of mass m inside the star during one oscillation cycle. The study of eigenfunctions is interesting as it gives us more information on the driving or damping of modes computed from different models. For the work integrals (which are normalized), the sign of the slope at a given depth tell us if a mode is locally driven or damped. If the slope is positive then the mode is driven while it is damped if the slope is negative. More generally, if the last value of the work integral is positive it means that the mode is globally excited and if its value is negative the mode is globally damped (we normalize W in the figures so that this surface value is the growth rate multiplied by the dynamical time $t_{dyn} = \sqrt{R^3/GM}$, in that way we are able to compare the results obtained).

Finally, one can note that the maximum driving occurs near the base of the convection zone. In the right panel of Fig. 3.2 we already see a huge difference between a FC and TDC treatment of the convection as with the former one we obtain a mode that is globally damped while with a TDC treatment we have an excited mode at the end. In addition, with the base of the convection zone located at around $\log q =$ -14, we conclude that the driving in the case of the TDC treatment is taking place a bit deeper in the star (just below the bottom of the convection zone) leading to a even more excited mode. These observations however are mostly visible at the blue edge and the dissimilarities between FC and TDC treatments tend to disappear as we look at lower effective temperatures (as illustrated in [Van Grootel, V. et al., 2012]). The left panel of Fig. 3.2 also shows two distinct behaviours of $\Re(\delta s)$. The main difference comes from the fact that, as shown just above, the convective lifetime is much smaller than the pulsation period at the blue edge. As a consequence, convection will adapt quasi instantaneously to the oscillations which is forbidden in a FC treatment but well authorized to happen in TDC models. Besides, as the superadiabatic gradient is extremely small in the deep regions (see Fig. 3.5), convection is very efficient there and so a small entropy gradient is sufficient to transport energy. This leads to the formation of a plateau of δs in the case of the TDC treatment as the entropy gradient is limited in this case (this plateau can move up and down with the oscillations) while in the FC treatment, the entropy gradient can take any (unrealistic high) value. However, even if the entropy gradient is smaller in the TDC treatment in the upper part of the convection zone, we see that at its base, there is a gain of heat ($\rho T \delta s$) greater than within the FC approximation. As a result, more energy is available and can be transformed in mechanical work leading to a more efficient driving of the oscillations. And indeed this is what we can observe in Fig. 3.2. To be more complete, we also have to take into account the fact that the upper part has much less influence on the excitation as the temperature and density dropped rapidly towards the surface. In addition, if we now consider the effective temperature of a model, this effect is mainly important at high effective temperatures (at the blue edge thus) but becomes less significant when going to the red edge as the convection zone goes deeper into the star leading to higher temperatures and densities inducing thus a $\rho T \delta s$ quite similar both in FC and TDC treatments (see [Van Grootel, V. et al., 2012]). This concludes our discussion on the differences that exist between FC and TDC treatments.

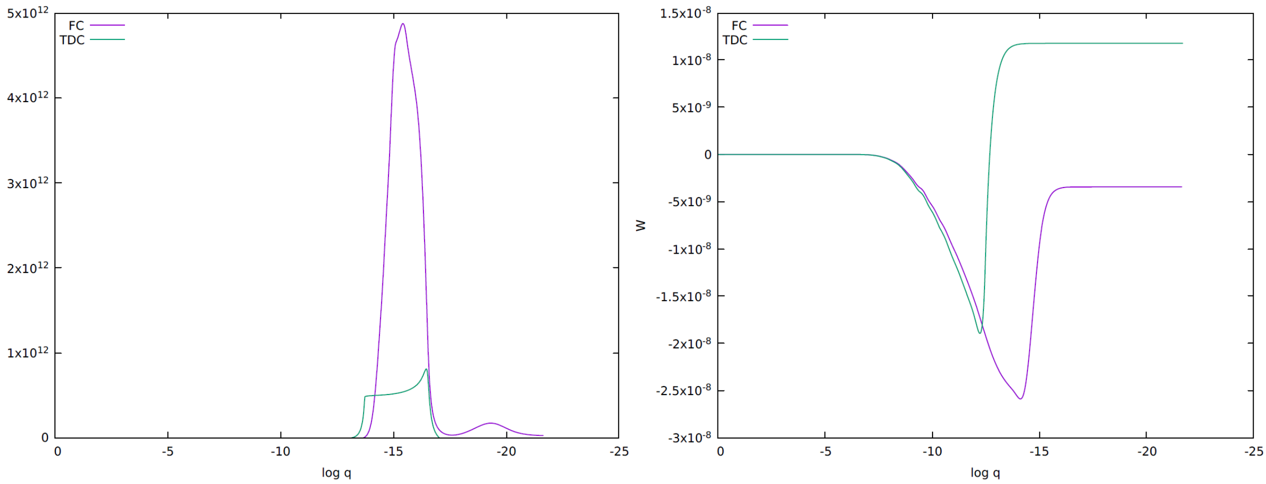

Figure 3.2: *Left panel:* entropy variations $\Re(\delta s)$ for a $\log g = 8$ white dwarf model with $T_{\text{eff}} =$ 12 000 K ($\ell = 1$, g_5 mode). *Right panel:* work integrals of the same mode

A final remark deserves to be made concerning the parameter β which was introduced in Eq. (2.6.4). Even if for simplicity we had omitted to use this parameter in the rest of the theoretical developments, in practice its use is necessary if one wants to avoid some non-physical unstable modes and oscillations in the work integral. As explained back in that section, we have chosen in all our calculations $\beta = (1, -1)$ which seems to work quite well ([Grigahcène et al., 2005] and [Van Grootel, V. et al., 2012]).

3.1 1D models

The beginning of our work consists in doing something similar to what was achieved in [Van Grootel, V. et al., 2012]. Namely we have applied the non-adiabatic code MAD which takes into account the TDC treatment to different white dwarf models to see how pulsation reacts to convection. In practice, we have first used the ML2 version of the MLT which sets the mixing length parameter $\alpha = 1$ and takes into account the following values for the numerical parameters : $a = 1$, $b = 2$ and $c = 16$. We do not take for now in consideration the perturbations of the turbulent pressure p_t or of the dissipation rate of turbulent kinetic energy into heat per gram ϵ_2 or any other improved models based on 3D simulations. This will come in the following section.

We applied the code to $\log g = 8$ (corresponding more or less to white dwarfs with a mass of $0.6M_{\odot}$) white dwarf models with an effective temperature varying from 14 000 K to 6 000 K by step of 500 K. The results obtained are quite comparable with the ones found by [Van Grootel, V. et al., 2012], with in our case less white dwarf models employed for time restriction. The results we obtained are illustrated in Fig. 3.3 which shows the spectrum of $\ell = 1$ excited g-modes. At different effective temperatures ($T_{\text{eff}} = 10$ 000 K, 8 500 K, 8 000 K and 7 500 K), white dwarf evolutionary models did not converge correctly and gave the temperature of the models used just before. For that reason and to avoid non-physical results we did not use the data obtained at these temperatures in our plots. Apart from that, we have found something similar to the Fig. 7 of [Van Grootel, V. et al., 2012] with the same conclusions that can be drawn. Firstly, the theoretical blue edge of the instability strip found here at $T_{\text{eff}} = 12$ 000 K is relatively similar to the empirical blue edge (see Fig. 1.1). Secondly, and this is certainly the biggest issue, the theoretical red edge predicted by our models is far from being close to the one observed. Indeed, we find excited modes down to $T_{\text{eff}} = 7$ 000 K while the empirical value is of the order of $T_{\text{eff}} = 11$ 000 K for a model of that mass. With a difference of several thousands of degrees in the effective temperature, we see that this approach with a parametrized 1D ML2/α=1.0 model is totally insufficient to reproduce the observed red edge.

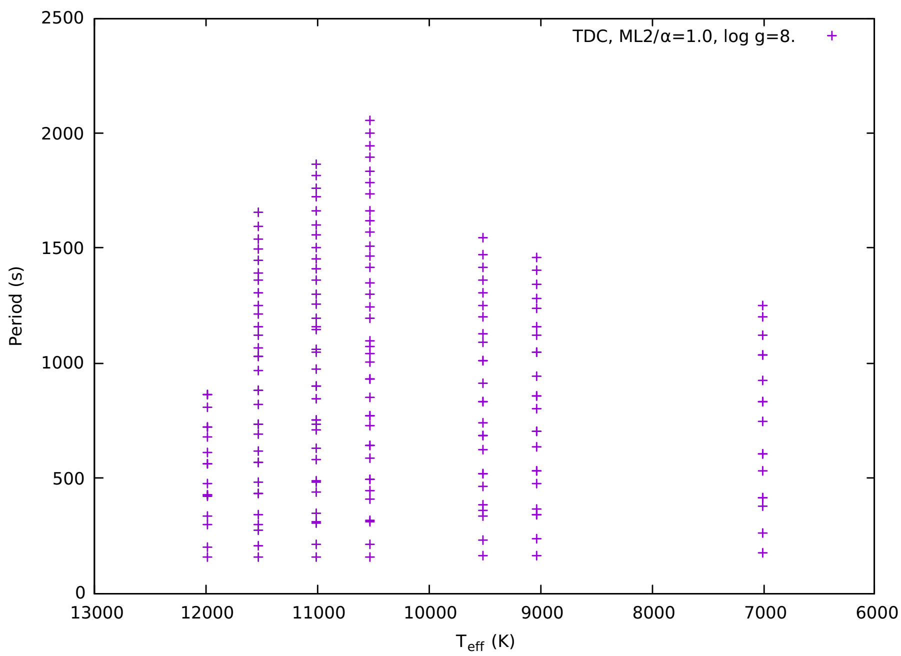

Figure 3.3: Periods in seconds obtained for the unstable $\ell = 1$ g-modes at various temperatures using our TDC treatment with the ML2/α=1.0 version of the MLT for a $\log g = 8$ white dwarf.

3.2 From 1D to 3D models

As a first step (cf. previous section) we have used models based on the ML2 flavour of the MLT fixing to 1.0 the mixing length parameter. However, we could not predict correctly the value of the red edge with this method. Indeed, we used in this case a 1D treatment of the convection but as introduced in Section 2.7, 3D simulations are able to give a much more realistic description of the convection. This is why we have also tried to use two other types of models relying more on 3D simulations with the hope of finding results closer to the empirical boundaries.

The first one is based on the calibration of the mixing length parameter α using 3D simulations in the upper part of the white dwarf as it was done in [Tremblay et al., 2015]. Indeed, in the basic 1D model, we have arbitrarily set the value of the mixing length parameter equal to one following the ML2 but a better suited value for α can be found. Basically, α is calibrated from comparisons between 3D simulations and a grid of 1D envelopes with a varying mixing length parameter. The α chosen is the one that fits the best the results obtained for the temperature and the pressure from 3D simulations at the bottom of the 3D simulation. Its value is then used to compute 1D MLT envelopes. In this approach, 3D simulations are only used to fit a parameter in the 1D models and once α is calibrated, the different quantities are deduced from this new calibrated 1D MLT model. As we will see, the results obtained are already closer to the case of a full 3D treatment but some discrepancies remain. In the future, when we will refer to these 1D models fitting 3D simulations we will talk about " *1D calibrated* models ".

The second idea is again based on the use of 3D simulations but in a greater extent. This time we use the free parameters Ω and α at our disposal to try to fit to the averaged quantities obtained from 3D simulations in the upper envelope. We thus try to reproduce with our 1D MLT models what is obtained directly from the 3D stratification in the lower regions of the convection zone and we directly use the results obtained from 3D simulations in the upper part. It differs from the previous 1D calibrated models in the sense that in the previous case, once α was calibrated, all the quantities obtained in the envelope were coming from 1D models independently of the results of 3D simulations. In what follows, we will name these models "*3D*". In deeper regions, we use back the 1D MLT as 3D simulations do not have a huge effect there. As a result, there is a matching point between 1D and 3D models. Most physical quantities are computed and fitted in order to avoid any discontinuity. However, as we will see, it is not always possible and especially for derived quantities. To sum up, this type of "patched" model consists in a combination of a 1D MLT treatment in the inner part on one hand and temporal and horizontal averages of 3D hydrodynamical simulations for the upper-surface layers on the other hand.

Using 3D simulations and doing pertinent averages we can then obtain some important quantities such as the convective flux F_c, the turbulent pressure p_t or the superadiabatic gradient $(\nabla - \nabla_{ad})$. All these quantities have values different from what we had in the framework of the MLT. Once their values are obtained, we can inject them in different equations in order to obtain γ, α and finally Ω. With these fitted parameters, we then get a more generalized MLT giving results closer to what is obtained from 3D hydrodynamical simulations. For γ, we use the expression of the turbulent pressure (Eq. (2.3.3)) and the definition of the convective efficiency γ given by $\gamma = \tau_R/\tau_c = \tau_R V/l$. Replacing τ_R by its value obtained in the previous chapter (Eq. (2.2.11)) and taking into account Eq. (2.4.26) we have :

$$\begin{aligned}\gamma &= \frac{c_p\,\rho^2 l\,\kappa}{c\,\sigma\,T^3}V \\ &= \frac{c_p\,\rho^2 \alpha\,H_p\,\kappa}{c\,\sigma\,T^3}\sqrt{\frac{2}{\rho}}p_t^{1/2}.\end{aligned}$$

Combining the previous equation and the equation of the turbulent pressure we obtain :

$$\frac{p_t}{\gamma^2} = \frac{\frac{A}{(A+1)\Lambda}\frac{1}{2}\frac{P_T}{P_\rho}p}{\left(\frac{c_p\,\rho^2\,H_p\,\kappa}{c\,\sigma\,T^3}\right)^2\frac{2}{\rho}p_t}\frac{\gamma}{\gamma+1}(\nabla - \nabla_{ad}) \tag{3.2.1}$$

which gives the following relation for γ :

$$\chi\gamma^3 = \gamma + 1 \tag{3.2.2}$$

where

$$\chi = \frac{\frac{A}{(A+1)\varLambda}\frac{1}{2}\frac{P_T}{P_\rho}p(\nabla - \nabla_{ad})}{\left(\frac{c_p\,\rho^2\,H_p\,\kappa}{c\,\sigma\,T^3}\right)^2 \frac{2}{\rho}p_t^2} = \frac{\frac{A}{(A+1)\varLambda}\frac{1}{4}(c\,\sigma)^2\frac{P_T}{P_\rho}(\nabla - \nabla_{ad})}{\left(\frac{c_p\,\kappa}{T^3\,g}\right)^2 p\,\rho\,p_t^2}$$

is a quantity that can be computed from the averaged quantities obtained with 3D simulations. Once we have determined γ by resolving Eq. (3.2.2), we can easily establish the relation for α. Indeed, isolating α in Eq. (3.2.1) one gets :

$$\alpha = \frac{\gamma\,c\,\sigma\,T^3\,g}{c_p\,\rho\,\kappa\sqrt{2\rho\,p_t}}.$$

Finally, as soon as γ and α are determined thanks to the previous relations, we can find the value of $\varOmega$ using this time the definition of the convective flux (Eq. (2.4.22)) given by :

$$F_c = \frac{\varOmega}{2}\alpha\rho\frac{l}{\tau_c}c_pT\frac{\gamma}{\gamma+1}(\nabla - \nabla_{ad}).$$

We then isolate $\varOmega$ in this expression and we get :

$$\begin{aligned} \varOmega &= 2F_c\frac{\gamma+1}{\gamma(\nabla - \nabla_{ad})\alpha\,\rho\,l\,f_c\,c_p\,T} \\ &= \frac{2}{\alpha}F_c\frac{1}{\rho\,l\,f_c\,c_p\,T}\frac{\gamma+1}{\gamma}\frac{1}{\nabla - \nabla_{ad}} \end{aligned} \tag{3.2.3}$$

where $f_c = 1/\tau_c = V/l = \frac{\sqrt{2p_t/\rho}}{\alpha H_p}$ is the inverse of the convective lifetime.

Nonetheless, using quantities obtained from 3D simulations as such is not all we can do to improve the accuracy of the results. One can also look at the non-local aspects. Actually, if one uses directly the results acquired from 3D simulations (F_c, p_t, $(\nabla - \nabla_{ad})$ and the other thermodynamics quantities) to solve Eqs. (3.2.2) (3.2.1) (3.2.3), the approach would only be local. But as convection is a non-local process[2], we will try to take it into account. As it was introduced in [Spiegel, 1963], one can see the following non-local approach as an analogy to the radiative transfer treatment. To keep it simple, we consider that the local solutions (obtained from the MLT and noted with the subscript "l") are similar to source terms while the non-local solutions (noted with "nl" as subscript) are averages obtained using these two expressions :

$$\begin{aligned} p_{t,nl}(\zeta_0) &= \int_{-\infty}^{+\infty} p_{t,l}\exp(-b|\zeta - \zeta_0|)d\zeta, \\ F_{c,nl}(\zeta_0) &= \int_{-\infty}^{+\infty} F_{c,l}\exp(-a|\zeta - \zeta_0|)d\zeta \end{aligned}$$

where $d\zeta = dr/l$ with l being the mixing length. a and b are free non-local parameters (introduced by [Balmforth, 1992]). One can then take the second order derivative of these quantities which gives :

$$\begin{aligned} d^2p_{t,nl}/d\zeta^2 &= b^2(p_{t,nl} - p_{t,l}), \\ d^2F_{c,nl}/d\zeta^2 &= a^2(F_{c,nl} - F_{c,l}). \end{aligned} \tag{3.2.4}$$

[2] Indeed, one cannot consider a local treatment as the greatest turbulent movements are greater than the scale height of the mean stratification ([Dupret et al., 2006])

With these new ideas in mind, if one obtains, by taking horizontal and time averages from 3D simulations, quantities such as the turbulent pressure or the convective flux then they will be regarded as non-local quantities. To find their local counterparts that are needed to determine (γ, α and Ω), the non-local values are directly injected into the system of Eqs. (3.2.4). However, to solve this system we have to know beforehand the values of the free parameters a and b. This can be done by looking at the overshooting region : in this region, the local quantities disappear (see Fig. 3.4 for example) so that the two parameters can be obtained simply by fitting an exponential function to the non-local quantities acquired from 3D simulations. The overshooting region (i.e.

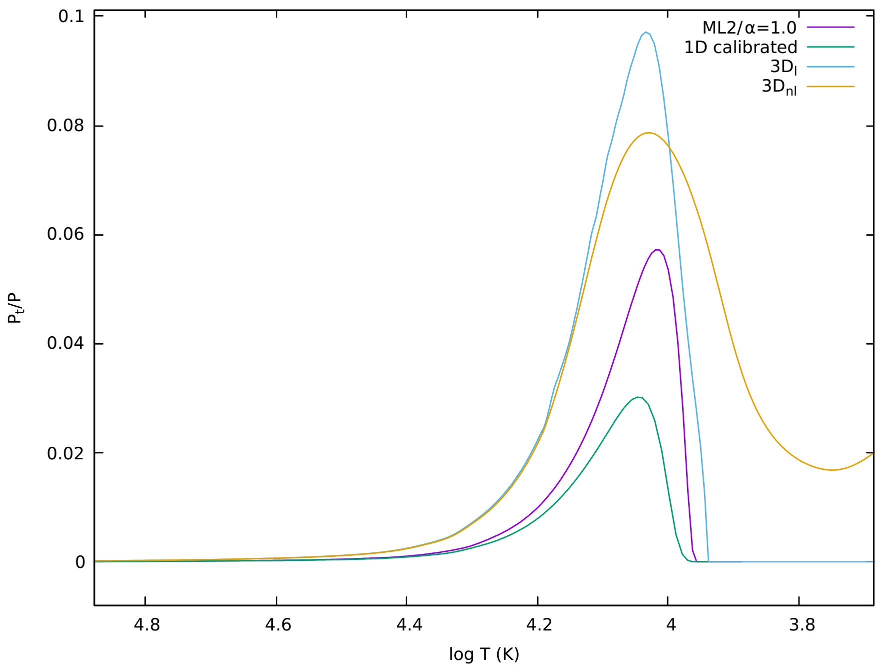

Figure 3.4: Turbulent pressure compared to the total pressure using different treatments : ML2/α=1.0, 1D calibrated, local 3D and non-local 3D for a $\log g$ = 8 model with T_{eff} = 12 000 K.

the convective region above the Schwarzschild boundary) is indeed directly related to the non-local character of convection. In truth, when a convective element crosses the Schwarzschild boundary, it is not its speed which becomes suddenly null but its acceleration and if it had a non-zero velocity at that time, it will decelerate in the so-called overshooting region until its velocity reaches zero. Fig. 3.4 illustrates also quite well the different results we obtain when using different models or when considering for a same model a local or non-local approach. When we compare the various models we see that the turbulent pressure has a greater impact with 3D simulations than with 1D models even if it remains relatively small compared to the total pressure (with a ratio of maximum 0.1). The non-local 3D curve (in yellow) clearly justifies our use of a non-local formalism as it takes well into account the reality in the overshooting region.

Fig. 3.5 illustrates the superadiabatic gradient ($\nabla - \nabla_{ad}$) for a ML2/α=1.0, 1D calibrated and 3D model. Again we see that the models do not give the same results at all in the convection zone. When we go towards the centre of the star (towards higher temperatures), we notice a discontinuity in the superadiabatic gradient obtained from 3D models. In fact, this discontinuity happens at the branching point between 1D models and 3D simulations. At this place, the models have been parametrized in such a way that they ensure the continuity for different quantities (such as the turbulent pressure) but it could not be done for derivative quantities such as the

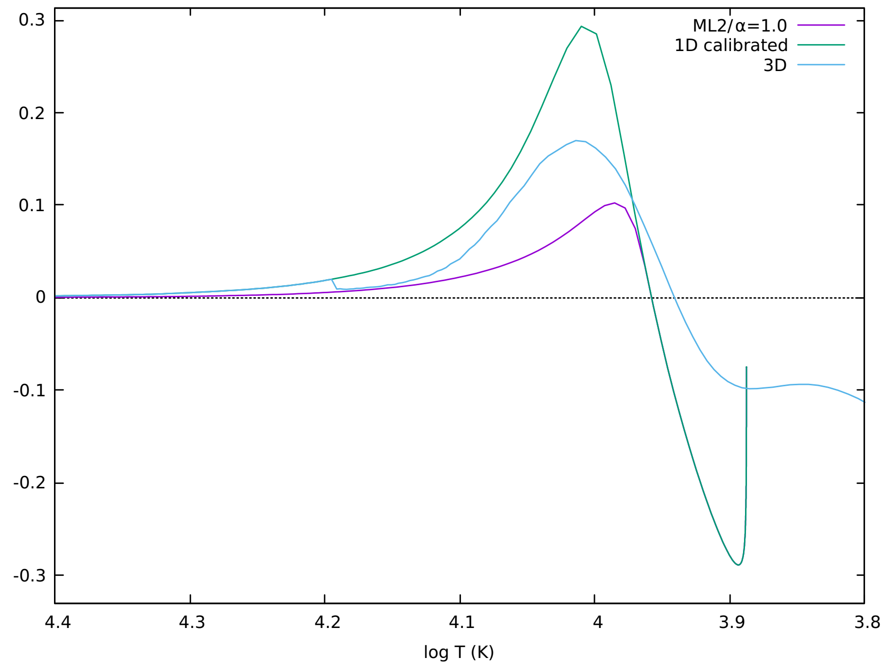

Figure 3.5: $\nabla - \nabla_{ad}$ obtained using three different treatments : ML2/α=1.0, 1D calibrated and 3D for a $\log g = 8$ model with $T_{\rm eff} = 12\,000$ K.

superadiabatic gradient. From this point towards the centre of the star both 1D calibrated and 3D models are in fact the same and are based on a 1D MLT model.

3.3 Results

Now that we have presented with an increasing power of accuracy three ways to model and predict the edges of the instability strip of ZZ Ceti white dwarfs, we will establish and compare the results obtained for some interesting representative evolutionary sequences. Our hope in this approach is to be able to better reproduce the empirical edges than what was done with a ML2/α=1 model as the two last models presented in the previous section are supposed to give more realistic results.

We present in Fig. 3.6 the spectrum of excited $\ell = 1$ g-modes for a $\log g = 9$ evolutionary sequence using the three different TDC models. This choice of white dwarf sequence might not be the most suitable as we can see on Fig. 1.1 that ZZ Ceti stars observed with excited modes in the instability strip have lower masses (typically between $\log g = 7.8$ and $\log g = 8.6$). However, we have already mentioned in Section 3.1 that some white dwarfs models had not been able to give us good results. Moreover, as it was presented in this section, we have calibrated the α parameter to fit 3D simulations in the 1D calibrated model but it was not all the time possible to find a converging value for α. As a result, for some evolutionary sequences, we had not acquired a sufficient amount of data to present and interpret them. For these reasons, we have mainly used an evolutionary sequence of $\log g = 9$ to apply the MAD code to, because of the good number of models for which we were able to find a value for α. Still, we have also applied the different codes to white dwarf models of different masses ($\log g = 7$, 7.5, 8, 8.5, 9, 9.5) and the case of $\log g = 8$ will also be illustrated later as it is a pertinent value to represent a ZZ Ceti pulsator.

In Fig. 3.6, for a better visual aspect, we have shifted by 100 K towards the blue edge the

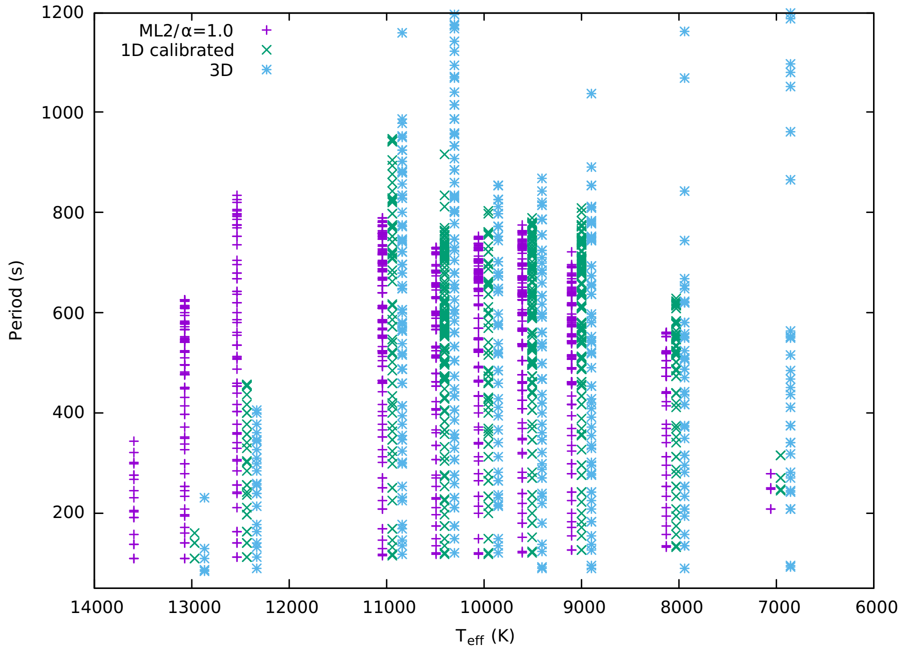

Figure 3.6: Periods in seconds obtained for the unstable $\ell = 1$ g-modes at various effective temperatures using our TDC treatment with the ML2/α=1.0 version of the MLT, 1D α calibrated model or 3D simulations for a $\log g = 9$ white dwarf.

results obtained from the ML2/α=1 computation and by 100 K towards the red edge the results predicted by 3D hydrodynamical simulations. The main difference that we observe between the results obtained with pure 1D models (ML2/α=1.0) and those based on 3D simulations (1D calibrated and to a greater extent 3D) is the location of the predicted blue edge. Even if the hot boundary of the ZZ Ceti instability strip had been already quite successfully determined in previous works ([Van Grootel, V. et al., 2012]) using the ML2/α=1.0 version of the TDC treatment, the results that we obtain here with models based on 3D simulations (1D calibrated and 3D) give a slightly smaller effective temperature on that side which remains consistent with the empirical values found[3]. However, as could be expected from models still based in some way to the simple MLT, the predicted red edge is again found at effective temperatures much too low compared to the empirical red edge of an evolutionary sequence model of that mass. It seems that even our improved treatment of the convection and the use of 3D simulations to parametrize more precisely the free parameters are not sufficient to reproduce correctly the red boundary. This tendency to get a lower effective temperature at the blue edge and a much lower predicted temperature at the red edge extend to all the evolutionary models we have tested. Between the two boundaries, it seems that the models are globally more excited when taking into account 3D simulations than what is found using only the ML2 flavour of the MLT.

Fig. 3.7 shows the results obtained for the case of a $\log g = 8$ model for which we have extracted some eigenfunctions in order to analyse and determine more precisely what are the possible driving or damping mechanisms in action. In what follows, we will focus more on the blue edge of the instability strip as it appears that our results differ the most there from the ones obtained with ML2/α=1 models. We first look at the entropy variations presented in Fig. 3.8. In this figure, the purple, green and blue lines were obtained for an unstable g mode (ℓ =1

[3]Besides, one should keep in mind our relatively low resolution on the effective temperature (500 K) along the evolutionary sequence which may lead to this small shift.

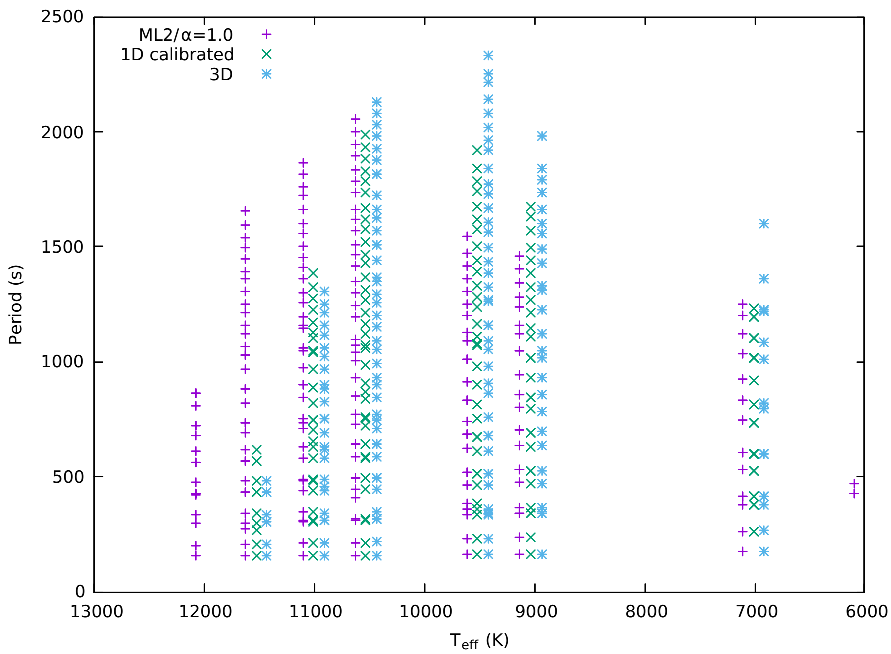

Figure 3.7: Periods in seconds obtained for the unstable $\ell = 1$ g-modes at various temperatures using our TDC treatment with the ML2/α=1.0 version of the MLT, 1D α calibrated model or 3D simulations for a $\log g = 8$ white dwarf.

g5 mode) picked from a $\log g = 8$ and $T_{\text{eff}} = 11\ 500$ K white dwarf model while the yellow curve was obtained from a similar mode but for a model at higher effective temperature ($T_{\text{eff}} = 12\ 000$ K). In fact, this last curve corresponds to the one obtained earlier with the TDC treatment in Fig. 3.2. From Fig. 3.7 we can see that at $T_{\text{eff}} = 11\ 500$ K the modes are globally more excited with ML2/α=1.0 models than with 1D calibrated or 3D models (as we had already concluded before). This observation can also be made now from the entropy variations perspective. Indeed, as we have explained at the very beginning of this chapter, what matter the most to have a driving effect on the oscillations (and thus more excited modes) is the energy input at the base of the convection zone where the temperature and the density are the highest. As we go towards the surface, the temperature and the density decrease rapidly and so even if the plateau of entropy is much higher in this region, it will not affect that much the oscillations. On Fig. 3.8, we see if we look closely that the purple curve (ML2/α=1.0) has a plateau extending deeper in the star than 1D calibrated or 3D models, it even begins slightly before the base of the convection zone (which is located at around $\log g$ = -14 for MLT2/α=1.0 computations). In fact, for 1D calibrated and 3D models, the mixing length determined for the calibration tends to be smaller than one. In consequence, as the size of the convection zone is proportional to this parameter, taking a smaller α into account reduces the size of the convection zone. The base of the convection zone is thus located in a less deep region with a lower temperature and density and so it explains why the driving is less pronounced there than it was with a ML2/α=1 model. From this discussion, one may conclude that the driving mechanism is in the case of the blue edge mainly driven by the position and the size of the convection zone and not by the type of models we apply. This conclusion can be even more supported if we look now at the additional curve obtained for a higher effective temperature (in yellow in Fig. 3.8). Indeed, the size of the convection zone (and especially the position of its base) is also influenced by the effective temperature of the model. As explained in [Van Grootel, V. et al., 2012], a larger

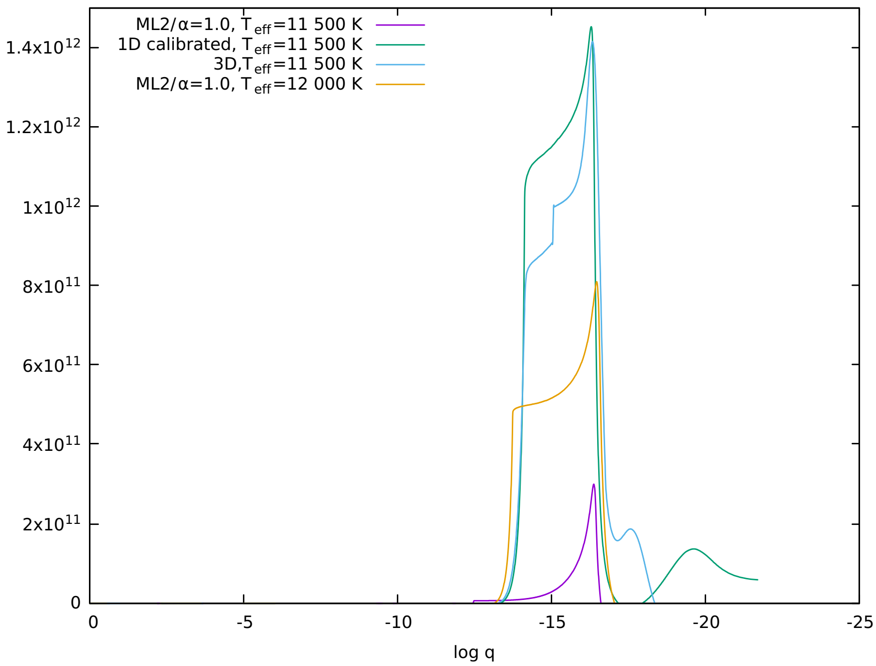

Figure 3.8: Entropy variations $\Re(\delta s)$ of a $\log g$ = 8 white dwarf model at two different effective temperatures (ℓ =1 g5 mode) with our TDC treatment (ML2/α=1.0, 1D calibrated model and 3D). The discontinuity at $\log q$ = -15 for the blue curve stems from the branching point between 1D and 3D models

opacity bump will develop as the temperature decreases due to ionization and recombination of neutral hydrogen. As the superficial boundary remains more or less at the same depth, the base will move deeper into the star. In our case, by taking a mode at a higher effective temperature (yellow curve) obtained from ML2/α=1 model we see that we can nearly mimic the results acquired from 1D calibrated and 3D models at a lower effective temperature even if the models considered are totally different. In conclusion, whatever the mixing length parameter α chosen, the model considered or the effective temperature, the driving of the instability is controlled by the position of the base of the convection zone in the star. This parameter is the one that matters the most at the blue edge. Nonetheless, the same reasoning is not true any more if we consider the red edge as all our discussion on the gradient entropy plateau cannot be applied in that case.

Fig. 3.9 presents the work integrals obtained for the same modes as for the entropy variations. The most striking fact is again the similitude between the results of 1D calibrated and 3D models at T_{eff} = 11 500 K and ML2/α=1.0 models at T_{eff} = 12 000 K. This comforts once more our previous reasoning as we see that the minimum of the work integrals (corresponding to the base of the convection zone) are nearly located at the same depth for these different models.

Other tools were also at our disposal, as we have discussed in the theoretical chapter and more especially in Section 2.6.5, our TDC treatment offers many possibilities to take into consideration or not various terms and their perturbations. Therefore, we have also used for a same model different variants depending on our choice concerning the perturbation of the turbulent pressure and the perturbation of the dissipation rate of turbulent kinetic energy into heat. In practice, we had the opportunity to take of well none of them into account, of well the first one (δp_t) or the other ($\delta\epsilon_2$), or both of them at the same time. In these various cases we will be referring each time to icop=0, icop=1, icop=2 or icop=3 respectively. The results obtained for a

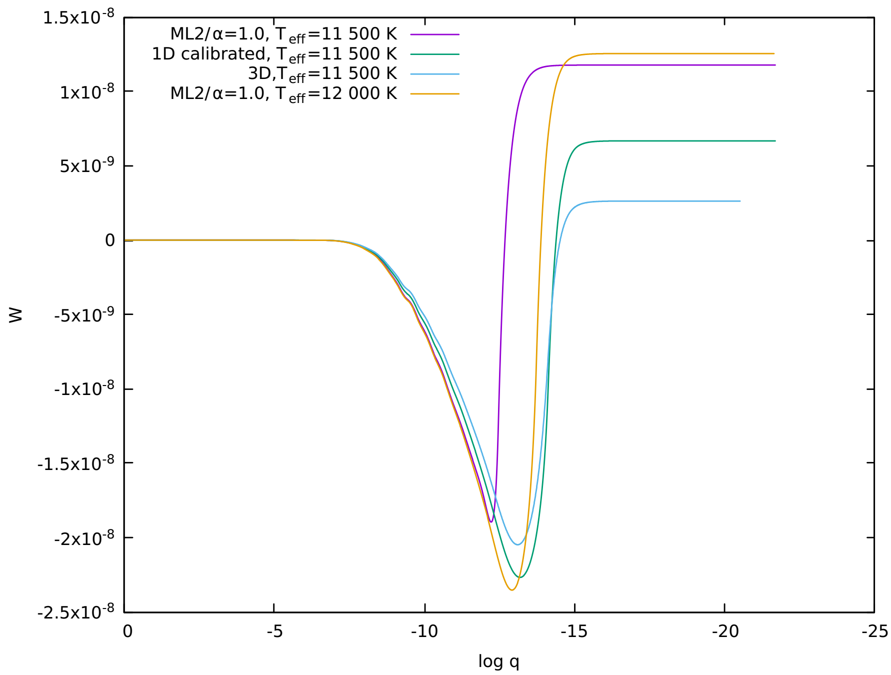

Figure 3.9: Work integrals of a $\log g$ = 8 white dwarf model at two different effective temperatures (ℓ =1 g5 mode) with our TDC treatment (ML2/α=1.0, 1D calibrated model and 3D).

$\log g$ = 9 evolutionary sequence for all four cases are shown in Fig. 3.10 with again the four different results shifted to have a clearer vision of the excited modes and their periods. For all these cases we used 3D hydrodynamical simulations (3D models) as they give the most realistic results. From the figure, we directly see that the results are relatively similar in all four cases with only small negligible discrepancies at some effective temperatures. In fact, this should not surprise us so much for two reasons.

Firstly because we have seen that the perturbation of the turbulent pressure and the one of dissipation rate of turbulent kinetic energy into heat had opposite effects on the damping or excitation rate of modes (through the work integral, cf. Section 2.6.5). Besides, it is theoretically not suitable to take only one of the perturbations into account while neglecting the other one at the same time (which is what happens when using icop=1 or icop=2) as the importance of one in comparison to the other depends on other factors such as the behaviour of Γ_3 and the shape of the convective elements through the choice of A (see Eq. (2.6.25)). In the case where we used icop=3, we have obtained nearly the same results as when we used icop=0 in our models, we can thus assume that both effects are compensating each other perfectly and so the unstable modes remain pretty much the same as if we had ignored both perturbations from the beginning (icop=0).

Secondly, when we have introduced in the previous section the improvements brought to 1D MLT models to fit better 3D hydrodynamical simulations, we have shown in Fig. 3.4 the ratio between the turbulent pressure and the total pressure. For 3D models, this ratio took values of maximum 0.08 which means that the turbulent pressure is quite small and its perturbation will only have a small impact on the results. In addition, as we have said, both the perturbation of the turbulent pressure and the perturbation of rate of dissipation of turbulent kinetic energy are of the same order which means that if the turbulent pressure is small then $\delta\epsilon_2$ is also small. This argument is illustrated in Fig. 3.10 if we look at the unstable modes obtained with icop=1

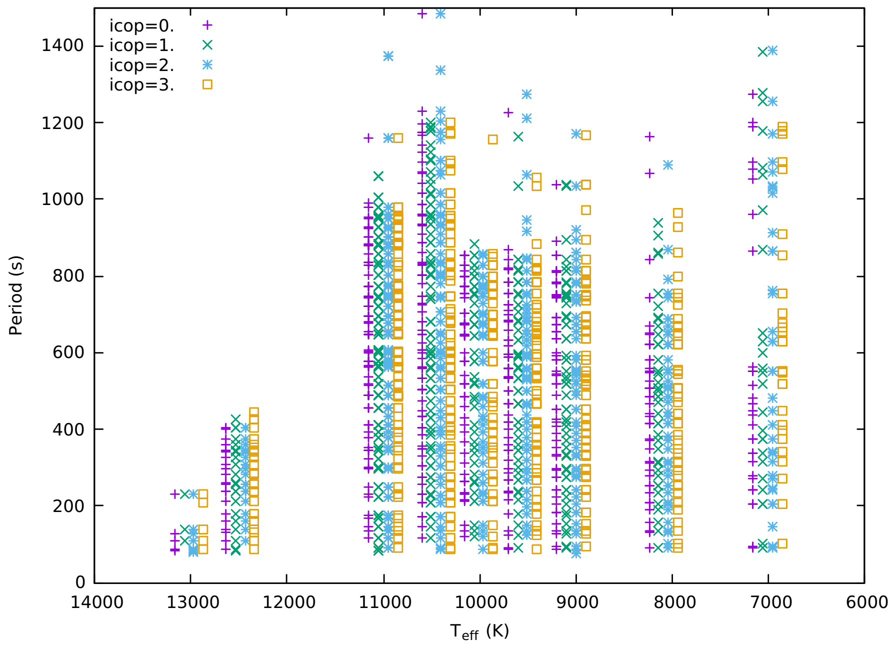

Figure 3.10: Periods in seconds obtained for the unstable $\ell = 1$ g-modes at various temperatures using 3D hydrodynamical simulations for a $\log g = 9$ white dwarf with the four different possibilities for the icop value.

and icop=2 models which appear to have the same periods as the ones obtained from models neglecting both perturbations.

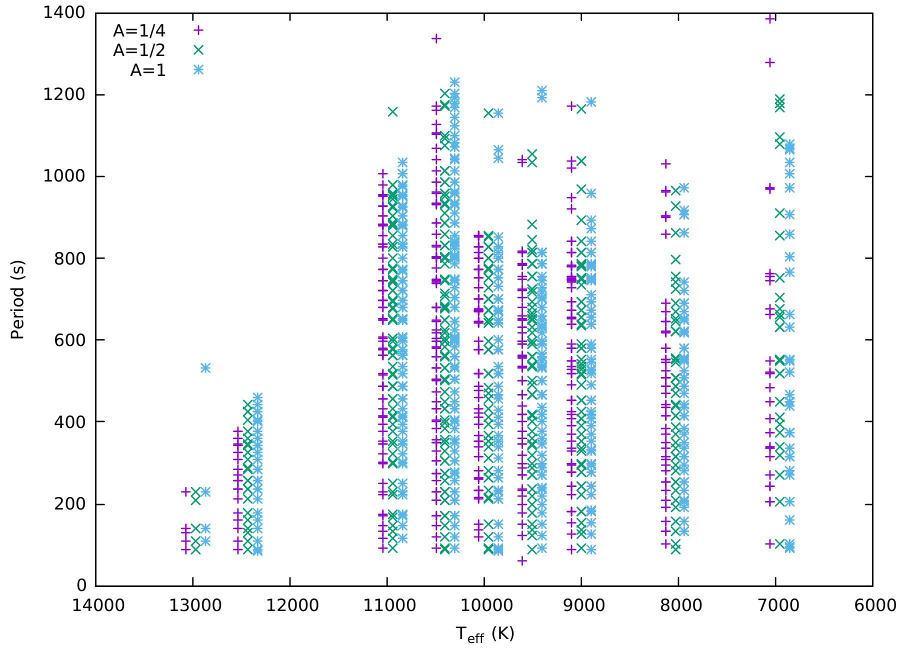

Figure 3.11: Periods in seconds obtained for the unstable $\ell = 1$ g-modes at various temperatures using our TDC treatment with the ML2/α=1.0 version of the MLT, 1D α calibrated model or 3D simulations for a $\log g$ =8 white dwarf with icop=3.

Nonetheless, even if it has not been yet mentioned in this chapter, all the models were computed with a constant value for the anisotropy parameter A fixed to 1/2 (isotropic turbulence). But as the value of A can influence the relative importance of the perturbation of p_t or the perturbation of ϵ_2, we have tried to vary it to see potential consequences. To stay consistent with the MLT in the stationary case, as A and the parameter Λ appears in the same relation (Eq. (2.4.25)), the code was written in a way that it automatically adapts the value of Λ when the user modifies the value of A. In consequence, modifying A does not affect directly the perturbation of the turbulent pressure as we have seen in the theoretical chapter that $\delta p_t/p_t = \delta\rho/\rho + 2\overline{\delta V_r}/V_r$ where the second term in the RHS is given by Eq. (2.6.14) in which both A and Λ appear. What remains of the influence of A lies in the definition of the dissipation rate of turbulent kinetic energy into heat through Eq. (2.6.18) and its link to the turbulent pressure. For a model with $A > 1/2$ we will have using Eq. (2.6.18) a greater effect of the turbulent pressure compared to the dissipation rate of turbulent kinetic energy. On the contrary, if $A < 1/2$ we obtain the opposite effect and in this case the turbulent pressure will have a smaller impact on the convection in comparison to the dissipation rate. We have tried three different values for A to compute an evolutionary sequence model of $\log g = 9$ with icop=3 using 3D simulations. The results are presented in the Fig. 3.11 for $A = 1/4$, $A = 1/2$ and $A = 1$. Globally, we do not see any general trend in this figure suggesting that the effect of A on the excitation or damping rate of modes remains small. This was expectable because of the small value of the turbulent pressure and thus of the dissipation rate of turbulent kinetic energy as both are related. Still, this small comparison helps to confirm what we have already concluded in the previous talk about the different values for the parameter icop.

Chapter 4

Conclusion

In Chapter 2 of this work, we have done all the developments leading to the time-dependent convection treatment based on mixing-length theory as presented in [Grigahcène et al., 2005]. The aim of this treatment is to take into account the interaction that exists between convection and pulsation. To obtain such a theory, many approximations were made, neglecting important aspects of the convection such as the whole cascade of energy. These approximations were for example the assumed expressions of the closure equations of momentum and energy as well as their perturbations, introduced to linearise and close the problem. In addition, with the incentive to do even better, we have also shown how three-dimensional hydrodynamical simulations were able to improve the description of convection. However, this has a cost and new free parameters were then introduced in the equations to match to our 1D models.

But all in all, when we have tested the models in Chapter 3 on the particular case of ZZ Ceti stars and their instability strip, we have seen that even with the improvements brought through the addition of 3D simulations, the results were still not satisfying enough. For the blue edge, the results obtained using 3D simulations were a little bit different from what was obtained with pure 1D models. Nevertheless, they remain coherent with the empirical values and show again that the main factor influencing the excitation on that side is the size and more precisely the location of the convection zone. Indeed, we have also tried to modify other factors that could have been possibly influencing the damping or driving of the modes (perturbation of the turbulent pressure and dissipation rate or the anisotropy factor A) but no significant changes were found. The same conclusion was made in [Van Grootel, V. et al., 2012] when comparing FC and TDC treatments. Concerning the red edge, the predicted temperature is again far too low compared to the empirical result found. Even when taking non-local effects or the perturbation of several other terms into account we could still not predict correctly the boundary.

However, this is not a fatality but it rather suggests that we certainly need to develop a new theory, possibly more complex but also more complete than a theory only based on the mixing-length theory. This new theory should maybe take in consideration non-linear effects. A more promising idea would be to correctly model the behaviour of stationary waves having the right global oscillation frequencies in the 3D box corresponding to a simulation. It would consist in studying and modelling the impact of a turbulent three-dimensional hydrodynamic on the modes by perturbing the hydrodynamics equations and solving the linear system of partial differential equations obtained. Finally, we could estimate the impact of this 3D convection on the damping or driving of the different modes by injecting the solutions obtained previously in the work integral.

Bibliography

[Aerts et al., 2010] Aerts, C., Christensen-Dalsgaard, J., and Kurtz, D. W. (2010). *Asteroseismology*.

[Balmforth, 1992] Balmforth, N. J. (1992). Solar pulsational stability - I. Pulsation-mode thermodynamics. , 255:603–649.

[Bohm and Cassinelli, 1971] Bohm, K. H. and Cassinelli, J. (1971). Convective Envelopes and Acoustic Noise Generation in White Dwarfs. *aap*, 12:21.

[Böhm-Vitense, 1958] Böhm-Vitense, E. (1958). Über die Wasserstoffkonvektionszone in Sternen verschiedener Effektivtemperaturen und Leuchtkräfte. Mit 5 Textabbildungen. , 46:108.

[Canuto and Mazzitelli, 1991] Canuto, V. M. and Mazzitelli, I. (1991). Stellar turbulent convection: A new model and applications. *Astrophys. J.*, 370:295–311.

[Dupret, 2018] Dupret, M.-A. (2017-2018). Lecture notes in stellar stability and asteroseismology.

[Dupret et al., 2006] Dupret, M.-A., Goupil, M., Samadi, R., Grigahcène, A., Gabriel, M., et al. (2006). A non-local mlt treatment fitting 3d simulations. *Proceedings of SOHO 18/GONG 2006/HELAS I, Beyond the spherical Sun*, page 78.

[Dupret et al., 2006] Dupret, M.-A., Samadi, R., Grigahcene, A., Goupil, M.-J., and Gabriel, M. (2006). Non-local time-dependent treatments of convection in A-G type stars. *Communications in Asteroseismology*, 147:85–88.

[Fontaine and Brassard, 2008] Fontaine, G. and Brassard, P. (2008). The Pulsating White Dwarf Stars. , 120:1043.

[Fontaine et al., 1982] Fontaine, G., McGraw, J. T., Dearborn, D. S. P., Gustafson, J., and Lacombe, P. (1982). On the statistics of ZZ Ceti stars. , 258:651–660.

[Freytag et al., 2012] Freytag, B., Steffen, M., Ludwig, H.-G., Wedemeyer-Böhm, S., Schaffenberger, W., and Steiner, O. (2012). Simulations of stellar convection with CO5BOLD. *Journal of Computational Physics*, 231:919–959.

[Gabriel et al., 1974] Gabriel, M., Scuflaire, R., Noels, A., and Boury, A. (1974). Influence de la Convection sur la Stabilité des Oscillations Nonradiales des Etoiles. *Bulletin de l'Academie Royale de Belgique*, 60:866–887.

[Gough, 1977] Gough, D. O. (1977). Mixing-length theory for pulsating stars. , 214:196–213.

[Grigahcène et al., 2005] Grigahcène, A., Dupret, M.-A., Gabriel, M., Garrido, R., and Scuflaire, R. (2005). Convection-pulsation coupling. I. A mixing-length perturbative theory. , 434:1055–1062.

[Houdek and Dupret, 2015] Houdek, G. and Dupret, M.-A. (2015). Interaction Between Convection and Pulsation. *Living Reviews in Solar Physics*, 12:8.

[Ledoux and Walraven, 1958] Ledoux, P. and Walraven, T. (1958). Variable Stars. *Handbuch der Physik*, 51:353–604.

[Ludwig et al., 1999] Ludwig, H.-G., Freytag, B., and Steffen, M. (1999). A calibration of the mixing-length for solar-type stars based on hydrodynamical simulations. I. Methodical aspects and results for solar metallicity. , 346:111–124.

[Prandtl, 1925] Prandtl, L. (1925). 7. bericht er untersuchungen zur ausgebildeten turbulenz. *ZAMM - Journal of Applied Mathematics and Mechanics / Zeitschrift für Angewandte Mathematik und Mechanik*, 5(2):136–139.

[Sonoi et al., 2017] Sonoi, T., Belkacem, K., Dupret, M. A., Samadi, R., Ludwig, H. G., Caffau, E., and Mosser, B. (2017). Computation of eigenfrequencies for equilibrium models including turbulent pressure. , 600:A31.

[Spiegel, 1963] Spiegel, E. A. (1963). A Generalization of the Mixing-Length Theory of Turbulent Convection. , 138:216.

[Starrfield et al., 1982] Starrfield, S., Cox, A. N., Hodson, S., and Pesnell, W. D. (1982). Linear theory radial and nonradial pulsations of DA dwarf stars. In *Pulsations in Classical and Cataclysmic Variable Stars*, page 78.

[Tassoul et al., 1990] Tassoul, M., Fontaine, G., and E. Winget, D. (1990). Evolutionary models for pulsation studies of white dwarfs. *The Astrophysical Journal Supplement Series*, 72:335–386.

[Tremblay et al., 2015] Tremblay, P.-E., Ludwig, H.-G., Freytag, B., Fontaine, G., Steffen, M., and Brassard, P. (2015). Calibration of the mixing-length theory for convective whife dwarf envelopes. *The Astrophysical Journal*, 799(2):142.

[Tremblay, P.-E. et al., 2013] Tremblay, P.-E., Ludwig, H.-G., Steffen, M., and Freytag, B. (2013). Pure-hydrogen 3d model atmospheres of cool white dwarfs. *A&A*, 552:A13.

[Unno, 1967] Unno, W. (1967). Stellar Radial Pulsation Coupled with the Convection. *Publications of the Astronomical Society of Japan*, 19:140.

[Van Grootel, V. et al., 2012] Van Grootel, V., Dupret, M.-A., Fontaine, G., Brassard, P., Grigahcène, A., and Quirion, P.-O. (2012). The instability strip of zz ceti white dwarfs - i. introduction of time-dependent convection. *A&A*, 539:A87.

[Winget et al., 1982] Winget, D. E., van Horn, H. M., Tassoul, M., Fontaine, G., Hansen, C. J., and Carroll, B. W. (1982). Hydrogen-driving and the blue edge of compositionally stratified ZZ Ceti star models. , 252:L65–L68.